



# Report on the integrated geomodels of Los Humeros and Acoculco

D3.1

# Report on the integrated geomodels of Los Humeros and Acoculco

D3.1

Final Version 13

Authors:

Philippe Calcagno, Eugenio Trumpy, Luis Carlos  
Gutiérrez-Negrín, Domenico Liotta, Gianluca Gola

with the collaboration of:

Claudia Arango Galván, Denis Avellán, Kristian Bär,  
Eivind Bastesen, Ásdís Benediktsdóttir, Caterina  
Bianco, Damien Bonté, Andrea Brogi, Gerardo  
Carrasco-Núñez, Guillermo Cisneros, Natalia  
Cornejo, Paromita Deb, Gwladys Evanno, Gylfi Páll  
Hersir, Victor Hugo Garduño-Monroy, Emmanuel  
Gaucher, Guido Giordano, Gabriela Gómez, Federico  
Lucci, José Luis Macías Vásquez, Adele Manzella,  
Gianluca Norini, Emmanuel Olvera Garcia, Luigi  
Piccardi, Bety Román, Alessandro Santilano, Tania  
Andrea Toledo Zambrano, Loes Vaessen, Walter  
Wheeler, the EU-MX GEMex Task 3.1 team, and CFE  
staff

Work package WP3

05/2020

Website: <http://www.gemex-h2020.eu>



The GEMex project is supported by the  
European Union's Horizon 2020  
programme for Research and Innovation  
under grant agreement No 727550

# Table of Contents<sup>1</sup>

<b>List of figures</b>	<b>5</b>
<b>List of tables</b>	<b>8</b>
<b>Executive summary</b>	<b>10</b>
<b>1 Introduction</b>	<b>11</b>
<b>2 Methodology</b>	<b>13</b>
2.1 Way of working	13
2.2 Geomodelling	13
<b>3 Los Humeros</b>	<b>15</b>
3.1 Geological and geothermal framework	15
3.2 Data and information	16
3.3 Integration	16
3.3.1 Geological piles description	17
3.3.2 Wells computation and description	19
3.3.3 Preliminary geomodels	21
3.3.4 Local geomodel update	23
3.3.5 Volcanic lineaments	26
3.3.6 Cluster analysis	32
3.3.7 Integrated geomodel	36
3.4 Interpretation – Conceptual model of the geothermal system	42
<b>4 Acoculco</b>	<b>46</b>
4.1 Geological and geothermal framework	46
4.2 Data and information	46
4.3 Integration	47
4.3.1 Preliminary geomodel	48
4.3.2 First geomodel update	50
4.3.3 Second geomodel update	51
4.3.4 Integrated geomodel	53
4.4 Interpretation – Conceptual model of the geothermal system	60
<b>5 Conclusion</b>	<b>62</b>
5.1 Way of working	62
5.2 Achievements	63
5.3 Perspectives	65

---

<sup>1</sup> The content of this report reflects only the authors' view. The Innovation and Networks Executive Agency (INEA) is not responsible for any use that may be made of the information it contains.

<b>6</b>	<b>Acknowledgement</b>	<b>67</b>
<b>7</b>	<b>References</b>	<b>68</b>

## List of figures

Figure 1: Location of the Los Humeros regional, local and integration areas, and Acoculco regional and local/integration areas, east of Mexico City in the Trans-Mexican Volcanic Belt (dashed blue area). Area locations are shown on the 90m Digital Elevation Model SRTM. Coordinate system is WGS84/UTM zone 14N. Figure modified from Calcagno et al. (2018). .....	11
Figure 2: Example of the integrated platform as a common thread enhancing the cooperation and the interaction of the scientific fields applied. The final model is a co-directed, mutual, shared, and robust interpretation. The methods illustrated here are examples usually involved in geothermal exploration (taken from Calcagno, 2015). .....	12
Figure 3: Interpolation method illustrated for two geological objects, red and blue (see Lajaunie & al., 1997; and Calcagno et al., 2008). (a) Input data for the interpolation: 3D points (location of geological interfaces) and 3D vectors (azimuth and dip of geological structures). (b) 3D potential field interpolation: The geological interfaces are modelled by isovalues of the potential field. ....	14
Figure 4: The main versions of the Los Humeros geomodels during the GEMex project. ....	17
Figure 5: Geological description, version 2017 (excerpt from Calcagno et al., 2018). ....	18
Figure 6: Geological description, version 2018. The three units of G3 are different from the version 2017 (see Figure 5). ....	19
Figure 7: The deviation data from CFE (left hand side) are transformed in survey data (right hand side). ....	20
Figure 8: Process to compute well deviation. ....	20
Figure 9: Deviated wells computation. Focus on the Azimuth angle calculation. ....	21
Figure 10: The Los Humeros regional geomodel of the four geological groups (see Figure 5). Coordinate system is WGS84/UTM zone 14N. ....	22
Figure 11: The Los Humeros local geomodel of the nine geological units (see Figure 5). Coordinate system is WGS84/UTM zone 14N. ....	23
Figure 12: New fieldwork data led to the update of almost all the faults of the local model of Los Humeros and to the addition of Fault 1 to Fault 4. Coordinate system is WGS84/UTM zone 14N (after Calcagno et al., 2020). ....	24
Figure 13: Fifty-six wells were used for the update of the Los Humeros local model. Ten of them are deviated. They are described according to the 2018 geological pile description presented in Figure 6. DEM is displayed as a grid including the fault network traces (see Figure 12). View from SE. ....	25
Figure 14: The 3D geomodel of Los Humeros updated at the local scale for the nine geological units (see Figure 6). It includes the updated faults (Figure 12) and fifty-six wells (Figure 13). Coordinate system is WGS84/UTM zone 14N (after Calcagno et al., 2020). ....	25
Figure 15: Criteria used for estimating the tectonic control on volcanic alignments (after Paulsen and Wilson, 2010, with modifications in Olvera Garcia et al., 2019); (a) Reliability criteria for assessment the vent alignments. The number of vents, the orthogonal distances of the volcanic center from the best-fit line (standard deviation), the values of elongate vents (index of elongation- see b and d), the angular deviation of elongate volcanic long axes from the trend of the best-fit line and the spacing distance between vents are used to assess the reliability of alignments. C.A.R = Crater Axial Ratio; (b) Morphology of vent shapes from circular to elongated as a consequence of	

deformation; (c) Parameters of alignment and volcanic vents as listed in a; (d) Axial ratio describing ellipticity of a volcanic vent (index of elongation).....	26
Figure 16: Yellow points indicate the location of the monogenic volcanoes considered in the computation as proposed by Paulsen and Wilson (2010). .....	27
Figure 17: Location of the monogenetic vents and ellipse shapes of the volcano centers used for the evaluation of the parameters given in Table 3.2. The eruptive fractures are interpreted on the basis of the volcanic morphological features (see Figure 15) and the values from the linear ridge results. ....	29
Figure 18: Map illustrating the areal density of monogenic volcanoes (black dots) after Lesti et al. (2008). The red lines are the fault traces as derived applying the methodology proposed by Paulsen and Wilson (2010). ....	30
Figure 19: Location of the monogenetic vents (black dots) and isolines delimiting areas with equal density of volcanic vents. ....	31
Figure 20: Interpretation in terms of fault-zones channelling magma to surface. The Maztaloya fault is also indicated as a reference. ....	31
Figure 21: Cross plots (upper) and normalized density plots (lower) of selected couples of geophysical datasets. The patterns of the relations $V_p$ - $V_p/V_s$ , the Resistivity- $V_p/V_s$ and the Resistivity-Density are displayed. ....	32
Figure 22: 3D visualization of the cluster volumes (a, c and e) and cluster distributions along selected cross-sections (b, d and f) exploiting the $V_p$ - $V_p/V_s$ (a and b), Resistivity- $V_p/V_s$ (c and d) and Resistivity-Density (e and f) datasets. The results refer to the unsupervised Gaussian Mixture Model method with seven clusters. ....	33
Figure 23: 3D model illustrating the distribution of the geophysical data by means of the cluster supervised methodology. Considered intervals are listed on the right side of the figure. See GEMex D5.12 for more information on the adopted methodology. North is indicated by the Y-axis. The well path are displayed. ....	34
Figure 24: Horizontal (slice 1 at 400 m a.s.l), E-W and N-S vertical sections (slices 2 and 3, respectively) from the 3D model shown in Figure 23. North is indicated by the Y-axis. ....	35
Figure 25: Horizontal sections (slice 1) from the 3D model shown in Figure 23. The yellow box indicates the cluster of geophysical data compatible with the occurrence of fluids. Location of boreholes (white lines) and main faults (red surfaces) are also indicated. ....	35
Figure 26: Vertical sections (slice 2 and 3) from the 3D model shown in Figure 23. The yellow box indicates the cluster of geophysical data compatible with occurrence of fluids. Location of boreholes (white lines) is also indicated. ...	36
Figure 27: Fifty-six wells are described according to the four groups' version 2018 of the geological pile presented in Figure 6. DEM is displayed as a grid including the fault network traces (see Figure 28). Coordinate system is WGS84/UTM zone 14N. View from SE. ....	37
Figure 28: The fault network constructed in the Los Humeros integrated geomodel, along with the wells. Surfaces visualization is semi-transparent to facilitate the reading of the picture. Purple: regional faults; brown: caldera structures; red: local faults. Coordinate system is WGS84/UTM zone 14N. ....	38
Figure 29: A clipped view of the Los Humeros integrated geomodel including wells, fault network, and the four geological groups: basement (green), pre-caldera rocks (blue), rocks from the caldera (purple), post-caldera rocks (brown). Coordinate system is WGS84/UTM zone 14N. ....	39

Figure 30: The Los Humeros integrated geomodel displaying wells, faults trace, and the four geological groups: (a) post-caldera rocks, (b) rocks from the caldera, (c) pre-caldera rocks, (d) basement. Coordinate system is WGS84/UTM zone 14N. Views from SE.....	39
Figure 31: The Los Humeros integrated geomodel displaying faults in transparency, seismic events (coloured dots) and $V_p/V_s$ 3D grid model (GEMex D5.3). Coordinate system is WGS84/UTM zone 14N. View from SW. ....	40
Figure 32: A top view of the the Los Humeros integrated geomodel displaying fault traces and Antigua fault full surface, wells and cluster 15 (see section 3.3.6). Top view.....	41
Figure 33: The Los Humeros integrated geomodel displaying faults in transparency, seismic events (coloured dots) and simulated temperatures 3D grid (GEMex D6.3). (a) whole temperature grid, view from SW; (b) temperature above 350°C, top view; (c) temperature above 350°C, view from W. Coordinate system is WGS84/UTM zone 14N.....	42
Figure 34: Interest area (green) to be searched to a depth >3.5 km for superhot geothermal resources in Los Humeros. Blue line: caldera related structures; brown area: the more recent lava-flows; red: faults; pink area: highest CO2 emissions in air. ....	45
Figure 35: The schema reports the main Acoculco geomodel updates, its presentation into the GEMex project context, the scale and if the model was scientifically disseminated. ....	48
Figure 36: Lithologic column for well EAC-1 and EAC – 2 (Lorenzo-Pulido et al., 2010).....	49
Figure 37: The two main cross-sections used for modelling the Acoculco area. Symbols: 1 – vulcanite (Pliocene-Holocene); 2– Quaternary dyke; 3 – skarn and marble; 4 – crust involved in thermal anomalies through time: magma chambers originating the different volcanic events are supposed to be developed within this volume; 5 – Jurassic-Cretaceous limestone; 6 – crystalline rocks, mainly phyllite (Paleozoic); 7 – Neogene-Quaternary normal to oblique slip faults; 8 – thrust faults related to the Laramide orogenesis (Oligocene) (Calcagno et al., 2018).....	49
Figure 38: a) The Acoculco regional fault model. Twenty-six faults are modelled. Coordinate system is WGS84/UTM zone 14N. b) The Acoculco regional geological model (Calcagno et al., 2018).....	50
Figure 39: The 3D visualisation of the updated faults system including the ‘Damage zones’, modelled as delimited by two sets of NNW-SSE striking parallel faults. Coordinate system is WGS84/UTM zone 14N (Calcagno et al., 2020).	51
Figure 40: The updated regional 3D geomodel of Acoculco with the new faults and the ‘Damage zones’. Coordinate system is WGS84/UTM zone 14N (Calcagno et al., 2020). ....	51
Figure 41: The second updated regional 3D geomodel of Acoculco with the new faults. Coordinate system is WGS84/UTM zone 14N. a) The computed geological map, in orange, red and blue the updated faults network; b) the 3D view of the new faults network; c) the two computed cross-sections (AA’ and BB’); d) the 3D view of the second updated Acoculco geomodel. ....	52
Figure 42: The second release of the local 3D geomodel of Acoculco with the detailed faults network. Coordinate system is WGS84/UTM zone 14N. a) The computed geological map, red and blue the detailed faults network; b) the 3D view of the new faults network; c) the two computed cross-sections (AA’ and BB’); d) the 3D view of the local Acoculco geomodel. ....	53
Figure 43: Part of the cross-section 10bis’ on the left and part of the cross-section AA’ on the right: VES is represented by the blue to light blue color ramp where colder colors stay for low resistive rocks while warmer color are referred to higher resistivity rocks. The blue dots (not in the vertical profile) are referred to the 60 $\Omega$ .m layer extracted from the 3D resistivity model. Inside the black box a good correspondence between the bottom of the volcanites and the 60 $\Omega$ .m layer. ....	54

Figure 44: Low to high density and low resistivity (60 $\Omega.m$ ) domains (clusters 11, 21, 31) coming from the supervised clustering that could partially represent the volcanites. ....	55
Figure 45: High resistivity-high density domains from the supervised clustering model together with the simplified lithostratigraphic sequence of the two boreholes in the area of study. The borehole EAC-1 results partially inside a first volume of this kind of rocks, while a second volume occurs toward N from the EAC-2 borehole.....	56
Figure 46: Blue dots represent the high resistivity-high density domain from the supervised clustering model imported in the AA', BB', 7 and 8 cross-sections. The occurrence of this cluster could suggest the presence of metamorphosed limestones in skarn facies and a former hydrothermal fluids circulation. ....	57
Figure 47: In both pictures are reported the blue dots that are related to the 750° degree isotherm from the regional thermal model and representing the shape of the supposed new younger intrusion. The blue dots position helped to infer the shape of the young intrusion within the previously (old) emplaced granite. ....	58
Figure 48: (Left) 2D map of the modelled faults at local scale (in light blue the NW-SE strike slip faults and in red the NE-SW normal faults). The pink dots represent the high resistivity – high density cluster domain projected in the surface. The fault in <i>Alcaparrosa</i> area is included in the indicated cluster (within the orange box). (Right) 3D representation of the faults and the high resistivity – high density cluster domain (in green). Within the black box the fault cutting the cluster.....	58
Figure 49: the map here reported is the 3km high pass filter from the density data, the colder color represent the lower density contrast while the warmer the higher density contrast. The distribution of the NE-SW normal faults (red) and the NW-SE strike slip faults (light blue) overlap the aforementioned map with monogenetic volcano cones (orange dots). Only close to the NF_1 it is recognizable the cones alignment with this fault. ....	59
Figure 50: The integrated local 3D geomodel of Acoculco. Coordinate system is WGS84/UTM zone 14N. a) The computed geological map, red and blue the detailed faults network; b) the 3D view of the new faults network; c) the two computed cross-sections (AA' and BB'); d) the 3D view of the local Acoculco geomodel. In this geomodel the bottom of the volcanites and part of the skarns are checked with geophysical data and cluster analysis, the young magmatic intrusion is added thanks to the Regional thermal model and the fault in the <i>Alcaparrosa</i> manifestation area is added.....	60

## List of tables

Table 3.1: List and sources of dataset used for the construction of the Los Humeros geomodels. In the table is specified which data were used for the preliminary and updated geomodels as well as the additional data for the integrated geomodel. Moreover, the source of data is specified with the reference to the GEMex deliverable number when applicable. ....	16
Table 3.2: Table summarizing the computation provided about the alignments. See also Figure 17 for the numbering of the vent alignments. ....	28
Table 3.3: Examples of methods and data used to produce the Los Humeros integrated geomodel and the geothermal system interpretation (see section 3.4). More information regarding these data is available in Table 3.1. ....	38
Table 4.1: List of dataset used for the construction of the Acoculco geomodels. In the table is specify which data were used for the preliminary and updated geomodels as well as the additional data for the integrated geomodel. Moreover, the source of data is specified.....	47

Table 5.1: The main uses of the geomodels within the GEMex consortium. ....	63
Table 5.2: Main achievements of the geomodelling and integration process for Los Humeros and Acoculco. ....	64
Table 5.3: Main communications of the geomodelling and integration process for Los Humeros and Acoculco. Presentations done in GEMex meetings are not listed. ....	65

## Executive summary

The European-Mexican geothermal GEMex project aims at developing geothermal energy in the easternmost region of the Trans-Mexican Volcanic Belt. Two sites under development by the Comisión Federal de Electricidad (CFE, Mexican National Power Company) are investigated to assess possible superhot resources and to develop an Enhanced Geothermal System, respectively in Los Humeros and Acoculco.

European and Mexican partners constructed 3D geomodels at regional, local, and integration scales in a collaborative way on both sites. In a preliminary step, these models were set up using data available at the beginning of the project, including geological maps, cross-sections and well logs. In a second phase, they were updated thanks to the results from geological and geochemical field campaigns conducted by GEMex partners. The models were finally improved via the integration of additional information acquired during the project, e.g. geochemistry analysis and geophysical models, to strengthen the structures and infer the geothermal interpretation.

In Los Humeros, the structures were modelled from the geological map, additional field work, volcanos alignment study and results from the study of the exhumed geothermal system of Las Minas. The Los Humeros geological formations were described in four groups at regional and integration scales, and nine units at local scale. The CFE provided records for fifty-six wells to constrain the Los Humeros area at depth. Geophysical data such as resistivity from MT survey, Vp/Vs computation, 3D seismic events, and gravity were used in the integration process. The interpretation based on the integrated 3D geomodel tends to highlight a potential volume of rocks located to the south of the Los Humeros village and where fluids in superhot conditions can be explored at depth between 3.5 and 4.5 km.

In Acoculco, the data core to build the 3D geomodels was based on the recently published geological map for the area, two geological cross-sections and about 50 structural stations acquired in the field works performed during the GEMex project. The structural asset and lithological groups were set-up for regional and local scale. In addition, 3D geomodels were constrained with the two deep boreholes drilled by the CFE, resistivity from MT and density from gravity surveys. Although the presence of a conventional hydrothermal system cannot be excluded for the Acoculco area, the data collected and organised, the implemented integrated 3D geomodel and the resulting conceptual model is the base for further evaluation in order to assess the feasibility of the stimulation for an EGS development of the area.

The 3D geomodels of Los Humeros and Acoculco were used by the GEMex partners along the course of the project as input for computations and simulations. In addition to the knowledge produced, the outcomes of the geomodelling work include the geomodels themselves that are shared in open access, and scientific presentations and papers.

**Keywords:** Interdisciplinary integration, geological interpretation, geophysical interpretation, 3D geomodelling, geothermal system interpretation, geothermal exploration, enhanced geothermal system, superhot geothermal system, Los Humeros, Acoculco.

# 1 Introduction

GEMex is a European Union's Horizon 2020 research and innovation programme project (2016-2020) gathering 24 European partners in collaboration with a nine-partners Mexican consortium. It aims at developing two non-conventional geothermal resources, which are Enhanced Geothermal Systems (EGS) and SuperHot Geothermal Systems (SHGS), by designing reliable, efficient, and replicable methodologies. To reach this goal, GEMex deployed a comprehensive range of investigations: geological and geothermal context understanding, deep structures detection, reservoir characterization, and concepts for EGS and SHGS development, including a socio-economic approach. More information about the project structure and contents can be found in Jolie et al. (2018) and [www.gemex-h2020.eu](http://www.gemex-h2020.eu).

Two sites were dedicated to GEMex as the most representative examples of the SHGS and EGS: Los Humeros and Acoculco, respectively, both located East of Mexico City (Figure 1). They belong to the Trans-Mexican Volcanic Belt (TMVB), which is a continental volcanic arc crossing central Mexico, where the volcanic activity is reported to have started about 16 Ma ago (Ferrari et al, 1999) and has continued nowadays with some currently active volcanoes (e.g. Popocatepetl, Volcán de Colima). These young volcanic processes make the TMVB a favourable area for active geothermal fields.

Los Humeros and Acoculco were investigated at different scales during the work presented in this report (Figure 1).

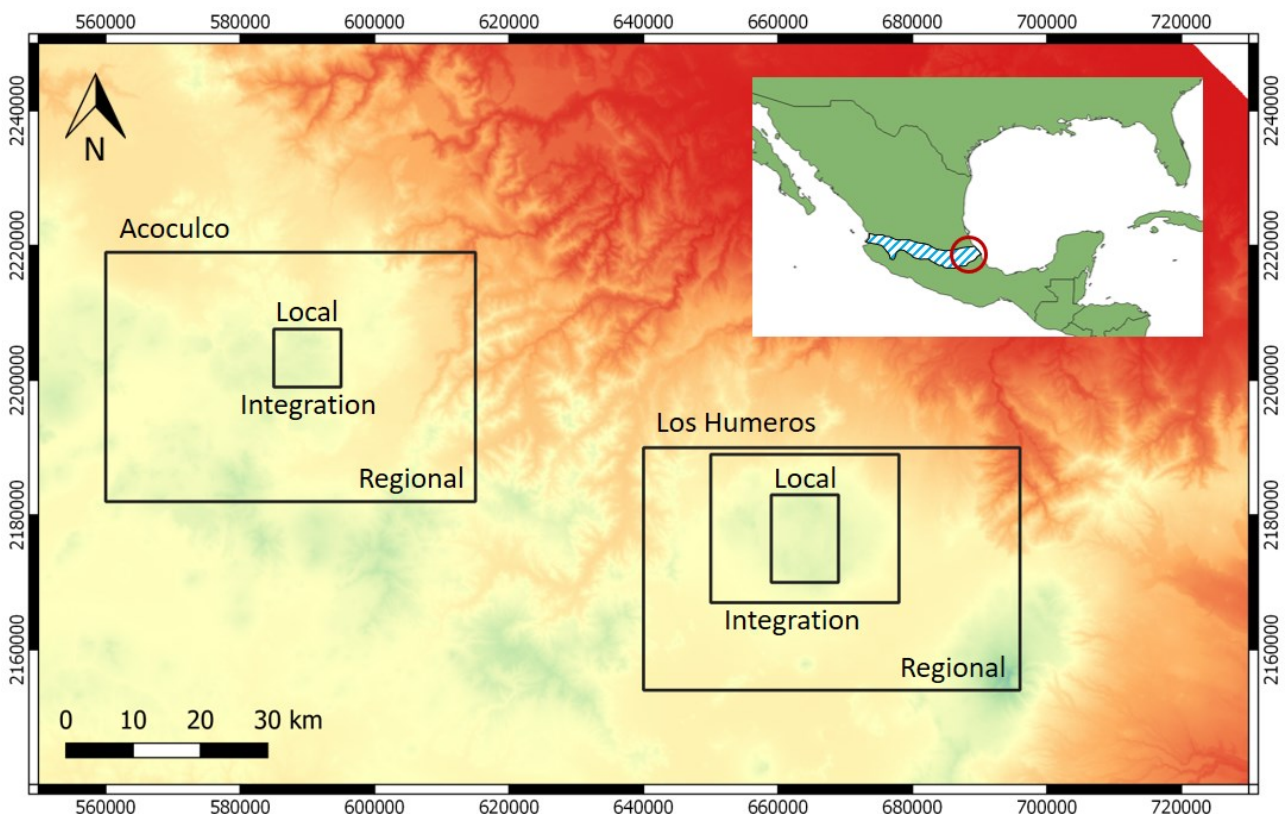


**Figure 1:** Location of the Los Humeros regional, local and integration areas, and Acoculco regional and local/integration areas, east of Mexico City in the Trans-Mexican Volcanic Belt (dashed blue area). Area locations are shown on the 90m Digital Elevation Model SRTM. Coordinate system is WGS84/UTM zone 14N. Figure modified from Calcagno et al. (2018).

Correct interpretation of subsurface structures, properties and simulation models in the exploration workflow is critically dependent on capability for 3D visualisation and consistency in 3D structural and compositional

interpretation (Houlding, 1994; Mallet, 2002; Wu, 2005). In the past decade significant advancement has been made in the development of 3D mapping, visualisation and modelling for geothermal purposes (Cloetingh et al., 2010; Calcagno, 2014). Multidisciplinary integration was a key factor for a robust and coherent knowledge of the areas that were investigated (Los Humeros and Acoculco). Associating data in a classic workflow methodology satisfies the forecasted objective to combine multi-discipline contributions. However, such a workflow makes collaborative scientific reasoning challenging because fields are used sequentially and individually. The GEMex project went a step forward by developing the contributions from the various disciplines together in a single 3D integration platform (Figure 2) instead of simply aggregating independent results (Calcagno, 2015). For instance, in this way, the geological interpretation benefits from the geophysics interpretation and vice versa. The geomodels constructed in GEMex are not the final result of a sequential weakly connected integration but a central tool of a cooperative interpretation process.

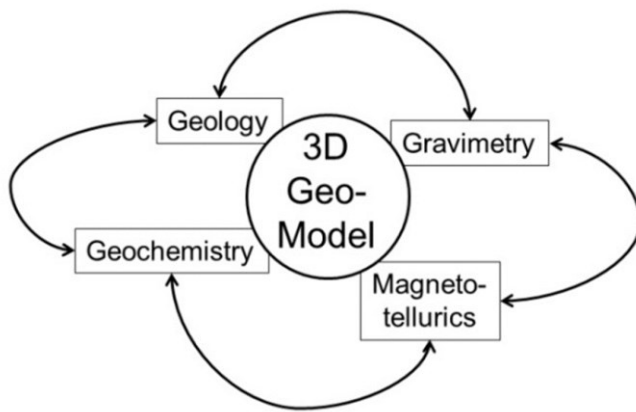


**Figure 2: Example of the integrated platform as a common thread enhancing the cooperation and the interaction of the scientific fields applied. The final model is a co-directed, mutual, shared, and robust interpretation. The methods illustrated here are examples usually involved in geothermal exploration (taken from Calcagno, 2015).**

Consequently, an important pillar of the GEMex ambition was to develop coherent, comprehensive, and reliable 3D geomodels to: (a) gather and place data and information from various disciplines, (b) serve as reference for further computations and simulations, (c) help to understand the geothermal systems. The existing information of the study areas were compiled in an integrated 3D model framework, which served as a reference framework for ongoing works. It was updated as new data and information come in and provided a platform to integrate various project results at different scales (Figure 1).

The main European and Mexican GEMex partners involved in this work were BRGM, CeMIE-Geo, CNR, UMSNH, UNAM, Uni Bari, Uni Roma 3, and Uni Utrecht.

The following chapters present the methodology that was used, the data and results of the integration process, which conducted to an interpretation of the geothermal systems at Los Humeros and Acoculco. Finally, conclusion and perspectives are provided both at the sites scale and at wider angle.

## 2 Methodology

### 2.1 Way of working

One of the main outcomes of constructing a geological model is a coherent interpretation in three dimensions. Merging the data in the same 3D space allows checking and correcting possible inconsistencies. Moreover, being able to visualize and to easily interact with the modelled geological objects is a powerful way of sharing a common view of the geology among a group of persons. The modelling process can then be used as a collaborative platform for exchange and debate, and for agreeing upon the geological interpretation.

Usually, a geomodel cannot be properly constructed by a single person, as such work not only relies on the merging of data, but also on integrating multiple knowledge sources and interpretations. The Los Humeros and Acoculco geomodels thus were constructed as a collaborative effort. Two teams, one dedicated to Los Humeros and the other to Acoculco, were created by scientists from Europe and Mexico. A loop was established through three main steps under the supervision of a referent geologist and a referent geophysicist: (i) data & knowledge, (ii) modelling, (iii) validation. The shapes of the models were discussed at the team level. Then, revised data and knowledge was input in a new loop until the models were fully validated by the partners.

Team members included geologists, volcanologists, structural geologists, geophysicists and modellers; one geologist and one geophysicist, specialists of each area, acted as consultants and advisors for interpretation by each team. The main GEMex partners involved in this work were BRGM, CeMIE-Geo, CNR, Uni Bari, UMSNH, Uni Utrecht, UNAM, ISOR, KIT, GFZ, and Uni Roma 3.

Considering the international mix of scientists in the teams, a critical issue of the collaboration resides in communication. In order to render the collaborative process as efficient as possible, tele-workshops dedicated to working sessions based on interactive exchanges were organized on a regular basis. Furthermore, protocols such as the use of pdf 3D files were set up for exchanging the 3D models, allowing the team members to visualize and check the steps of the construction.

The collaboration was a two-ways process. On the one hand, as described above, the interaction between partners allowed to set up and refine the geomodels. On the other hand, GEMex partners used the geomodels versions at different stages of their evolution to feed their own work and produce their results.

### 2.2 Geomodelling

To construct the geometry of the 3D geomodels, the interpolation of the data was performed using a co-kriging geostatistical method where 3D points located on the geological interface to be modelled and 3D vectors showing the dip of this geological interface are used at the same time (Lajaunie et al., 1997). The result of the interpolation is a 3D scalar potential field where isovalues represent geological interfaces (Figure 3). A geological pile describes the chronological and topological relations between the geological formations. It allows automatic management of the geological boundaries (gradual or erosional). The links between faults and formations are also described in the modelling process, to compute automatically how faults affect formations. When faults interact with each other, they are combined in a fault network for describing their

relations. This methodology is fully described in Calcagno et al. (2008) and implemented in the 3D GeoModeller package<sup>2</sup>.

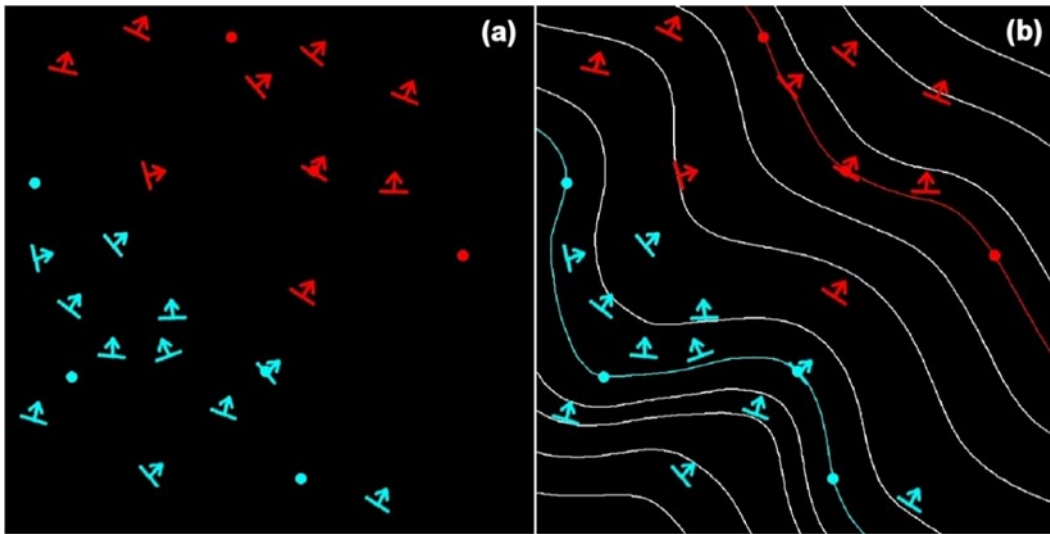


**Figure 3: Interpolation method illustrated for two geological objects, red and blue (see Lajaunie & al., 1997; and Calcagno et al., 2008). (a) Input data for the interpolation: 3D points (location of geological interfaces) and 3D vectors (azimuth and dip of geological structures). (b) 3D potential field interpolation: The geological interfaces are modelled by isovalues of the potential field.**

The geological and geothermal settings of Los Humeros and Acoculco are quite different as described above. The rationale behind the construction of the geological models considered these different contexts. In addition, particular attention was paid to ensure a coherent geological interpretation of both areas, especially when similar geological objects were present in both sites.

---

<sup>2</sup> 3D GeoModeller is a commercial software developed by BRGM and Intrepid Geophysics. For further information, please refer to Calcagno et al. (2008) and Guillen et al. (2008), and visit: <https://www.geomodeller.com>.

## 3 Los Humeros

### 3.1 Geological and geothermal framework

Los Humeros is one of the five geothermal fields currently in operation in Mexico, at an average elevation of 2800 masl. The field has been developed inside the Los Humeros caldera, which is a roughly circular caldera structure of ~18-20 km in diameter, with an inner and younger caldera, known as Los Potreros, with 5-8 km in diameter. The first collapse structure of Los Humeros was formed ~165 ka and the second around 70 ka, according to recent geochronological dates by Carrasco-Núñez et al. (2018). The last volcanic eruption phase occurred between 10 ka and less than 3 ka ago, and it is represented by two extreme volcanic sequences: one is of basic composition ( $\text{SiO}_2 < 55\%$ ) between 7-4 ka, and the other is acidic ( $\text{SiO}_2 > 65\%$ ) with ages of 10-3 ka. According to thermal-barometric modelling, the current heat source could be a differentiated magma chamber, stratified into several smaller pockets located at different depths that probably share the same feeding source located at the lower crust, perhaps up to 30 km depth for the olivine basalts (Lucci et al., 2020).

In Los Humeros, geothermal energy has been exploited since the 1990s by the Comisión Federal de Electricidad (CFE), when the first 5 MW power unit started operating. The current installed capacity in the Los Humeros geothermal field is 94.8 megawatts (MW) composed of three condensing power units of 26.6 MW each, and three back-pressure units of 5 MW each as backup, even though there are another five 5-MW each units out of operation. The power units are fed by approximately 25 production wells, and the residual brine is injected back to the reservoir. Power generation in the field is in the order of 500 gigawatts-hour annually (Gutiérrez-Negrín et al., 2020).

The exploited fluids are of conventional hydrothermal type, contained in the andesites that mainly conform the pre-caldera lithological group. The wells in Los Humeros produce a mixing with more than 85-90% of high-enthalpy steam and 10-15% water, and only one well (H-1 and its successors H-1D and H-49) produces mainly water. It is of sodium-chloride to bicarbonate-sulfate type with high content of boron, ammonia and arsenic. The chemical composition of water varies through time and depends on the depth of the well and the diameter of the production orifice, but it is low-salinity with partial equilibrium at temperatures of 280-310°C (Gutiérrez-Negrín et al., 2020). The geothermal field was chosen for developing the superhot part of the GEMex Project due to the high temperatures already measured in some of the wells (the maximum temperature reached almost 400°C), which indicates the probable presence of these superhot fluids, though they have not been exploited so far.

Geological information from only sixteen wells was available for the preliminary study (Calcagno et al., 2018), and from a total of fifty-six wells for the updated local and integration geomodels. Los Humeros today is a conventional hydrothermal system, with locally superhot fluids underground. The aim of GEMex is to obtain a better understanding of the geothermal field, especially of the location and main features of these superhot fluids and the way to exploit them.

The geothermal target for superhot fluids is assumed to be mostly located in the upper portions of the underlying basement, composed of limestones, mainly granitic intrusive rocks and metamorphic rocks as skarn, marble and hornfels. The deepest parts of the pre-caldera volcanic rocks (mainly hornblende andesites), may host also superhot fluids. In all the cases the permeability is basically secondary due to faults and fractures belonging to the two main structural systems recognized, roughly of NW-SE and NE-SW general orientations.

More information on the geological setting of Los Humeros is available in GEMex D3.2 and GEMex D4.1.

### 3.2 Data and information

A wide range of data and information were used to set up the Los Humeros geomodels. Digital Elevation Model (DEM), geological map and sections, wells, analogue model, geochemistry information, geophysical models were used to constrain the successive versions of the geomodels. Table 3.1 lists the main data and information input in the Los Humeros geomodels, along with their references.

Used for	Data	Reference
Preliminary and updated geomodels	DEM	Instituto Nacional de Estadística y Geografía (INEGI, 2016)
	Geological map	Carrasco-Núñez et al. (2017b)
	Geological cross-sections	Núñez et al. (2017a) and Norini et al. (2015)
	Faults system network	Norini's team GEMex field works
	Wells	CFE
Integrated geomodel	Analogue modelling	GEMex D3.5 and GEMex D3.6
	Regional fault system network	GEMex D4.2
	Geochemistry and hydrology	GEMex D4.3. and GEMex D3.3
	3D resistivity model	GEMex D5.2 and GEMex D5.8
	Seismic structures	GEMex D5.3
	Active seismic lines	GEMex D5.5
	3D gravity model	GEMex D5.6
	Integrated geophysical model	GEMex D5.10
	Results from cross-plotting data integration	GEMex D5.12
	Thermal modelling	GEMex D6.3 and GEMex D6.6

**Table 3.1: List and sources of dataset used for the construction of the Los Humeros geomodels. In the table is specified which data were used for the preliminary and updated geomodels as well as the additional data for the integrated geomodel. Moreover, the source of data is specified with the reference to the GEMex deliverable number when applicable.**

### 3.3 Integration

Constructing the Los Humeros geomodels was a collaborative process supported by many partners of GEMex. This chapter describes the steps followed during this process where three scales were investigated (Figure 1):

- A **local** scale focussing on the Los Humeros geothermal exploitation.
- A **regional** scale fitting the geological map (Carrasco-Núñez, 2017b).
- An **integration** scale shaped by the GEMex Task Force (WP8) mainly based on the extent of the geophysical surveys.

The Los Humeros geomodels were initiated at the very beginning of the GEMex project. Preliminary versions were constructed to give a coherent geological interpretation using the existing state of the art. They were updated using new data acquired in the field until the final integration using geophysical information. Figure 4 presents the main steps of the Los Humeros geomodels that have been produced during the project.

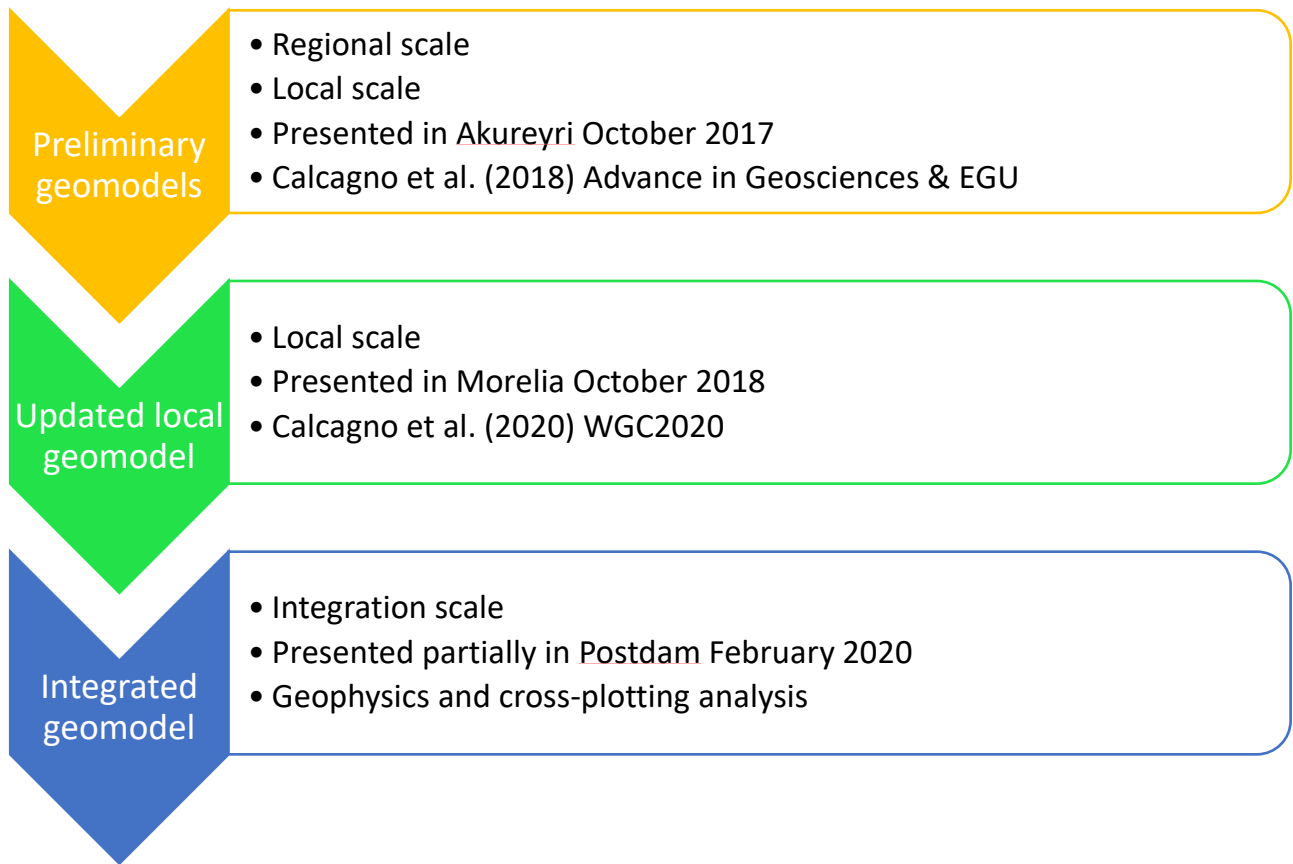


**Figure 4:** The main versions of the Los Humeros geomodels during the GEMex project.

### 3.3.1 Geological piles description

Two ways have been used to describe the underground lithology in Los Humeros, and correlate it with the abundant outcropping lithological units recognized at surface. Thus, the subsurface rocks have been described as groups at the regional and integration scales, and as units at the local scale (see Figure 1). Moreover, the lithology has been described following two approaches regarding the pre-caldera events.

The geological pile gathers lithology arranged in chronological order (see section 2.2). The version 2017 (Figure 5) of the geological pile is the one used to construct the preliminary regional and local 3D geomodels. For more information, see Calcagno et al. (2018).

#### **Version 2017**

Group	Unit	Rock	Age (Ma)
G1 Post-caldera	U1 Undefined pyroclastic	Tuff, pumice and some alluvium	< 0.003
	U2 Post-caldera	Rhyodacite, andesite, basaltic andesite, and olivine basalt lava flows	0.050 to 0.003
G2 Caldera	U3 Los Potreros caldera	Rhyodacitic flows	
		Zaragoza ignimbrite	0,069
	U4 Intermediate caldera	Faby tuff with andesitic-dacitic lava flows	0,07
		Rhyolitic and obsidian domes	0,074
	U5 Los Humeros caldera	Mainly composed of Xaltipan ignimbrite with minor andesitic and rhyolitic lava	0,165
G3 Pre-caldera	U6 Upper pre-caldera	Rhyolite, dacite, some andesite and tuff, and minor basalt	0.693 to 0.155
	U7 Intermediate pre-caldera	Mainly pyroxene andesite (Teziutlán andesite) with mafic andesite in the basal part and/or dacite	2.61 to 1.46
	U8 Basal pre-caldera	Mainly hornblende andesite (Alseseca andesite and Cerro Grande) and subordinate dacite	10.5 to 8.9
G4 Basement	U9 Basement	Middle Miocene granite	15, 12
		Cretacic limestone, shale and minor flint	~140
		Jurassic limestone and shale	~190
		Paleozoic granite and schist (Teziutlán Massif)	>251

Figure 5: Geological description, version 2017 (excerpt from Calcagno et al., 2018).

### Version 2018

By suggestion of WP6 researchers and CFE's geologists, it was decided to include a package of rocks of mainly pyroclastic origin within the Group G3, which the CFE identified in the lithological columns of its wells as lithic, vitreous or crystalline tuffs (Tobas Líticas, Tobas Vítreas, Tobas Cristalinas), among other denominations, which are usually located between the upper pyroxene andesites (AP) and the lower hornblende andesites (AH), see Figure 6. Although this pyroclastic unit does not have an outcropping unit to whom it can be correlated, and even it is uncertain that it is composed of pyroclastic rocks, it has been included in the model because its petrophysical properties are in any case different of the andesitic package.

Group	Unit	Rock	Age (Ma)
G1 Post-caldera	U1 Undefined pyroclastic	Tuff, pumice and some alluvium	< 0.003
	U2 Post-caldera	Rhyodacite, andesite, basaltic andesite, and olivine basalt lava flows	0.050 to 0.003
G2 Caldera	U3 Los Potreros caldera	Rhyodacitic flows	
		Zaragoza ignimbrite	0,069
	U4 Intermediate caldera	Faby tuff with andesitic-dacitic lava flows	0,07
		Rhyolitic and obsidian domes	0,074
	U5 Los Humeros caldera	Mainly composed of Xaltipan ignimbrite with minor andesitic and rhyolitic lava	0,165
G3 Pre-caldera	U-6 (AP) Upper pre-caldera volcanism	Pyroxene andesites (Teziutlán Andesites) with mafic andesites in the basal part and/or dacites	1.46-2.61
	U-7 (TV) Pyroclastic Rocks	Lithic, crystalline and vitreous tuffs identified in most of the wells, with no correlation with any outcropping unit	2.62-8.8
	U-8 (AH) Basal pre-caldera volcanism	Hornblende andesites (Alseseca Andesites & Cerro Grande), and dacites	8.9-10.5
G4 Basement	U9 Basement	Middle Miocene granite	15,12
		Cretacic limestone, shale and minor flint	~140
		Jurassic limestone and shale	~190
		Paleozoic granite and schist (Teziutlán Massif)	>251

**Figure 6: Geological description, version 2018. The three units of G3 are different from the version 2017 (see Figure 5).**

The geological pile description presented in Figure 6 is the one used to construct the updated local 3D geomodel. For more information, see the Calcagno et al. (2020).

### 3.3.2 Wells computation and description

Sixteen wells were provided by the CFE for the preliminary phase. The number of wells was increased to fifty-six for the update and integration phases. They have been used to constrain the 3D geomodels of the area.

On the one hand, wells have been described at the regional scale using geological groups. On the other hand, they have been described at the local scale using geological units. In addition, at the local scale, the units of Group 3 have been described in two ways (see section 3.3.1). That is why three descriptions are available for the same set of wells.

The geometry of the wells has been computed using the deviation data from the CFE. The objective was to transform the information on deviations provided by CFE into survey data to define the actual geometry of every well (Figure 7).

Deviation data					Survey data		
	X	Y	Depth (m)		Dip	Azimuth	Length
H-1D	661 906	2 175 064	0	→	90	0	100
H-1D	661 906	2 175 064	100		90	0	200
H-1D	661 906	2 175 064	200		90	0	300
H-1D	661 906	2 175 064	300		90	0	400
H-1D	661 906	2 175 064	400		90	0	500
H-1D	661 906	2 175 064	500		90	0	600
H-1D	661 906	2 175 064	600		90	0	700
H-1D	661 906	2 175 064	700		90	0	800
H-1D	661 906	2 175 064	800		90	0	900
H-1D	661 906	2 175 064	900		90	0	900
H-1D	661 900	2 175 065	1000		86.5618125	-84.005888	1000.18032
H-1D	661 889	2 175 062	1100		83.3578644	257.587528	1100.85606
H-1D	661 875	2 175 059	1200		82.031248	257.406434	1201.83109
H-1D	661 860	2 175 056	1300		81.0843907	258.826659	1303.0541
H-1D	661 845	2 175 054	1400		81.7593663	260.411787	1404.09739
H-1D	661 834	2 175 049	1500		82.9843761	247.618793	1504.85175
H-1D	661 822	2 175 045	1600		83.0105838	249.144332	1605.60044
H-1D	661 810	2 175 040	1700		82.4404021	250.479483	1706.47721
H-1D	661 796	2 175 035	1800		81.5136506	251.383374	1807.58423

Figure 7: The deviation data from CFE (left hand side) are transformed in survey data (right hand side).

The computation process that has been used is presented in Figure 8, with a focus on the Azimuth angle calculation in Figure 9.

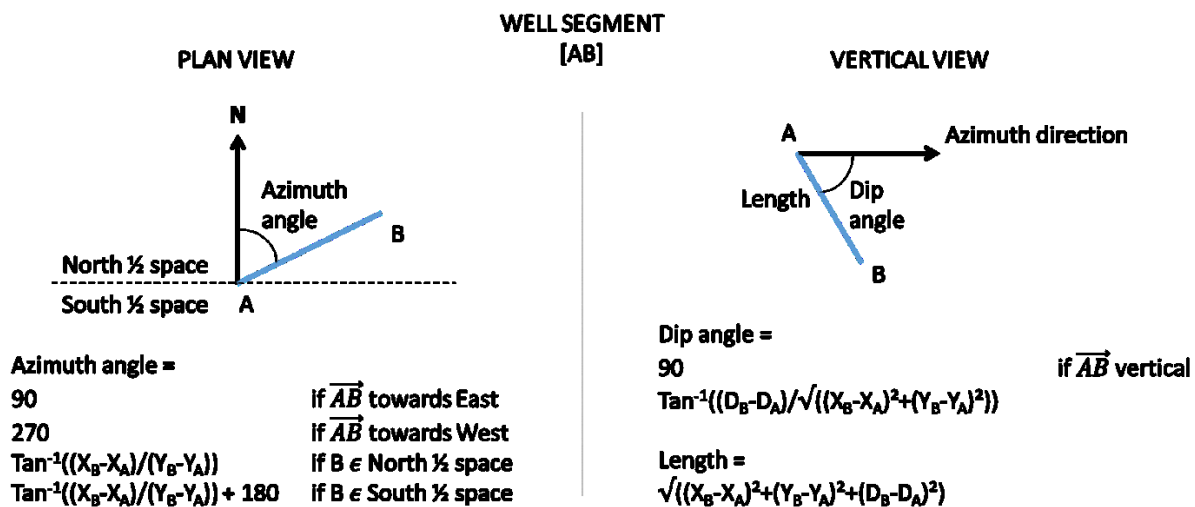
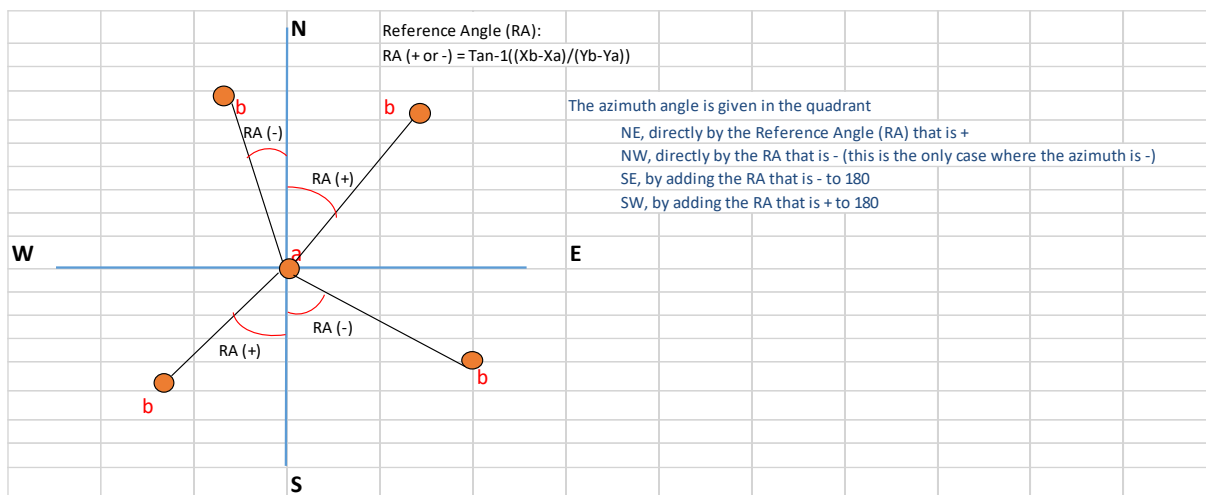


Figure 8: Process to compute well deviation.



**Figure 9: Deviated wells computation. Focus on the Azimuth angle calculation.**

The following files are located on the Virtual Research Environment of GEMex in the folder “202002\_LosHumeros\_WellsDescription\_2019update” at <https://data.d4science.net/nZcR> (Workspace > VRE Folders > CFE\_DATA).

They are related to the 2017 and 2018 versions of the geological descriptions (respectively Figure 5 and Figure 6). The local (9 units) and regional (4 groups) descriptions have been updated thanks to the improvement of 3D geomodels in 2019.

GEMex\_LH\_Wells\_Description\_Local\_2017

- GEMex\_LH\_Wells\_Description\_Local\_2017\_collar\_20181212.csv
- GEMex\_LH\_Wells\_Description\_Local\_2017\_survey\_20181212.csv
- GEMex\_LH\_Wells\_Description\_Local\_2017\_geology\_20181212.csv

GEMex\_LH\_Wells\_Description\_Regional\_2017\_2019update

- GEMex\_LH\_Wells\_Description\_Regional\_2017\_2019update\_collar\_20190618.csv
- GEMex\_LH\_Wells\_Description\_Regional\_2017\_2019update\_survey\_20190618.csv
- GEMex\_LH\_Wells\_Description\_Regional\_2017\_2019update\_geology\_20190618.csv

GEMex\_LH\_Wells\_Description\_Local\_2018\_2019update

- GEMex\_LH\_Wells\_Description\_Local\_2018\_2019update\_collar\_20191011.csv
- GEMex\_LH\_Wells\_Description\_Local\_2018\_2019update\_survey\_20191011.csv
- GEMex\_LH\_Wells\_Description\_Local\_2018\_2019update\_geology\_20191011.csv

### 3.3.3 Preliminary geomodels

The Los Humeros preliminary regional and local geomodels are fully described in Calcagno et al. (2018). They are available on the VRE at: <https://data.d4science.net/NA8B>. Each one comes with:

- Metadata sheet for more information
- GeoModeller files
- PDF3D file
- TSurf files

The geological map from Carrasco-Núñez et al. (2017b) and the two geological sections from Carrasco-Núñez et al. (2017a) and Norini et al. (2015) were the main references to set up the geomodels. In addition, the Comisión Federal de Electricidad (CFE) provided geological description of sixteen wells. Considering the lack of information available on their geometry, the wells were considered as vertical.

A selection of the main faults to be modelled at the regional and local scales was done. They all have a maximum extension of four kilometres (below ground level) corresponding to the interpretation of the brittle-ductile transition. For the modelling process, the geological formations were described as four groups and nine units, respectively at the regional and the local scales, using the version 2017 of the geological piles description (Figure 5).

The Digital Elevation Model (DEM) was provided by INEGI (Instituto Nacional de Estadística y Geografía).

### Regional model

Los Humeros regional geomodel is available on the VRE at: <https://data.d4science.net/NA8B>.

The geomodel at regional scale (56 km x 36 km x 12 km, i.e. down to 7 km b.s.l.) presents four geological groups: basement, pre-caldera rocks, rocks from the caldera, post-caldera rocks (version 2017, Figure 5). The geological map (Carrasco-Núñez, 2017b) and sections (Carrasco-Núñez et al., 2017a; Norini et al., 2015) were re-interpreted accordingly. The geological description of the wells made it possible to match all the information with the four groups selected for the modelling of the regional model.

Eleven complementary cross sections were used to constrain the regional model. They were drawn according to the two references cross-sections cited above to ensure a coherent interpretation, for instance in terms of geological formations thickness. The regional geomodel is presented on Figure 10.

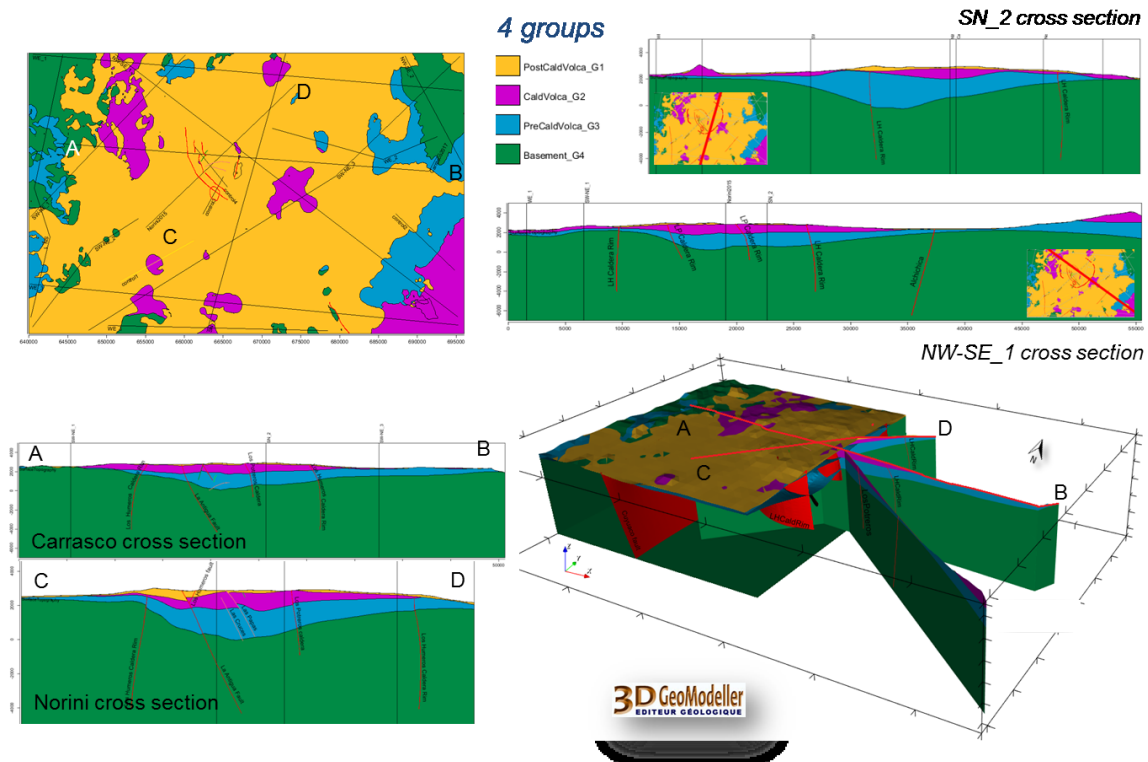


**Figure 10:** The Los Humeros regional geomodel of the four geological groups (see Figure 5). Coordinate system is WGS84/UTM zone 14N.

## Local model

Los Humeros local geomodel is available on the VRE at: <https://data.d4science.net/NA8B>.

The GeoModel at local scale (9.5 km x 12.5 km x 12 km, i.e. down to 7 km b.s.l.) presents nine units (version 2017, Figure 5). The geological map (Carrasco-Núñez et al., 2017b) and geological cross sections (Carrasco-Núñez et al., 2017a; Norini et al., 2015) have been re-interpreted accordingly. It was not possible to match the wells' description with the nine units for three of them among the sixteen wells available.

One complementary cross section was used to constrain the local model. The local geomodel is presented on Figure 11.

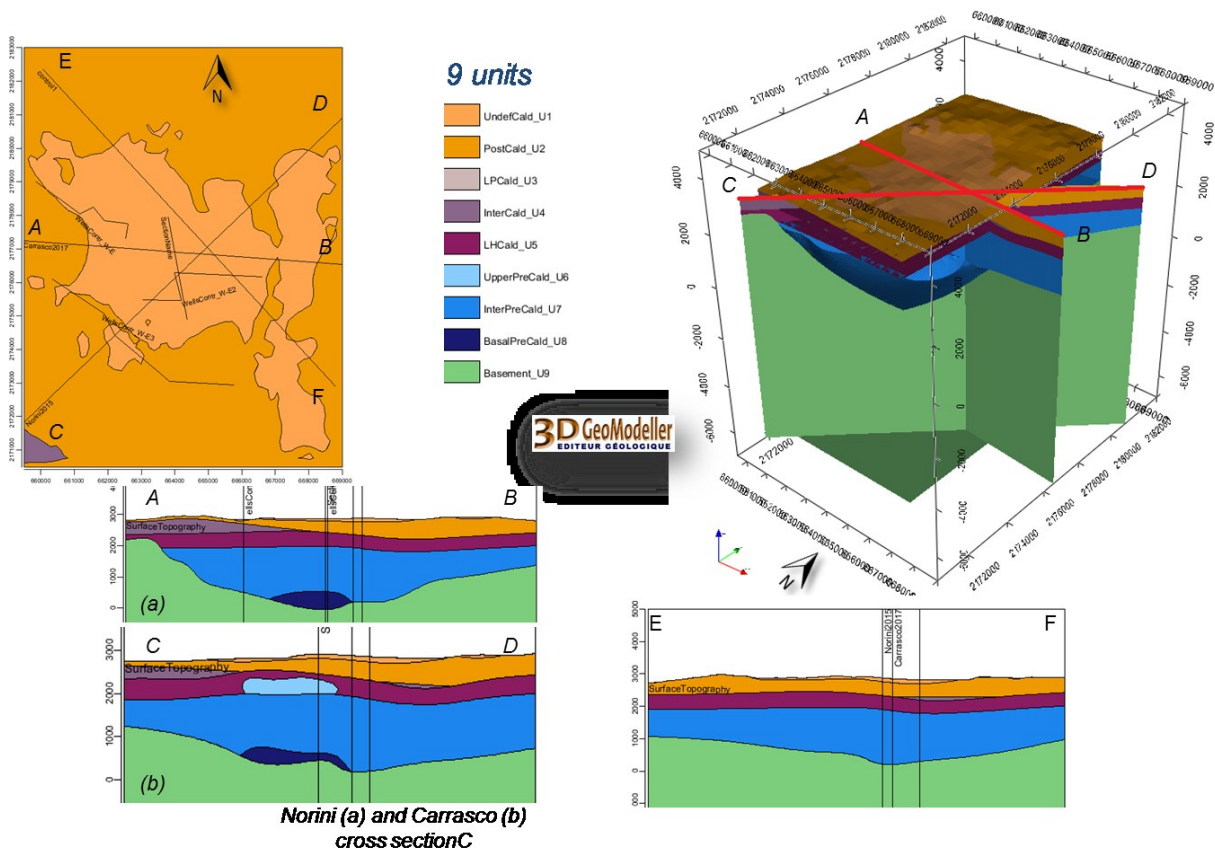


Figure 11: The Los Humeros local geomodel of the nine geological units (see Figure 5). Coordinate system is WGS84/UTM zone 14N.

### 3.3.4 Local geomodel update

The Los Humeros updated local geomodel is fully described in Calcagno et al. (2020). It is available on the VRE at: <https://data.d4science.net/kvqX>. It comes with:

- Metadata sheet for more information
- GeoModeller files
- PDF3D file
- Tsurf files
- VTK files

The update started with the refinement of the faults at local scale. They were updated after new fieldwork, mainly done by Norini's team in 2018 (Figure 12). The updated Los Humeros local fault model is available on the VRE: <https://data.d4science.net/qotN>.

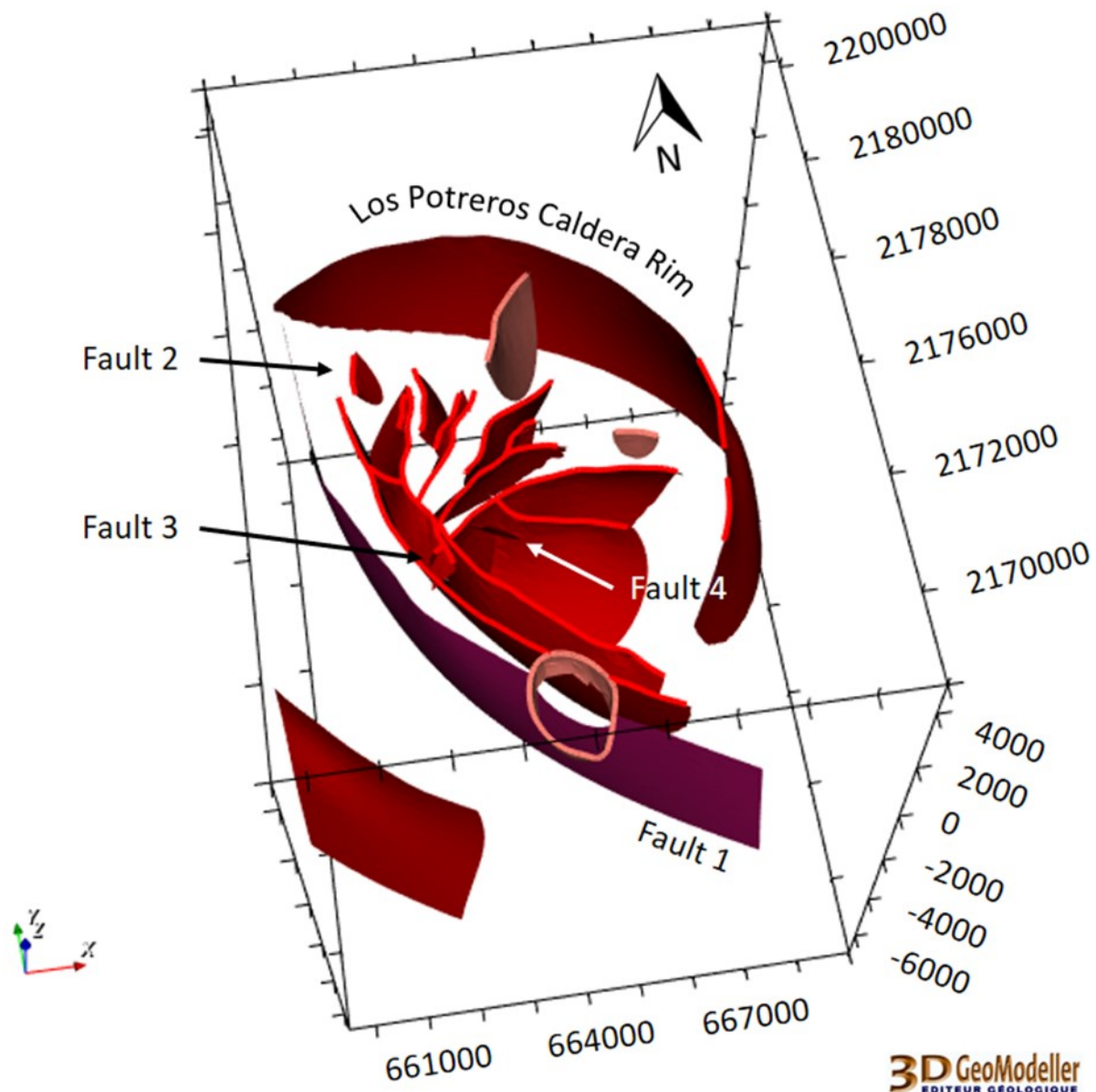


**Figure 12:** New fieldwork data led to the update of almost all the faults of the local model of Los Humeros and to the addition of Fault 1 to Fault 4. Coordinate system is WGS84/UTM zone 14N (after Calcagno et al., 2020).

In a second phase, the geological units were refined at local scale. This step is mainly based on a new description of the nine-units geological pile (version 2018, Figure 6) and on forty more wells from the CFE. A total of fifty-six wells were used to update the Los Humeros local area (Figure 13). The wells were provided especially via two models (geological and geophysical) existing before GEMex started. These models were analysed by the T3.1 team (Bär, 2017 and Bär, 2018). On top of that, the geometry of the wells was set up to take into account the deviation parameters given by CFE, see Figure 13 and section 3.3.2.

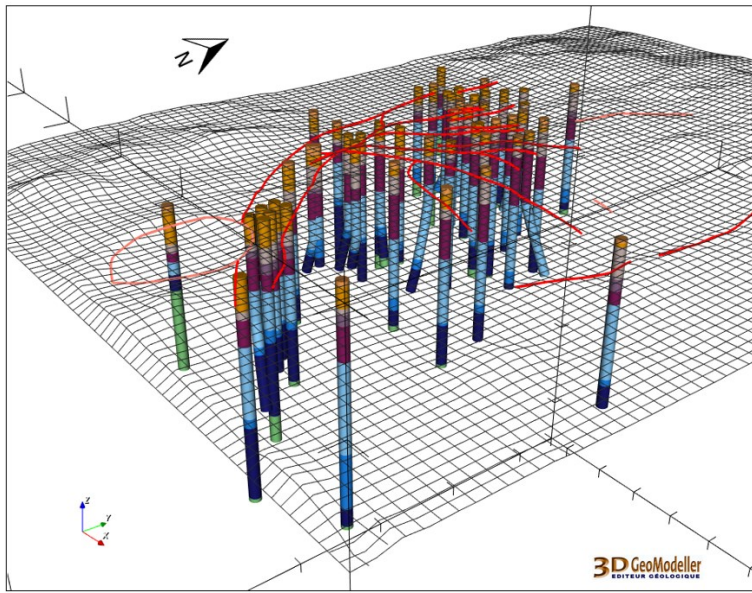


**Figure 13:** Fifty-six wells were used for the update of the Los Humeros local model. Ten of them are deviated. They are described according to the 2018 geological pile description presented in Figure 6. DEM is displayed as a grid including the fault network traces (see Figure 12). View from SE.

The updated geomodel at local scale is presented in Figure 14.

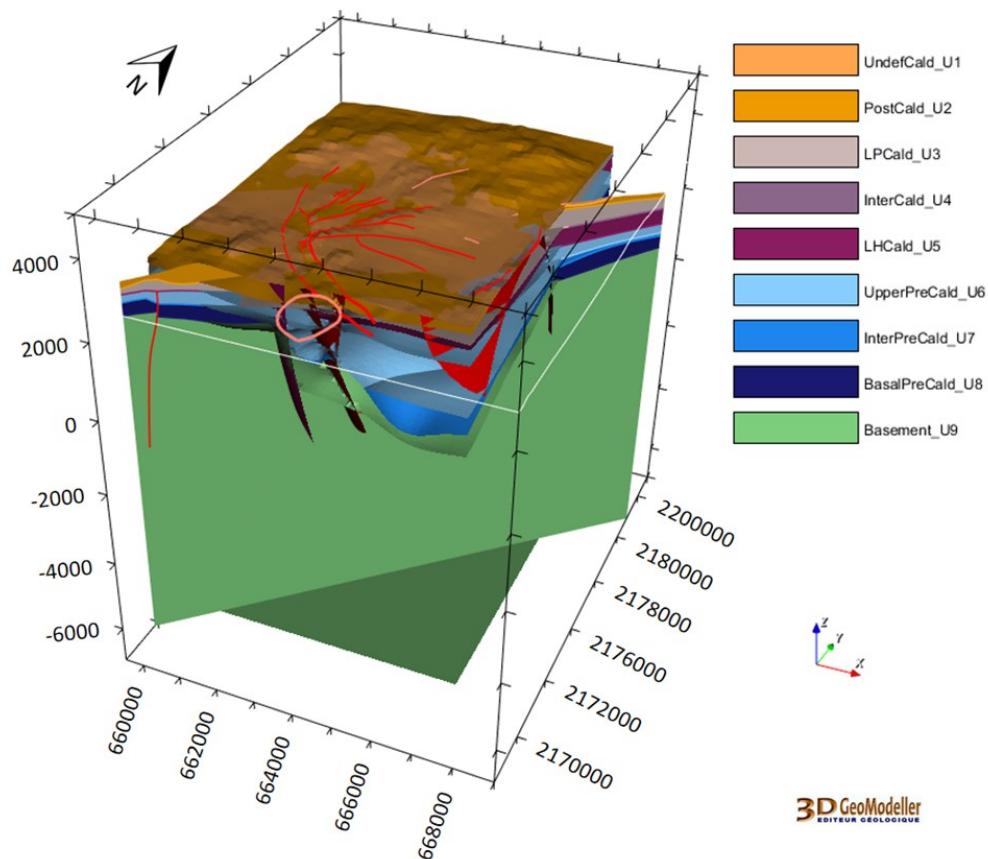


**Figure 14:** The 3D geomodel of Los Humeros updated at the local scale for the nine geological units (see Figure 6). It includes the updated faults (Figure 12) and fifty-six wells (Figure 13). Coordinate system is WGS84/UTM zone 14N (after Calcagno et al., 2020).

### 3.3.5 Volcanic lineaments

In order to obtain information on the existence of regional structures in the Los Humeros geothermal area, the T3.1 team used an approach based on the alignment of monogenetic volcanoes, which are considered as the surficial expression of deep magma feeding fracture systems. The criteria adopted were proposed by Paulsen and Wilson (2010) and Lesti et al. (2008). Paulsen and Wilson (2010) and are listed in Figure 15.

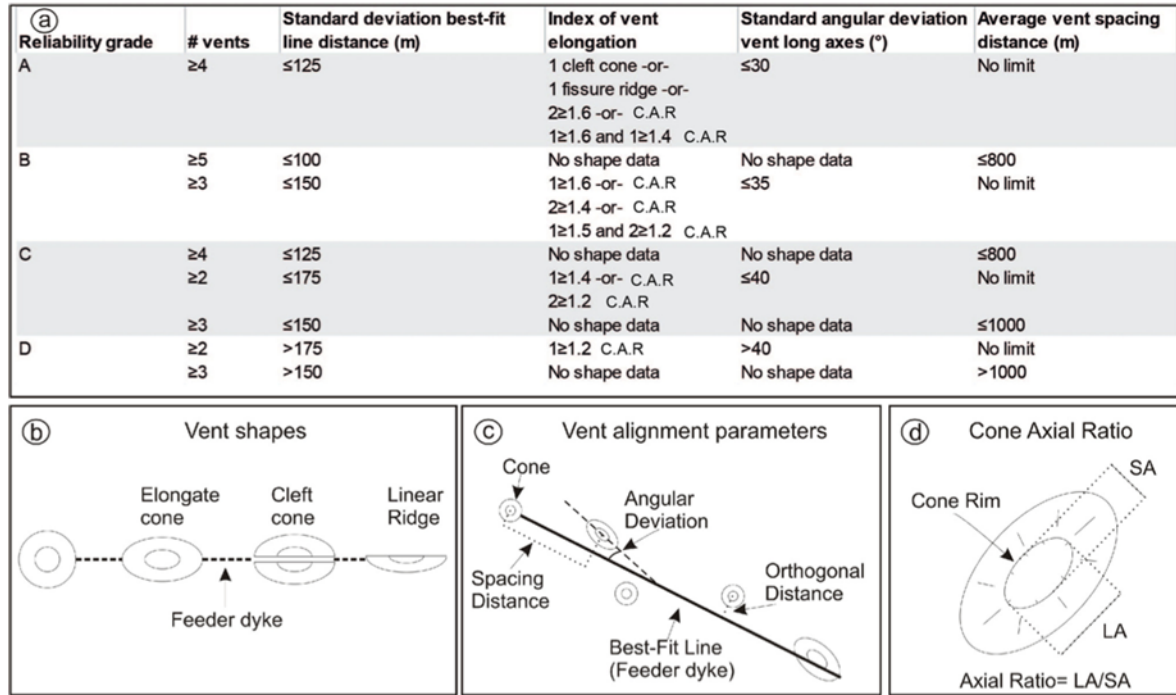


**Figure 15: Criteria used for estimating the tectonic control on volcanic alignments (after Paulsen and Wilson, 2010, with modifications in Olvera Garcia et al., 2019); (a) Reliability criteria for assessment the vent alignments. The number of vents, the orthogonal distances of the volcanic center from the best-fit line (standard deviation), the values of elongate vents (index of elongation- see b and d), the angular deviation of elongate volcanic long axes from the trend of the best-fit line and the spacing distance between vents are used to assess the reliability of alignments. C.A.R = Crater Axial Ratio; (b) Morphology of vent shapes from circular to elongated as a consequence of deformation; (c) Parameters of alignment and volcanic vents as listed in a; (d) Axial ratio describing ellipticity of a volcanic vent (index of elongation).**

After having determined the location of the monogenetic volcanoes in the caldera and surrounding areas (Figure 16) by integrating existing (GEMex D4.1) and new data, the reliability of the alignments was evaluated. The results are given in Table 3.2 while the number of alignments is labelled in Figure 17. On the basis of the ranking of the morphological features, the trend of the eruptive fractures was therefore derived (Figure 17). Almost half (7 over 15) of the considered alignments is classified in the higher ranks (A and B). Their length is comprised between 4 and 16 km, thus suggesting their importance at regional scale.

Two main trends are highlighted, NNW and NE-oriented respectively, both in the surroundings of the caldera (i.e. Perote plain) and in delimiting the caldera rim.

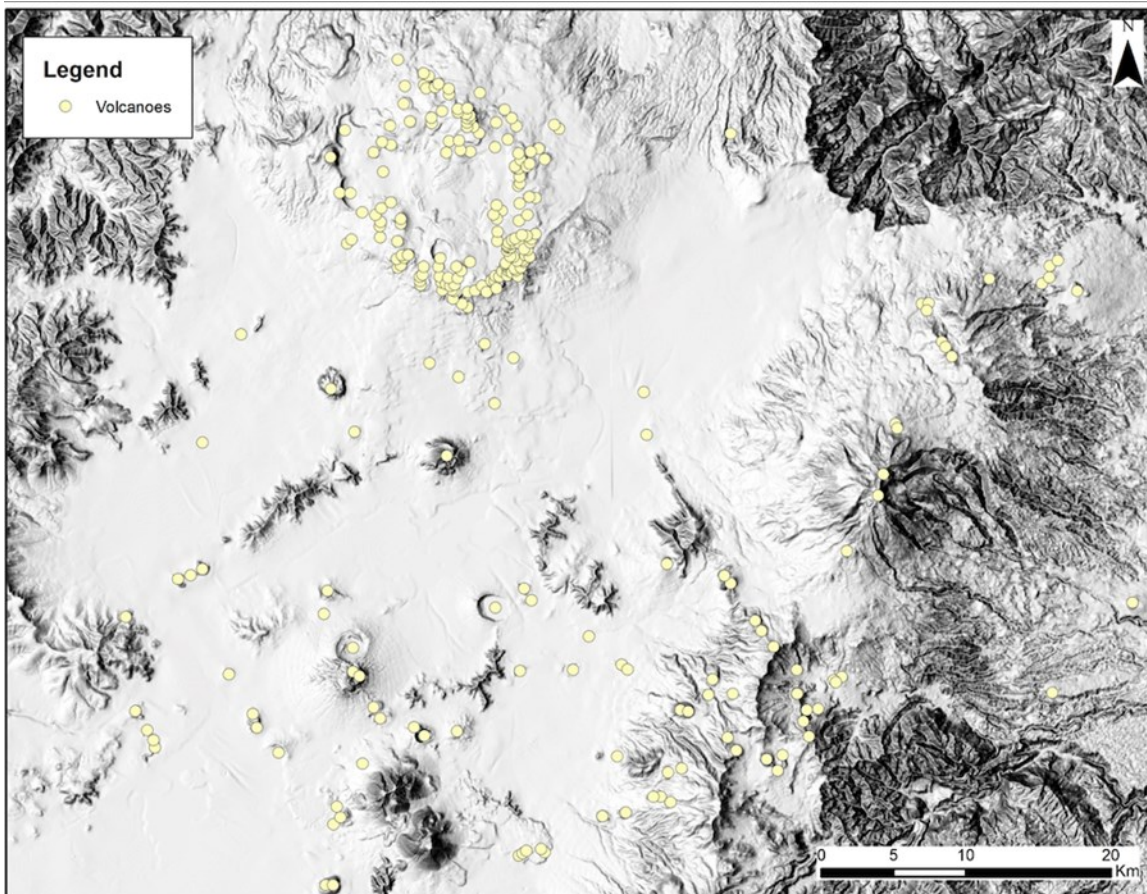


**Figure 16:** Yellow points indicate the location of the monogenic volcanoes considered in the computation as proposed by Paulsen and Wilson (2010).

Number of the vent alignment	Alignment grade	Length (km)	# vents	Linear ridge (LR), Cleft cone (CC), Ellipse cone (EC)	Standard deviation (m)	Average vent spacing distance (km)	Standard angular deviation (°)	Alignment azimuth (°)
1	A	16,15	9	4 EC	61	2,05	85	314
2	A	9,62	8	2	81	1,37	20	309
3	D	12,7	4	1	228	4,1	0	326
4	C	9,7	7	1	183	1,5	6	336
5	A	4,2	5	1 LR	57	1,1	0	330
6	B	22	8	2 LR	136	3,1	0	329
7	D	21,6	11	2 LR 1 EC	194	2,1	10	305
8	C	1,4	3		94	0,6		316
9	C	2,8	4		52	0,9		328
10	A	4,4	13	2 LR	87	0,2	15	64
11	D	1,9	4		243	0,6		46
12	C	1,79	3		53	0,8		63
13	C	4,8	3		30	2,3		77
14	C	1	4		23	0,3		63
15	C	0,6	3		5	0,05		56

**Table 3.2:** Table summarizing the computation provided about the alignments. See also Figure 17 for the numbering of the vent alignments.

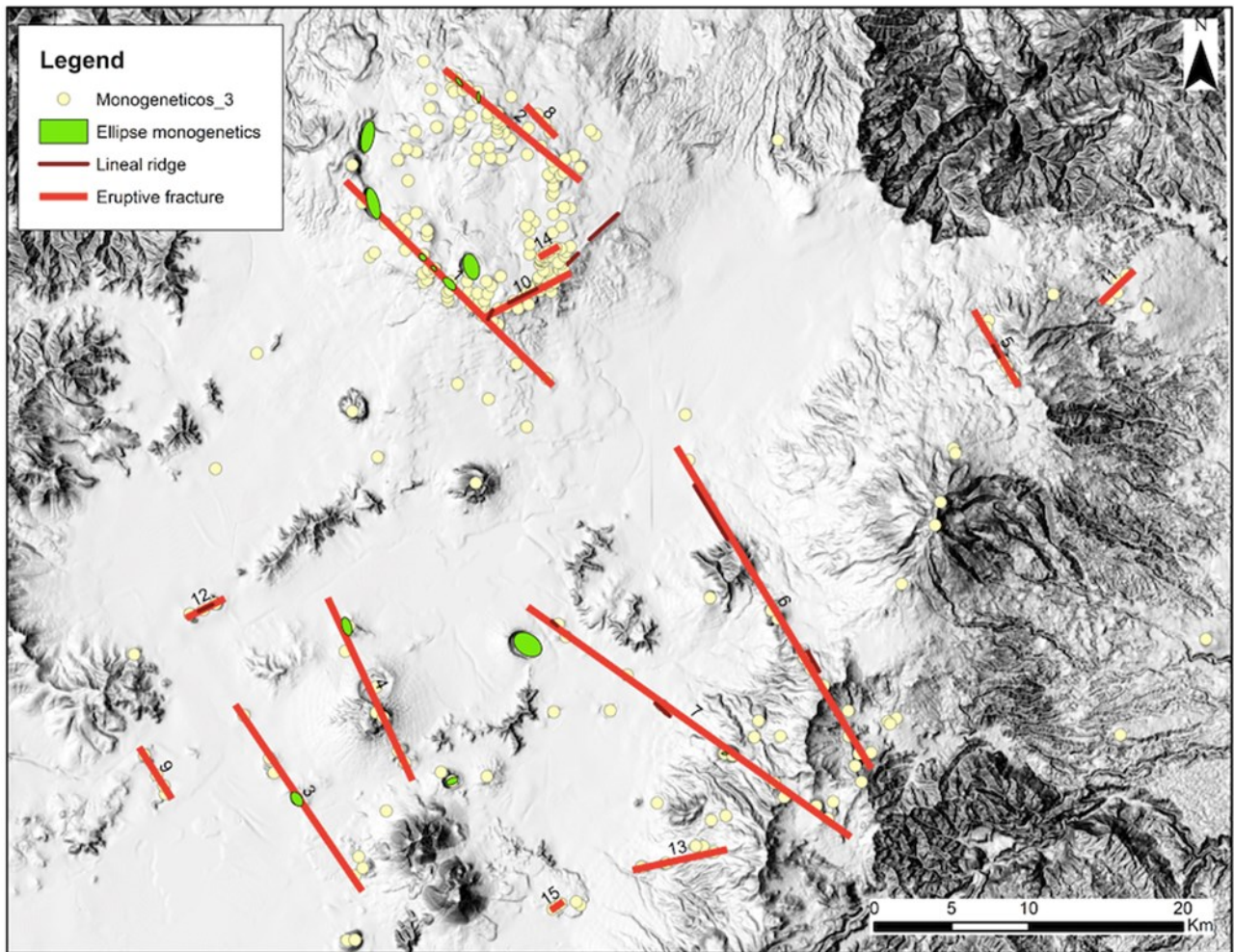


**Figure 17:** Location of the monogenetic vents and ellipse shapes of the volcano centers used for the evaluation of the parameters given in Table 3.2. The eruptive fractures are interpreted on the basis of the volcanic morphological features (see Figure 15) and the values from the linear ridge results.

The second methodology (Lesti et al., 2008) is based on indicating the density of monogenetic volcanoes by iso-lines, delimiting areas. This approach was applied to the regional (Figure 18) and to the Caldera scales (Figure 19). The results confirm the indications obtained from the above mentioned evaluation.

In particular, in addition to what already indicated in Figure 17, the study about the caldera area highlights an ENE-oriented lineament cross cutting the western border of the caldera, and minor fracture systems almost N-S oriented. Assuming these lineaments have the meaning of magma feeding fractures (Figure 20), a system of fault zones affecting the caldera is therefore reported. We assumed a simplified version of this fault-system, for the 3D model.

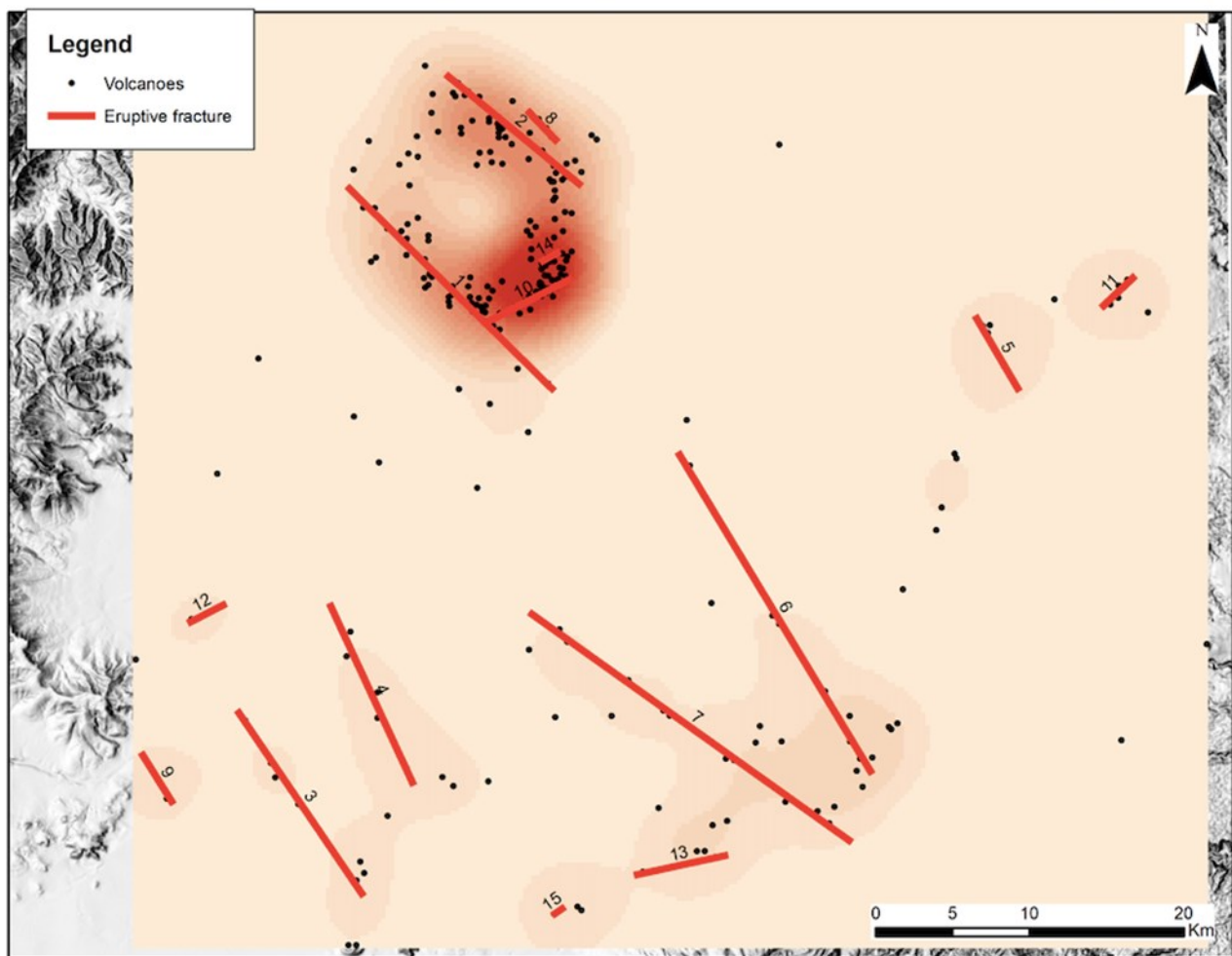


**Figure 18:** Map illustrating the areal density of monogenic volcanoes (black dots) after Lesti et al. (2008). The red lines are the fault traces as derived applying the methodology proposed by Paulsen and Wilson (2010).

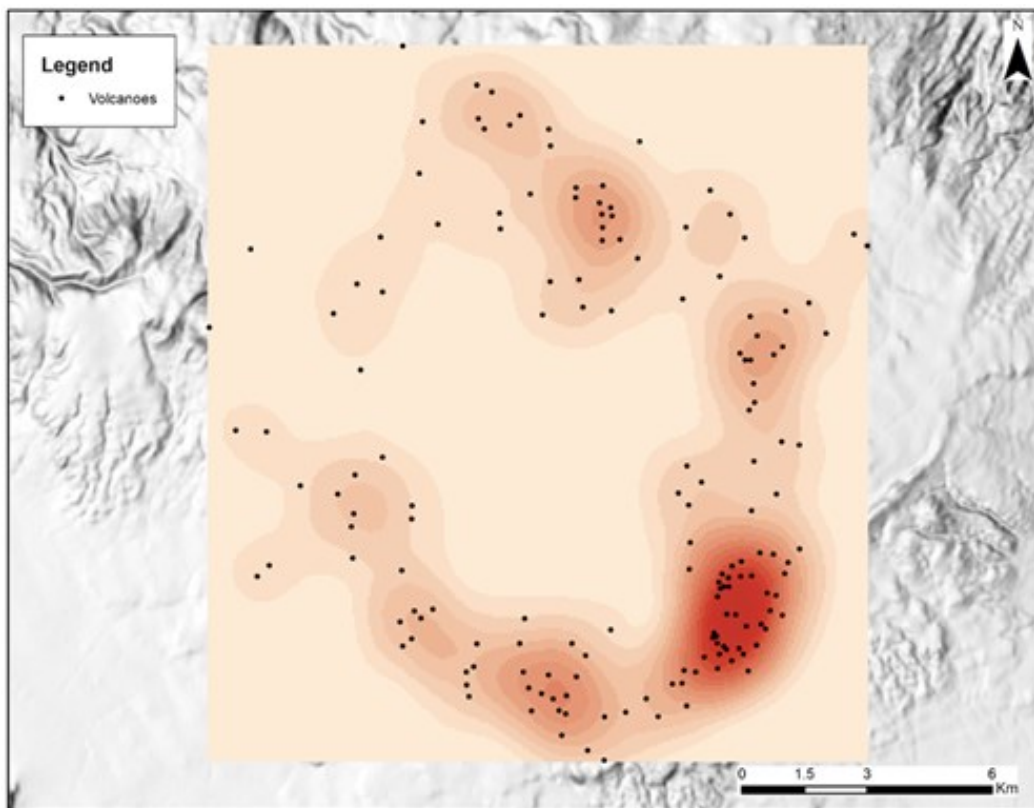


Figure 19: Location of the monogenetic vents (black dots) and isolines delimiting areas with equal density of volcanic vents.

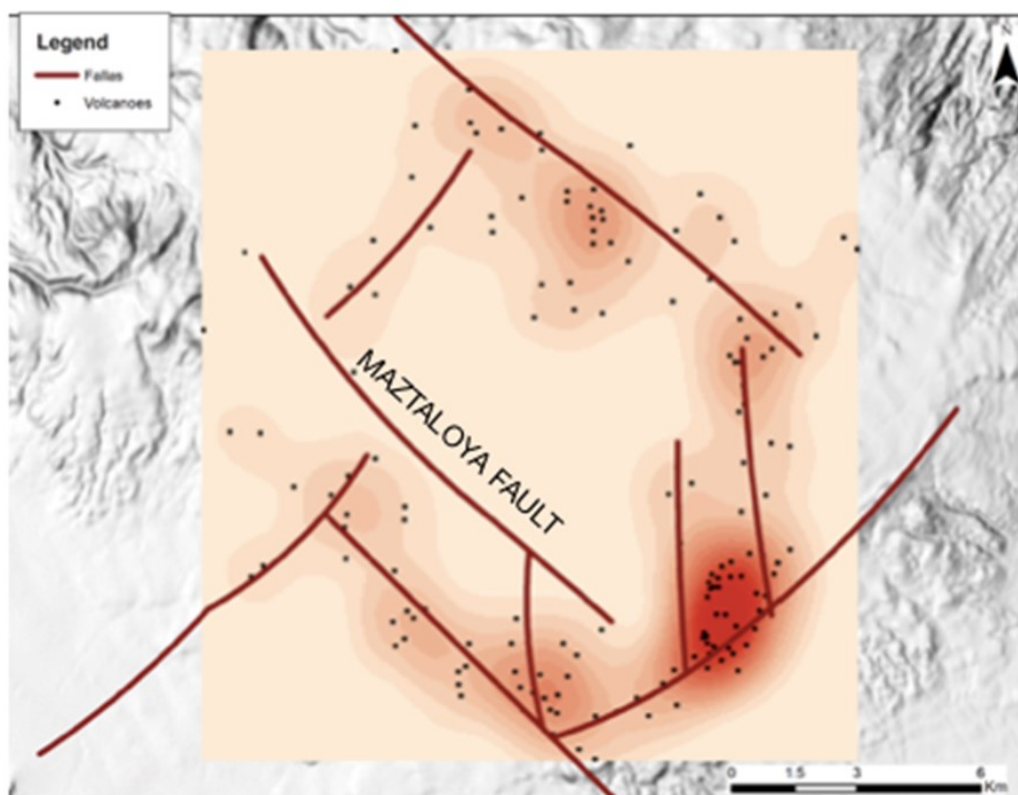
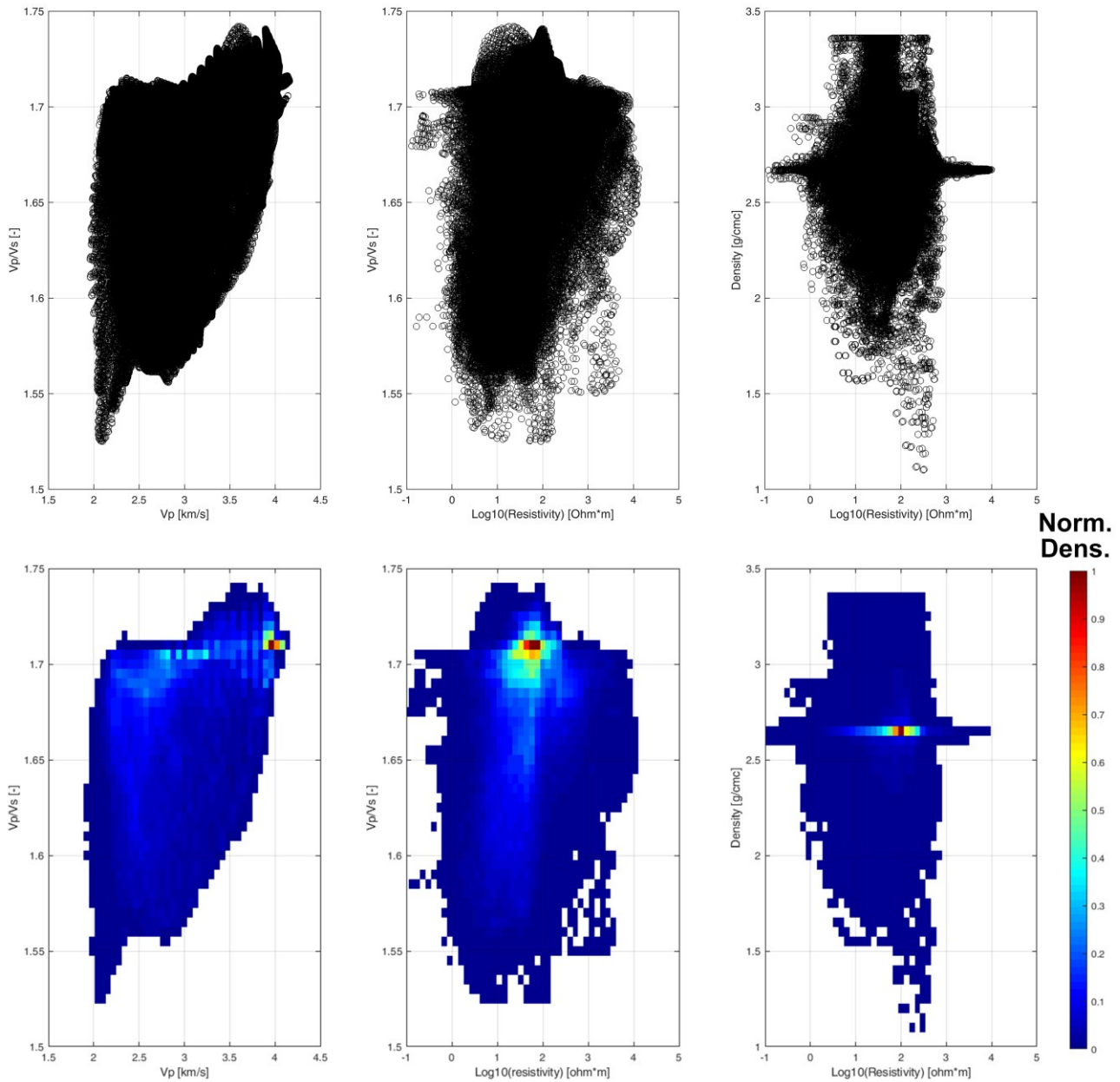


Figure 20: Interpretation in terms of fault-zones channelling magma to surface. The Maztaloya fault is also indicated as a reference.

### 3.3.6 Cluster analysis

Each single petrophysical parameter retrieved from geophysical surveys provided important relations with lithology, geological structures, fluid saturation and phase as well as underground physical conditions. An effective integration of the available geophysical data allowed an unambiguous, self-constrained characterization of the geothermal system. This has been attained by the development of different clustering procedures capable to identify patterns on the density distribution of cross-plotted data (Figure 21). We performed the cluster analysis by exploiting the available resistivity (GEMex D5.2 and GEMex D5.8), density (GEMex D5.6 and Carrillo et al., 2020), magnetization (Carrillo et al., 2020) and seismic-waves velocity (GEMex D5.3) models. The methodology and the results are presented in (GEMex D5.12). The clusters highlighted the principal geophysical features previously recognized by the joint visualization of the data (GEMex D5.10) in the Paraview platform.



**Figure 21: Cross plots (upper) and normalized density plots (lower) of selected couples of geophysical datasets. The patterns of the relations  $V_p$ - $V_p/V_s$ , the Resistivity- $V_p/V_s$  and the Resistivity-Density are displayed.**

We upgraded the cluster analyses employing the latest release of the geophysical datasets, in particular exploiting the new density and seismic velocity models. The new velocity model includes the Vp and Vp/Vs information, and the resolution parameters for each cell volume. In this new analysis we took advantage of the Spread parameter. The higher the value, more inversion artefacts there could be. Avoiding cells with a Spread  $> 3$ , we limited our analyses to a more constrained volume. On the other hand, we investigated a smaller volume extending in depth to about 3 km below ground level (0 m a.s.l.). Few output examples of the clustering are displayed in Figure 22.

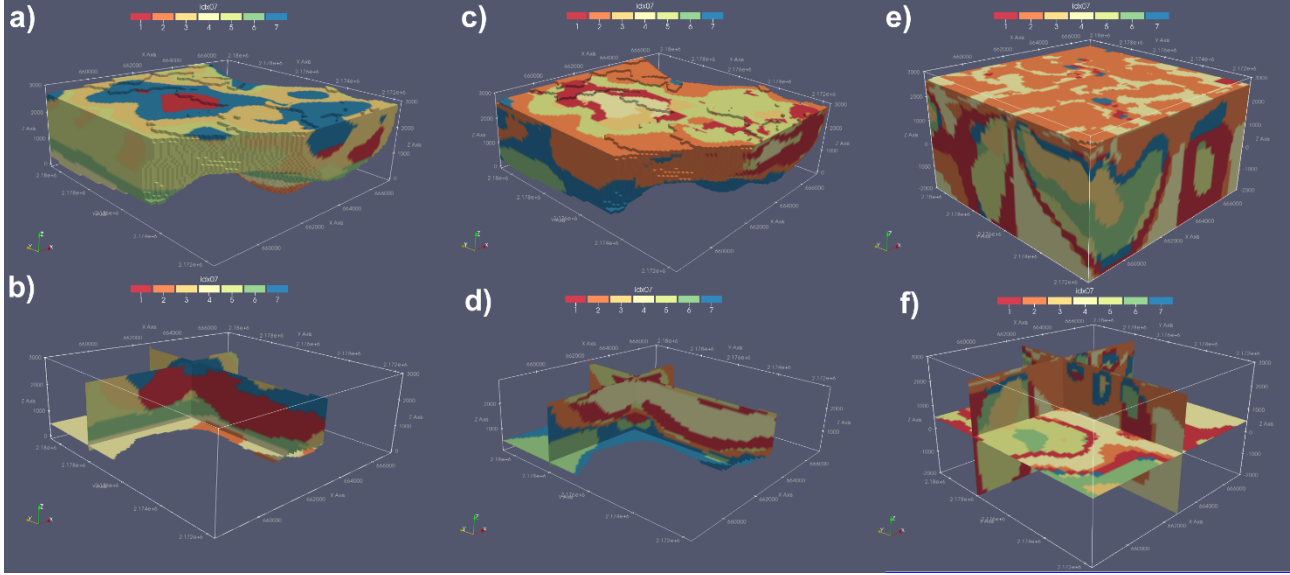


**Figure 22: 3D visualization of the cluster volumes (a, c and e) and cluster distributions along selected cross-sections (b, d and f) exploiting the Vp-Vp/Vs (a and b), Resistivity-Vp/Vs (c and d) and Resistivity-Density (e and f) datasets. The results refer to the unsupervised Gaussian Mixture Model method with seven clusters.**

The cluster methodology and results, reported in GEMex D.5.12 and mentioned above permitted to group different interval of geophysical values (Figure 23), in order to highlight volume of rocks where parameters indicate the same geological interpretation in terms of compatibility with the occurrence of geothermal fluids.

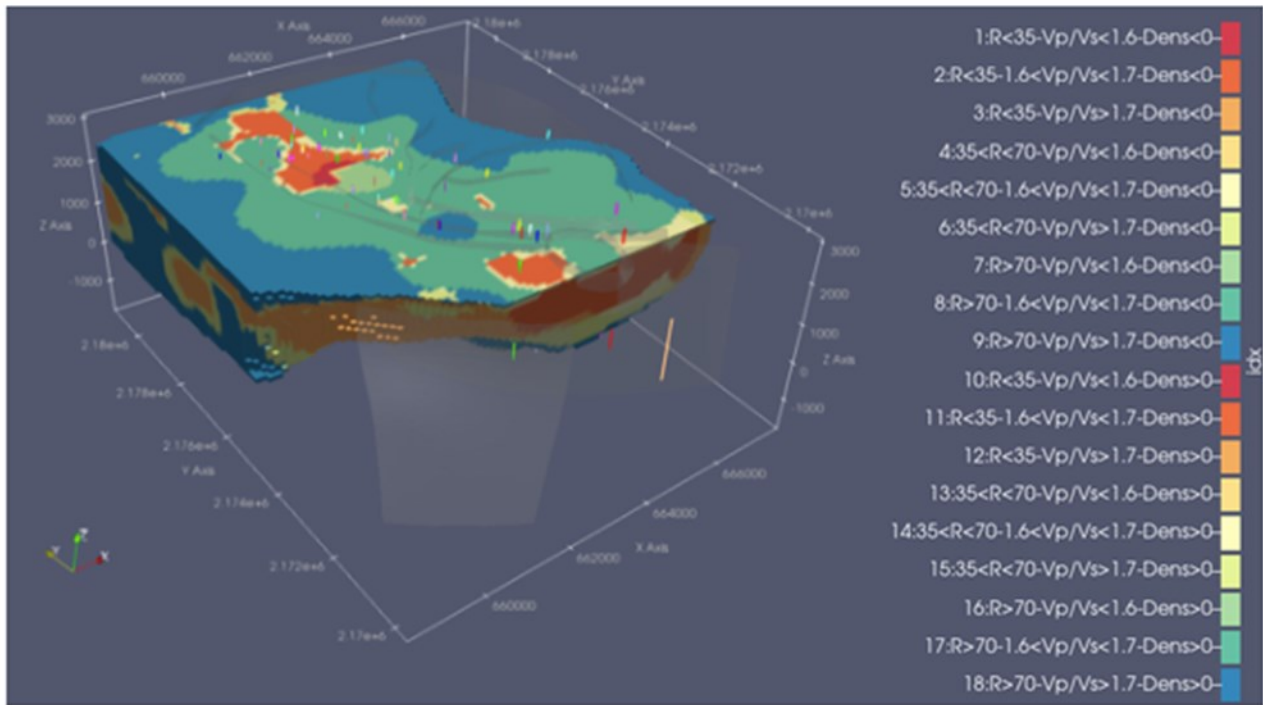


**Figure 23: 3D model illustrating the distribution of the geophysical data by means of the cluster supervised methodology. Considered intervals are listed on the right side of the figure. See GEMex D5.12 for more information on the adopted methodology. North is indicated by the Y-axis. The well path are displayed.**

In this regard, the class corresponding to low resistivity values ( $< 70 \Omega m$ ), high  $Vp/Vs$  ratio ( $> 1.7$ ) and low density contrast ( $< 0$ ) is deemed of interest.

Apart from superficial levels where the hydrothermal alteration influences the low resistivity values, the above mentioned conditions were contemporaneously recorded in few rock volumes, at about the sea level depth. Here, P and T values are supposed to indicate conditions for the presence of super-hot fluids, expected at about 4 km depth, based on the results of the study of the analogue exhumed geothermal system of Las Minas (GEMex D4.1).

Hence, we obtained three slices from the 3D model sections (Figure 24), in order to highlight parts where the mentioned geophysical parameters are favourable to the occurrence of geothermal fluids, although it should be kept in mind that the basal limit of the 3D cluster model was fixed at the sea level (about 3 km below surface), as a consequence of the procedure of acquisition of some geophysical data.

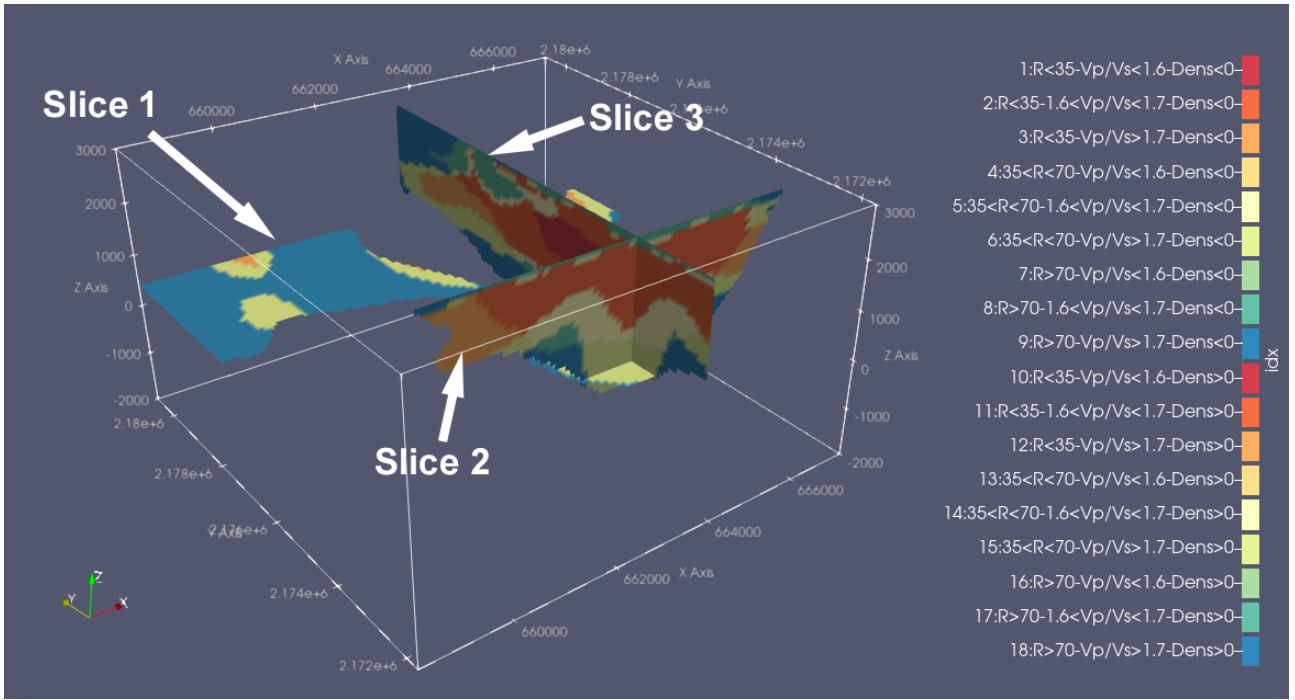


**Figure 24:** Horizontal (slice 1 at 400 m a.s.l), E-W and N-S vertical sections (slices 2 and 3, respectively) from the 3D model shown in Figure 23. North is indicated by the Y-axis.

Two suitable different volume of rocks with the favourable geophysical features can be recognized, at about the sea-level depth: to the North (slice 1, Figure 25) and in the central part of the geothermal area (slice 2 and slice 3, Figure 26), corresponding to an area to the south of the Los Humeros village.

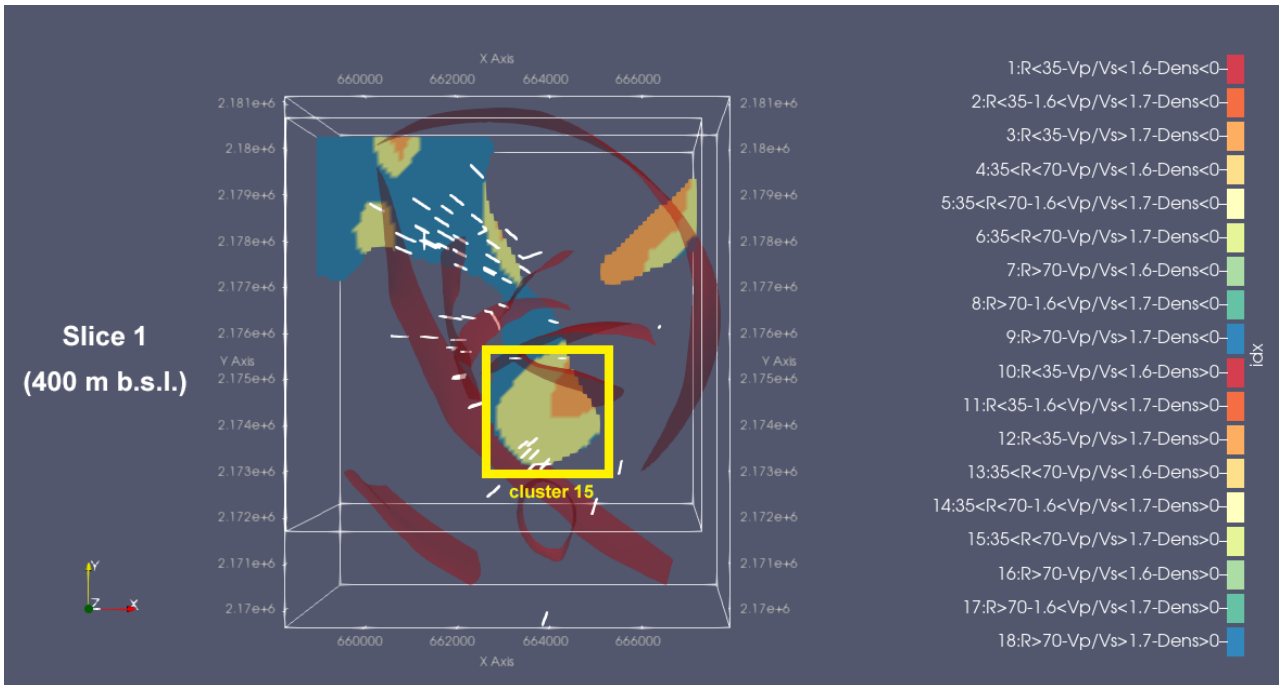


**Figure 25:** Horizontal sections (slice 1) from the 3D model shown in Figure 23. The yellow box indicates the cluster of geophysical data compatible with the occurrence of fluids. Location of boreholes (white lines) and main faults (red surfaces) are also indicated.

Regarding the volume to the North, although this is limited and close to the model margins, the cluster signature is valid, as also confirmed by the few wells above it.

Differently, the rock volume located to the south of Los Humeros village (Figure 26) is wider and apparently more promising, suggesting a deeper extension that may result compatible with superhot fluid conditions.

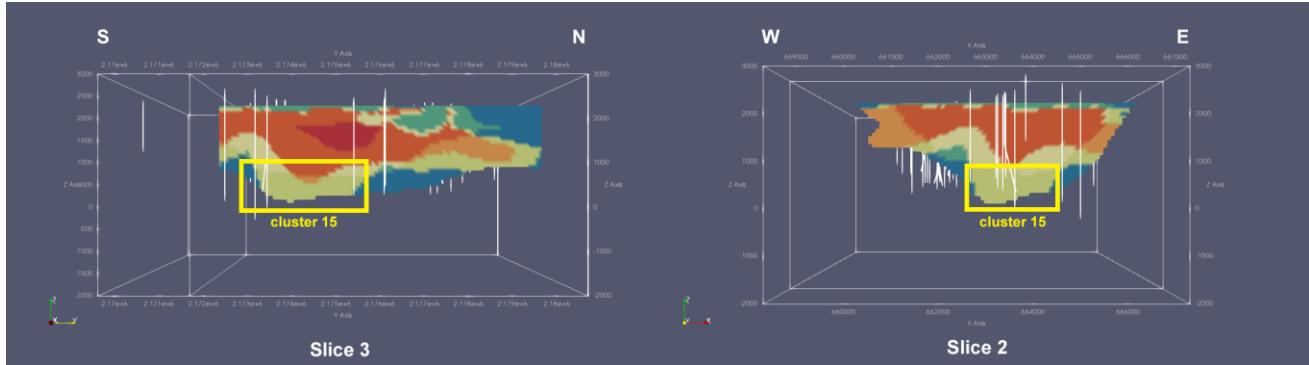


**Figure 26: Vertical sections (slice 2 and 3) from the 3D model shown in Figure 23. The yellow box indicates the cluster of geophysical data compatible with occurrence of fluids. Location of boreholes (white lines) is also indicated.**

### 3.3.7 Integrated geomodel

The Los Humeros integrated geomodel is available on the VRE at: <https://data.d4science.net/mm5C>. It comes with:

- Metadata sheet for more information
- GeoModeller files
- PDF3D file
- TSurf files
- VTK files

The preliminary and updated geomodels of Los Humeros (section 3.3.3 and section 3.3.4), constructed in the first part of GEMex, were mainly based on geological knowledge and data. In the second half of the project, inputs from other disciplines became available, such as analogue modelling, geochemical interpretation, and geophysical surveys. The integrated geomodel intends to (i) synthesize as much as possible these inputs to produce a coherent interpretation of the structures and formations, and (ii) combine them to give an interpretation of the geological system behaviour.

The size of the integrated geomodel (28 km x 22 km x 12 km, i.e. down to 7 km b.s.l.) has been set up by the GEMex Task Force (WP8) mainly to fit most of the geophysical surveys. The fifty-six wells (Figure 27) are described along the four groups' version 2018 of the geological pile (Figure 6): basement, pre-caldera rocks, rocks from the caldera, post-caldera rocks.

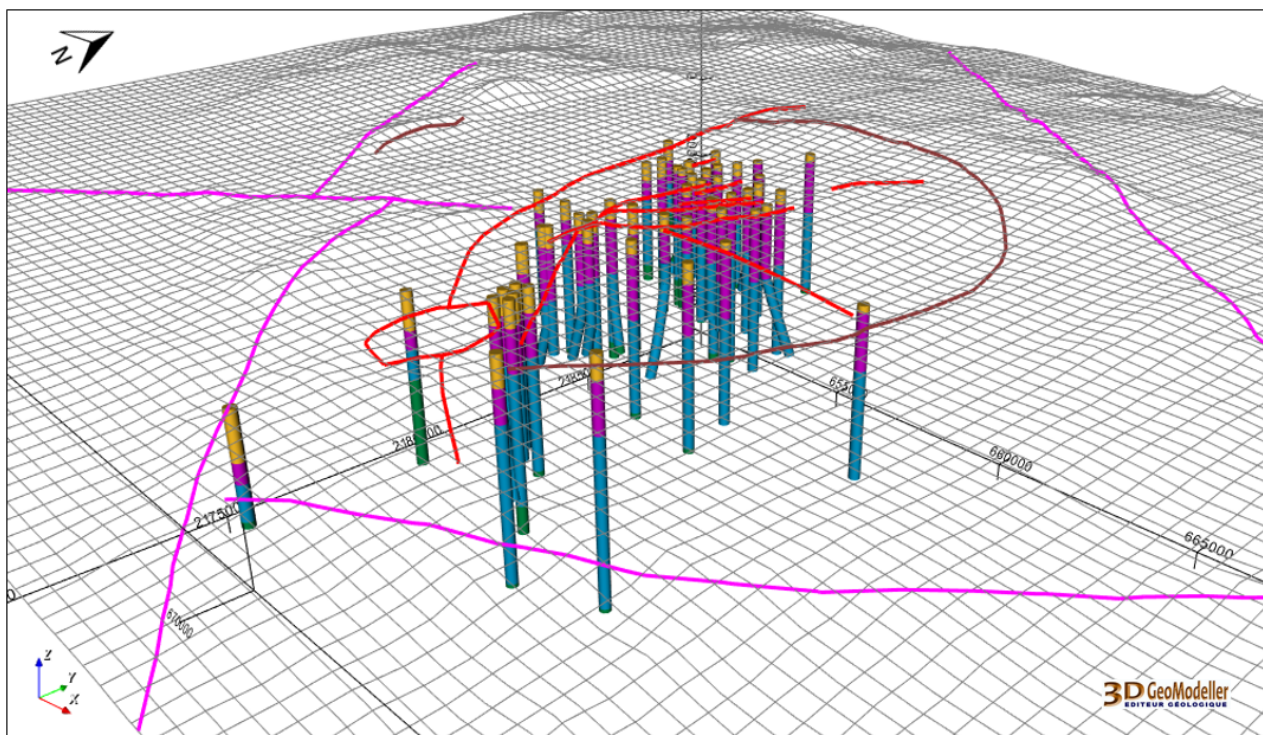


**Figure 27: Fifty-six wells are described according to the four groups' version 2018 of the geological pile presented in Figure 6. DEM is displayed as a grid including the fault network traces (see Figure 28). Coordinate system is WGS84/UTM zone 14N. View from SE.**

The integrated geomodel is an evolution of the preliminary regional model and the updated local model. Several methods and data were used in an interdisciplinary approach to produce the integrated geomodel of Los Humeros and to support the interpretation of the geothermal system presented in section 3.4. The Table 3.3 lists some examples of them.

Input	Use
Los Humeros regional geomodel	Framework for the evolution of the geomodel
Los Humeros local geomodel	Framework for the evolution of the geomodel
Fifty-six wells 2018 version	Constrain geological groups at depth
Volcanoes morphology and distribution	Regional faults traces interpretation (volcanoes alignment)
Geochemical study	Guide for the regional faults interpretation
Analogue modelling	Guide to interpret the shapes of the structures
CFE structural map (autoCAD)	Las Viboras fault interpretation
Gravity contrast regional map	Regional faults location
Gravity contrast regional map	Basement interpretation

Seismic events East cluster	Las Papas fault interpretation at depth
Resistivity (MT)	Rho<35 ohm.m to highlight possible presence of hot fluid
Vp/Vs	The current production zone is located in the range 1.6 to 1.7, higher values mark the shallow alteration zone
Gravity contrast local 3D grid	Negative contrast to highlight possible presence of hot fluid
Gravity contrast local 3D grid	Constrain the Antigua fault: range 0.2 to 0.713875 (max)

**Table 3.3: Examples of methods and data used to produce the Los Humeros integrated geomodel and the geothermal system interpretation (see section 3.4). More information regarding these data is available in Table 3.1.**

One of the main updates of the integrated model regards regional faults. A new regional fault network was interpreted from the volcanic lineaments study presented in section 3.3.5. This set of regional faults is interconnected with the updated local fault network described in section 3.3.4. Figure 28 displays the whole fault network at the integration scale within the 3D geomodel.

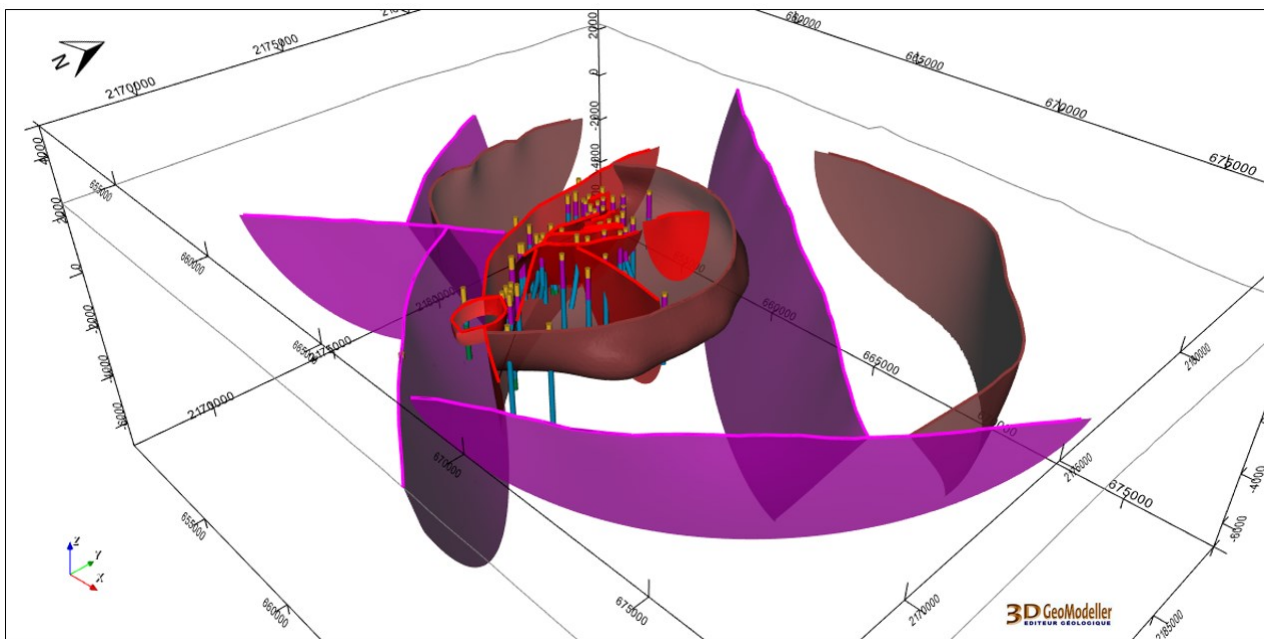


**Figure 28: The fault network constructed in the Los Humeros integrated geomodel, along with the wells. Surfaces visualization is semi-transparent to facilitate the reading of the picture. Purple: regional faults; brown: caldera structures; red: local faults. Coordinate system is WGS84/UTM zone 14N.**

The full integrated geomodel is presented in Figure 29 and Figure 30.

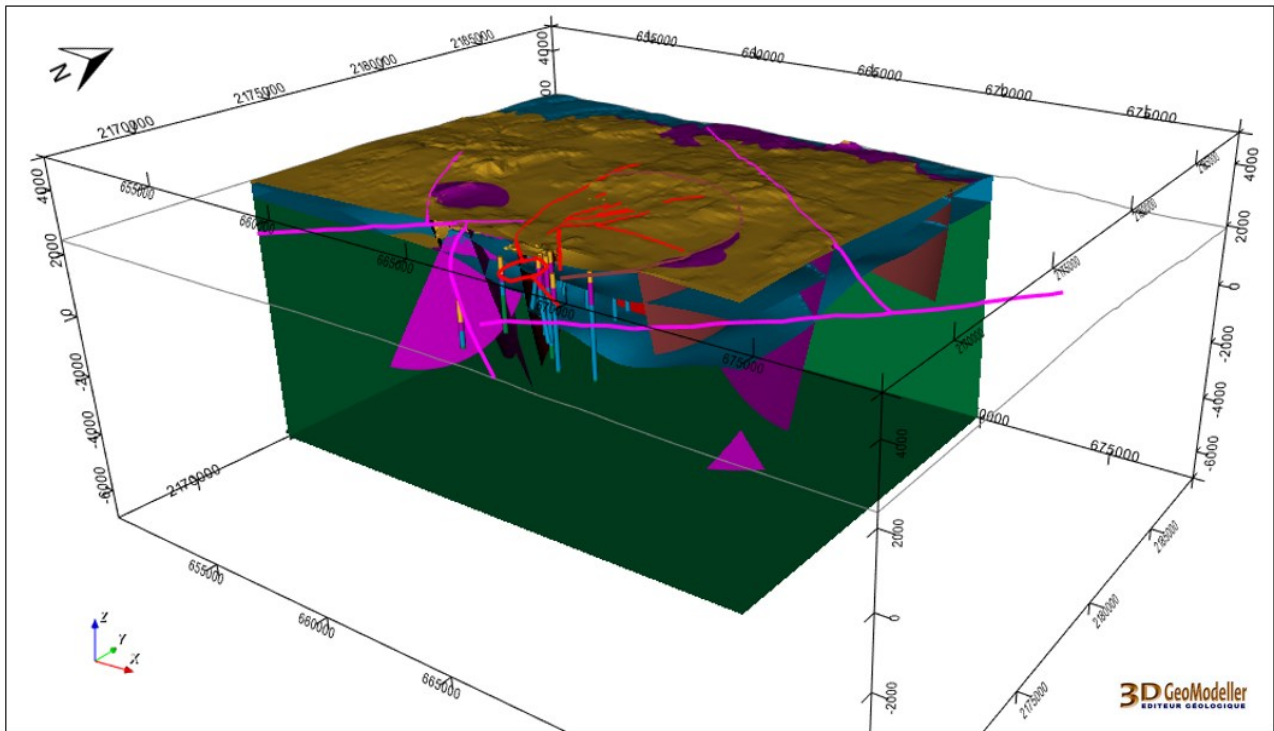


Figure 29: A clipped view of the Los Humeros integrated geomodel including wells, fault network, and the four geological groups: basement (green), pre-caldera rocks (blue), rocks from the caldera (purple), post-caldera rocks (brown). Coordinate system is WGS84/UTM zone 14N.

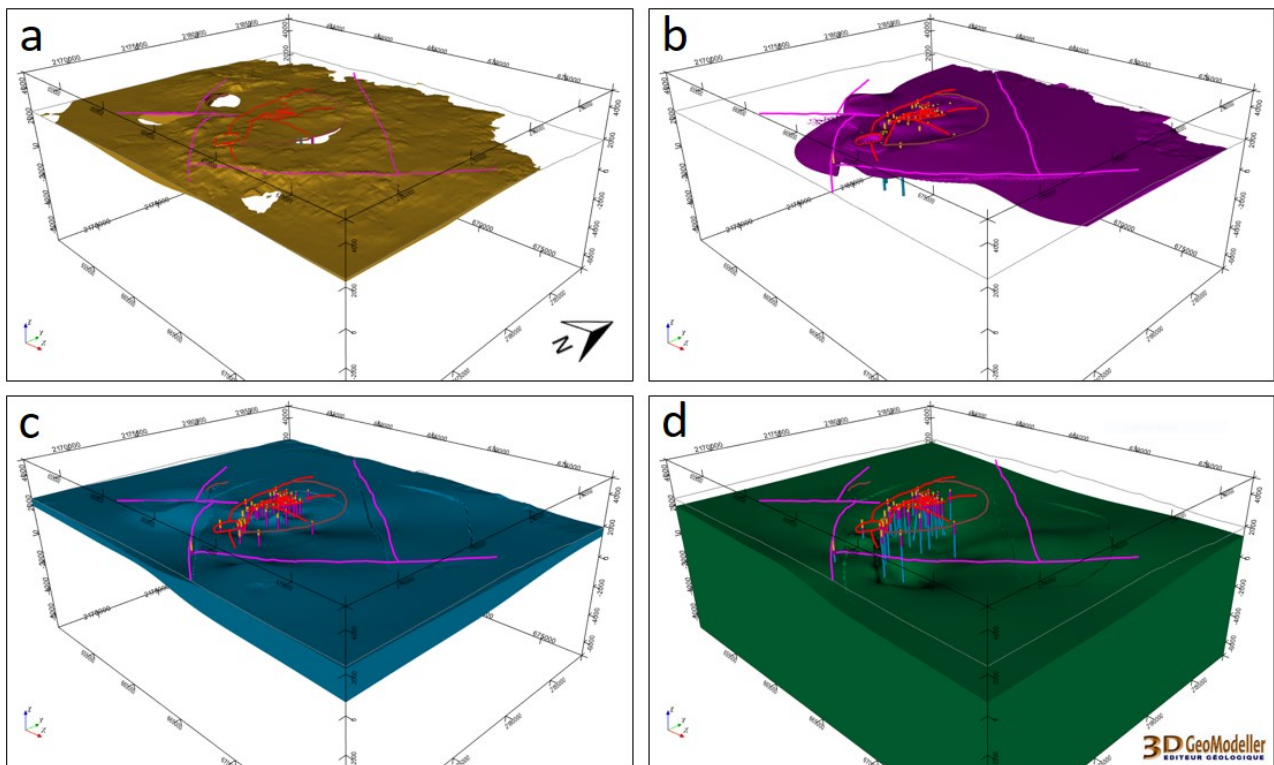
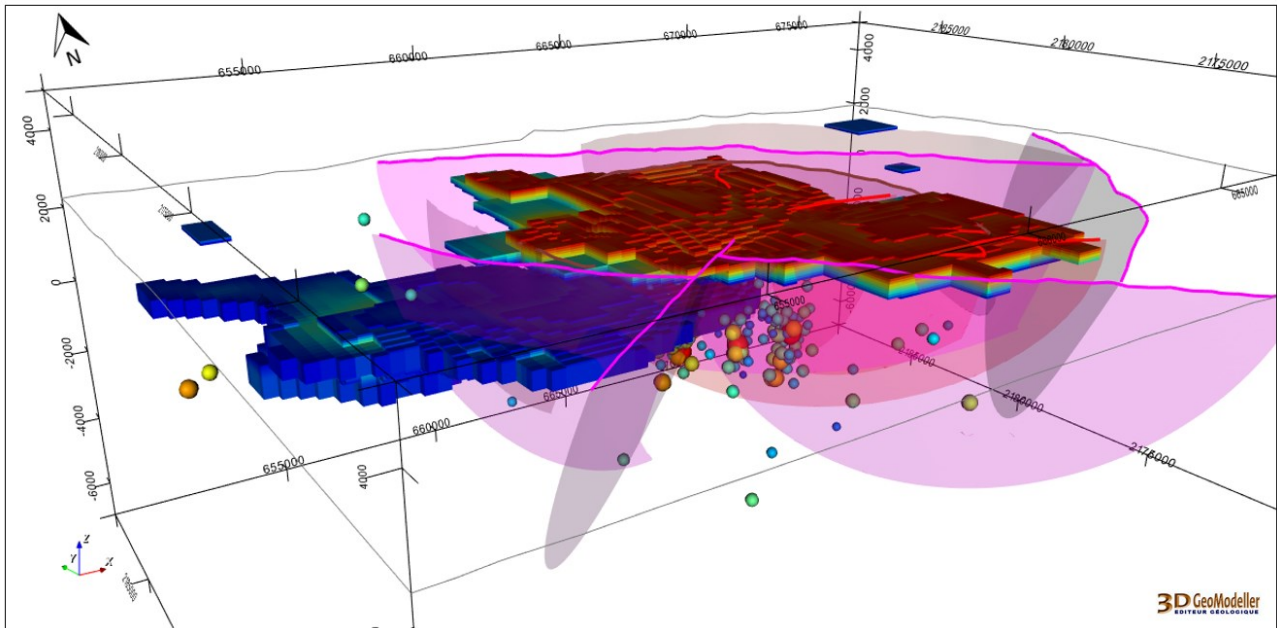


Figure 30: The Los Humeros integrated geomodel displaying wells, faults trace, and the four geological groups: (a) post-caldera rocks, (b) rocks from the caldera, (c) pre-caldera rocks, (d) basement. Coordinate system is WGS84/UTM zone 14N. Views from SE.

The integrated model allows to display information in the same 3D space to facilitate interpretation. For instance, faults, seismic events, and  $V_p/V_s$  model (GEMex D5.3) are shown altogether in Figure 31.



**Figure 31: The Los Humeros integrated geoscientific model displaying faults in transparency, seismic events (coloured dots) and  $V_p/V_s$  3D grid model (GEMex D5.3). Coordinate system is WGS84/UTM zone 14N. View from SW.**

The GEMex project used several geophysical methods to investigate the Los Humeros site. A way to manage the combination of several of them is to perform a cluster analysis. The cluster 15 highlighted by the study in section 3.3.6 is displayed along with the wells and the faults in Figure 32. This was used to support the interpretation of the Los Humeros geothermal system presented in section 3.4.

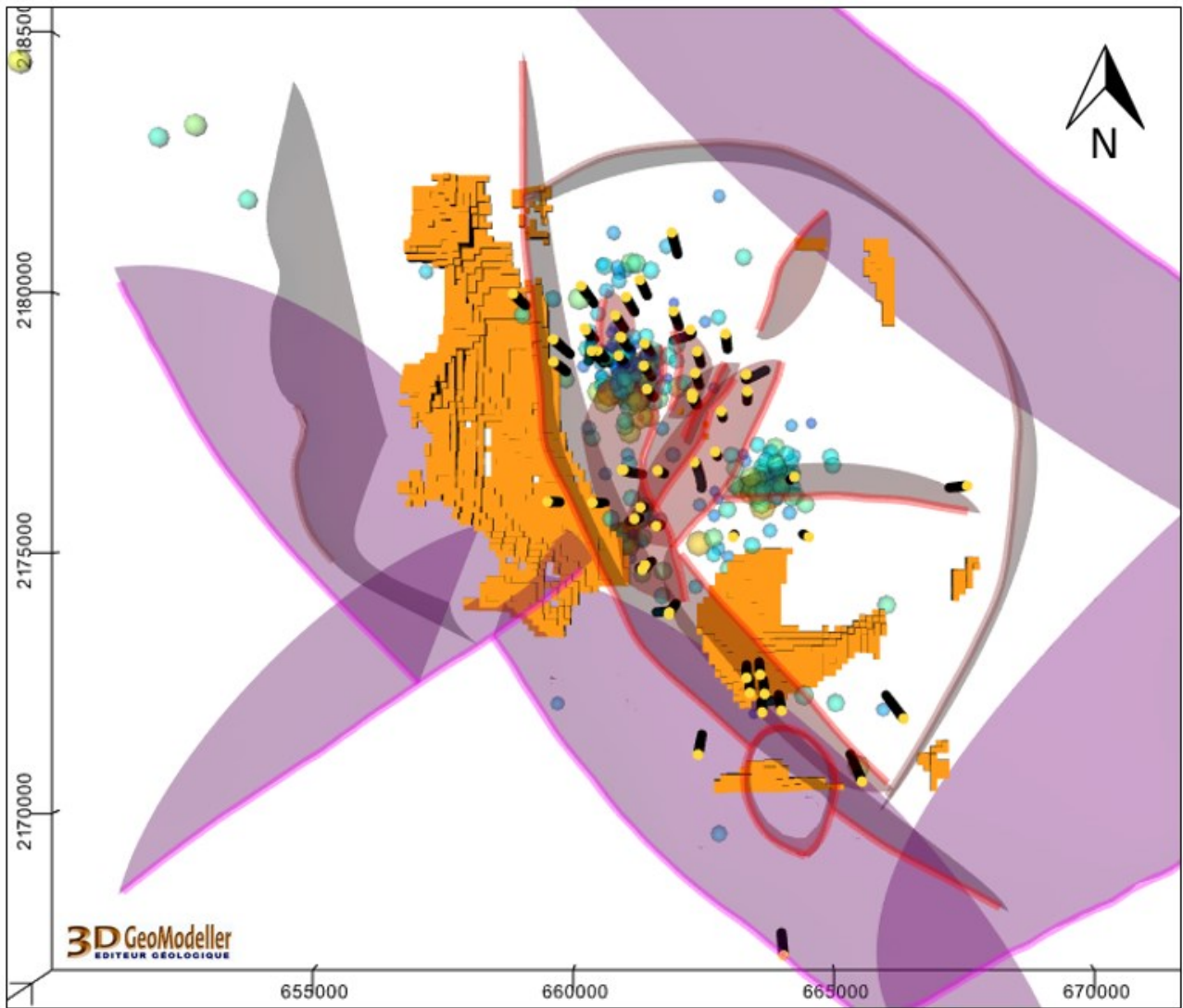


**Figure 32: A top view of the the Los Humeros integrated geomodel displaying fault traces and Antigua fault full surface, wells and cluster 15 (see section 3.3.6). Top view.**

Thermal modelling simulated the conductive-convective temperature distribution constrained by thermal data from boreholes and the above-mentioned geological-structural information. The latter were included into the numerical domain in terms of thermal conductivity, porosity and permeability distributions. The results image a dome-shaped thermal anomaly with highest magnitude of  $\sim 450^{\circ}\text{C}$  at 1000 m b.s.l. in the central sector of Los Humeros geothermal area (GEMex D6.3 and GEMex D6.6). The simulated temperatures are displayed in the integration scale geomodel along with faults and seismic events (Figure 33).

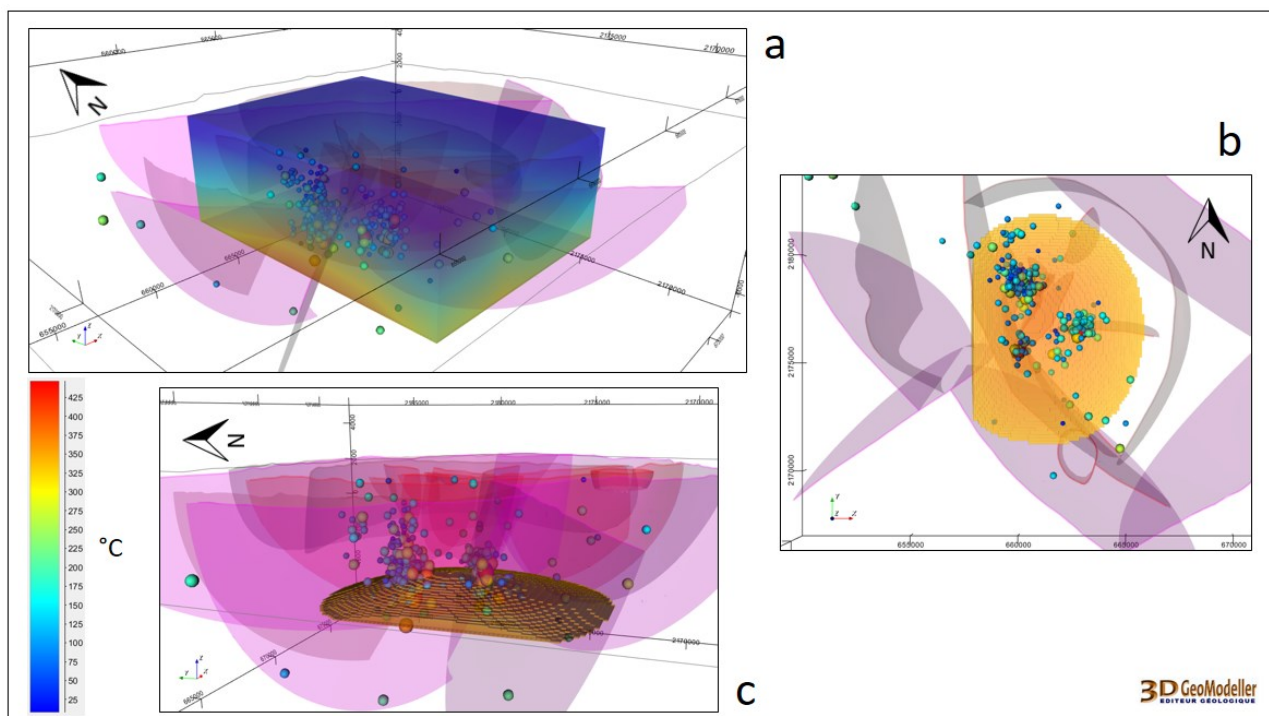


**Figure 33: The Los Humeros integrated geomodel displaying faults in transparency, seismic events (coloured dots) and simulated temperatures 3D grid (GEMex D6.3). (a) whole temperature grid, view from SW; (b) temperature above 350°C, top view; (c) temperature above 350°C, view from W. Coordinate system is WGS84/UTM zone 14N.**

### 3.4 Interpretation – Conceptual model of the geothermal system

The conceptual model of the Los Humeros geothermal system is based on the integration process described in section 3.3. This process combines the results obtained: (i) during the laboratory and fieldwork in the analogue exhumed system of Las Minas; (ii) during the laboratory and fieldwork, including geophysics, carried out in the active geothermal areas; (iii) the results of cluster analysis, pointing out volume of rocks with favourable parameters for the goals of this research. The outcome lead us to define the area to the south of the Los Humeros village as of interest for future studies and possible exploitation programs.

Studies on the Las Minas exhumed geothermal system (GEMex D4.2) indicated that the deep geothermal circulation (i.e. within the carbonate substratum) is controlled by fractures intersection and their damage zones. In particular, permeability was mainly controlled by the NNW-striking fractures, by their intersection with the NE-striking fractures and by the pre-existing foliations (i.e., bedding and granite/limestone boundary), where fluids were channelled when hydraulically connected to the main structural conduits. Hydrothermal fluid properties, studied by fluid inclusions and geochemical analyses, indicated circulation of hyper- to low- saline (meteoric) fluids, and from high (>600°C) to low (about 250°C) temperatures. Hyper-saline and hot to super-hot fluids were present at the deeper structural levels, while fluids with decreasing temperatures and salinity were recognized at shallower structural levels, these latter comparable with the present exploitation carried out in Los Humeros geothermal area (GEMex D4.2). Based on this, the lesson we learnt is that the research should be addressed to the identification of similar structural relationships in the Los Humeros basement by integration and interpretation of indirect methods, since the outcropping conditions are not favourable.

Petrological studies performed in samples from lavas indicate that the recent (<10 ka) volcanic evolution is characterized by small and diffuse magma pockets, located at different structural levels (GEMex D3.2). These have been favouring heat transfer and, presumably, trapping of hot to super-hot fluids. Regarding faults and

fractures, regional studies carried out in the surroundings of Los Humeros indicate three main groups of fractures: a) regional fractures connected to the extensional tectonics, active since Miocene (GEMex D4.1 and GEMex D4.2); b) fractures connected to the Laramide Orogeny in carbonate rocks (GEMex D4.1); c) fractures developed during the caldera collapse (GEMex D4.1). Looking to structures affecting the basement (i.e. where hot to super-hot fluids are located), the main point to be discussed is about the location of the regional fractures since outcrop analyses do not permit to clearly recognize them, as a consequence of the rheological behaviour of the Pleistocene-Holocene ignimbrite, hiding brittle deformation and widely covering the area.

An indirect way to analyse regional structures is proposed through the study of the morpho-tectonic lineaments (GEMex D4.1) and alignment of monogenetic volcanic vents (see section 3.3.5). Both methodologies suggested two main trends of fractures, NNW- and NE-striking, coherent with the previous knowledge and the Las Minas outcomes. These fractures are delimiting and affecting the Los Humeros caldera rim, reasonably representing pre-existing discontinuities, also activated during the caldera collapse. In this view, analogue models were tested in laboratory (GEMex D3.5), producing compatible geometries.

Moreover, the existence of regional structures is crucial to explain how meteoric waters can be channelled from the surroundings to depth, into the Los Humeros geothermal system, as it is documented by the waters geochemical analyses (GEMex D4.3 and GEMex D3.3). In addition, the study of the ground gas natural emission (GEMex D4.3) indicates a significant spot to the south of the Los Humeros village.

Geophysical studies carried out in the Los Humeros area (GEMex D5.3) indicate:

- Gravity data support discontinuities with the same trend of the regional structures, delimiting and passing through the volcanic caldera area.
- T-strike alignments (from MT data) are in agreement with the trend of the regional structures, suggesting these are passing through the caldera and delimiting the caldera rim. Interestingly, the SW-NE trend is interrupted by the NNW-SSE trend to the south of the Los Humeros village.
- MT-maps and cross-sections show the strong influence of the hydrothermal alteration on the values of the resistivity data. Nevertheless, structures delimiting the caldera remain well detectable.
- Cluster analysis (see section 3.3.6 and Figure 32) and interpretation of geophysical data (GEMex D5.10) indicate rock-volumes with parameters compatible with the occurrence of geothermal fluids. Based on its lateral extension, the most promising, is located to the south of the Los Humeros village, down to 3 and more km depth.
- Three principal and distinct earthquake clusters are recognized. One is located under the main production area, at the Los Humeros fault, east of the northern part of the Antigua fault, and related to the re-injection of residual brines. The second is in the centre of the Los Potreros caldera, between the Las Viboras and Las Papas faults. The third is a cluster at about 2-3 km in depth, located in the western border of the caldera by the Los Humeros village, far from the injection wells. This is apparently related to the NNW-SSE trending regional fractures, in agreement with the T-strike indications and the possible interaction with the structures related to the caldera collapse.
- Apart from the above mentioned, a significant aligned cluster of epicenters is marked along an almost SW-NE direction, intersecting the western rim of the Los Humeros caldera. This alignment is in agreement with the T-strike results and the morpho-tectonic lineaments (GEMex D5.3).

The thermal simulation (GEMex D6.3 and GEMex D6.6) leads to a dome-shaped thermal anomaly with highest magnitude of ~450°C at 1000 m b.s.l. in the central part of the Los Humeros geothermal area (Figure 33). In the same sector, the lack of earthquake hypocentres roughly follows the up-doming 350°C-isotherm. The low-resistivity, high Vp-Vs ratio and relatively low density volume imaged by cluster analysis set in the south-

eastern sector with the 300°C isotherm bounding the bottom of the above-mentioned cluster. In the same sector, super-hot conditions in the range 360-420°C at 1000 m b.s.l. cannot be ruled out.

The main conclusion points to a relatively small area located south of Los Humeros village as a crucial sector for a probable upflow of superhot resources (Figure 34). In this same area there are some wells producing a relevant liquid phase, higher than the average in the standard production well in Los Humeros that is less than 10% of the total production. Among these wells are H-1, H-1D and H-49, all located in the same well-pad, with production of separated brine between 45 up to a maximum of 75% of the total mass production, and well H-56 with separated brine between 25 and 31% of the total. Besides, close to these wells is well H-13D, currently used as injector, which denotes a good permeability. Thus, all of this seems to indicate a significant deep hydraulic conductivity. Basement structures hosting hot- to superhot fluids are therefore supposed to be present at depth ( $> 3$  km), in structural traps within the damage zone associated to the intersection between the regional NNW-SSE and SW-NE trending structures.

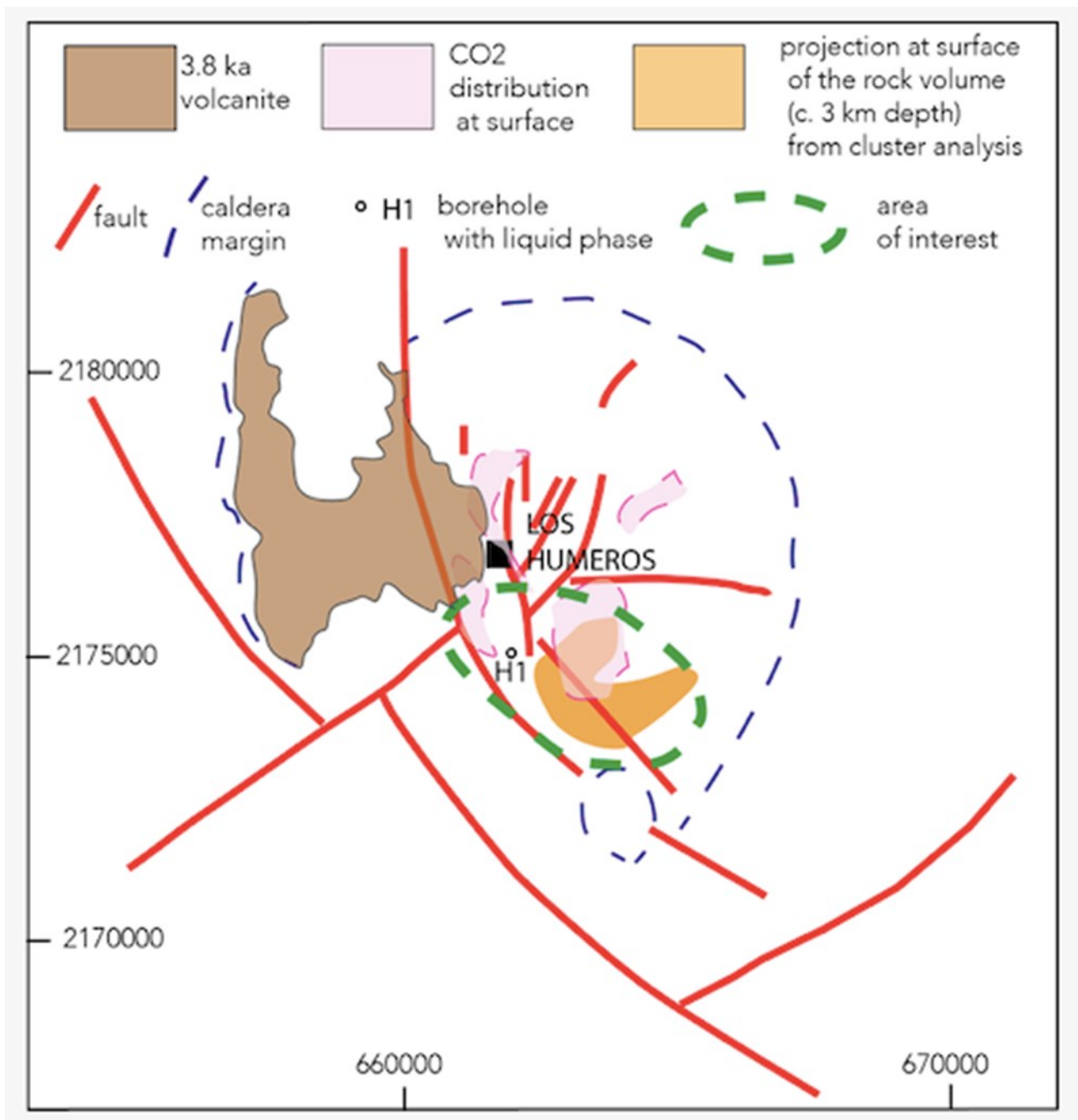


Figure 34: Interest area (green) to be searched to a depth >3.5 km for superhot geothermal resources in Los Humeros. Blue line: caldera related structures; brown area: the more recent lava-flows; red: faults; pink area: highest CO<sub>2</sub> emissions in air.

## 4 Acoculco

### 4.1 Geological and geothermal framework

The Acoculco area is also located at the eastern portion of the TMVB, where three important structural systems intersect each other: the NE–SW Tenochtitlan-Apan, the NW–SE Taxco-San Miguel de Allende, and the E-W Chapala-Tula fault systems, within a regional extensional regime (García-Palomo et al., 2017). The complex rests upon a basement formed by granite, Cretaceous limestone and marble, the Zacatlán-Chignahuapan basalt plateau and Miocene pre-caldera domes and lavas (13–3 Ma; Avellán et al., 2018).

The Acoculco Caldera was formed 2.7 Ma ago, with an explosive eruption that produced the Acoculco andesitic ignimbrite, with a volume of 127 km<sup>3</sup>. The eruption triggered the collapse of the magma chamber roof, giving place to an asymmetric caldera of sides of 18 and 16 km long, with rhombohedral to sub-circular geometry. Since then, volcanic activity has persisted up to around 60 ka, forming domes, cinder cones, fissure lava flows and two ignimbrite eruptions. So, several episodes of volcanism have taken place through reactivations of the system or associated magmatism of the nearby Apan-Tezontepec Volcanic Field (García-Palomo et al., 2017; Sosa-Ceballos et al., 2018; Avellán et al., 2018).

CFE has been awarded with the exploration permit in the area, and has drilled two exploratory wells: the EAC-1 in 1995 and the EAC-2 in 2008. The first well was finished at 1800 m depth and reached a maximum measured temperature of 307°C, while the well EAC-2 was completed at 1900 m depth with a maximum temperature of 264°C. None of the wells produced fluids (Lorenzo-Pulido et al., 2010), and so the zone seems susceptible to be developed by EGS technologies. The geothermal target must be located in the basement, composed of calcareous, granitic and metamorphic rocks, since the overlying volcanic rocks present a total width of 700 m (EAC-1) and 450 m (EAC-2), where maximum temperatures are considerably lower. In the well EAC-1 it was found an aplitic dyke dated  $0.183 \pm 0.036$  Ma (Sosa-Ceballos et al., 2018). Even though this age could have been reset by heat provided by younger intrusions or by magma flux, it suggests the presence of a recent heat source (Sosa-Ceballos et al., 2018). In addition, volcanic rocks show intense hydrothermal alteration (Lorenzo-Pulido et al., 2010).

More information on the geological setting of Acoculco is available in GEMex D3.4 and GEMex D4.1.

### 4.2 Data and information

To perform the Acoculco 3D geomodel, different datasets were imported into GeoModeller software package. The datasets were prepared in suitable formats to be included in the geomodel. Firstly, apart the Digital Elevation Model (DEM) of the study area, typical geological data sets were imported such as a geological map, a vector file with the main faults, two interpreted geological cross-sections and the litho-stratigraphic logs of the two deep boreholes drilled in the area. Afterwards, geophysical dataset were embedded to constrain and refine the geomodel. In particular, two partially overlapped 3D geophysical models referred to the resistivity and density petrophysical properties were imported. Moreover, the 1D-2D profiles from joint optimization of VES and TEM were considered. For Acoculco no seismic data were available because the installed seismic network in the GEMex project did not register any events for the period. Excluding the DEM (INEGI, 2016) geological map of Acoculco (Sosa-Ceballos et al. 2019) and the description of the two deep boreholes (Lorenzo-Pulido et al., 2010) all the other datasets were made available thanks to the multidisciplinary activities foreseen and carried out in the framework of the GEMex project, see Table 4.1 for details.

Used for	Data	Reference
Preliminary and updated geomodels	DEM	Instituto Nacional de Estadística y Geografía (INEGI, 2016)
	Geological map	Sosa-Ceballos et al. (2018)
	Geological cross-sections	Liotta's team on the basis of the Lopez-Hernandez et al. (2009)
	Faults system network	Liotta's team GEMex field works
	Boreholes Thermo-Litho-stratigraphy	Lorenzo-Pulido et al., 2010
Integrated geomodel	3D density model	GEMex D5.6
	3D resistivity model	GEMex D5.2
	3D Thermal model	GEMex D3.4
	Depth of shallowest resistive basement from joint optimization of VES and TEM	GEMex D5.2
	2D VES resistivity profile	GEMex D5.2
	Seismic data	GEMex D5.10
	Distribution of the morpho-tectonic lineaments	GEMex D4.2
	Geochemistry consideration	Internal discussion with Lelli, M.
	Results from cross-plotting data integration	GEMex D5.12

**Table 4.1: List of dataset used for the construction of the Acoculco geomodels. In the table is specify which data were used for the preliminary and updated geomodels as well as the additional data for the integrated geomodel. Moreover, the source of data is specified.**

The 3D density model is provided as differential density ( $\Delta\rho$ , g cm<sup>-3</sup>) with respect to the Bouguer density of 2.67 g cm<sup>-3</sup>. The 3D resistivity model from MT is provided as linear values of resistivity ( $\Omega$ .m). The 2D VES resistivity profile, obtained from the interpolation of 1D resistivity models each of them constrained with neighbour soundings, is provided as linear values of resistivity ( $\Omega$ .m). The information from the joint inversion of VES and TEM data by probabilistic method is provided as the depth, in m, of the shallowest resistive basement (GEMex D5.10).

### 4.3 Integration

The geomodel of Acoculco was carried out with an interdisciplinary approach thanks to the contribution of the different expertises that participated not only providing datasets but also contributing in the several discussion periodically organised to improve the geomodel.

The last version of the geomodel of Acoculco is the result of several steps schematically described in the Figure 35.

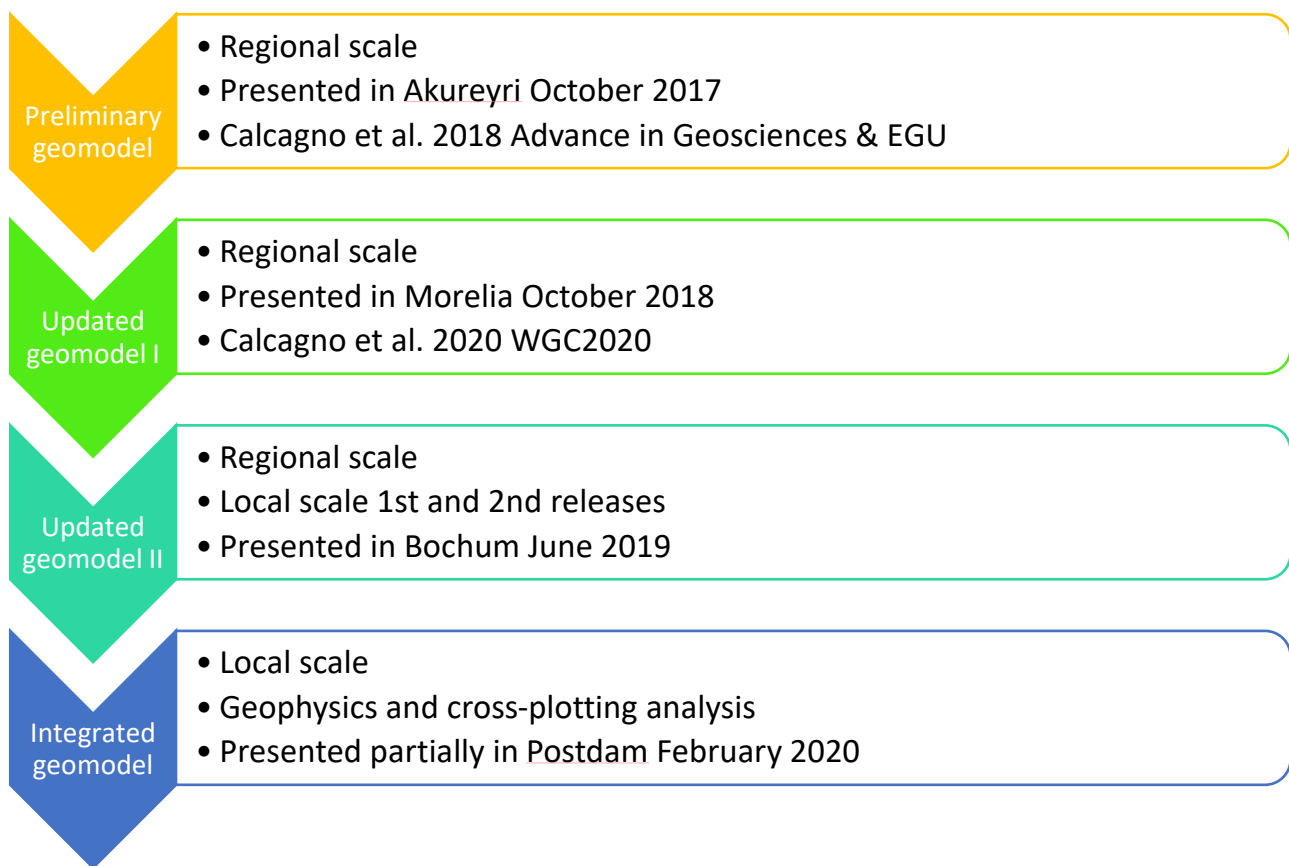


**Figure 35:** The schema reports the main Acoculco geomodel updates, its presentation into the GEMex project context, the scale and if the model was scientifically disseminated.

#### 4.3.1 Preliminary geomodel

The preliminary model is available in the VRE at the following link: <https://data.d4science.net/h2rg> together with the associated metadata sheet.

The preliminary model was carried out in the first year of the GEMex project and included mainly the existing data collected in the first months of the project. Since only two boreholes (Figure 36) drilled by CFE gave direct information on the underground, two interpreted geological cross-sections were prepared by Liotta's team to constrain the model under the surface (Figure 37). These cross-section followed the model proposed by López-Hernández et al. (2009). Apart the litho-stratigraphy of the two deep borehole obtained from Lorenzo-Pulido et al., 2010 a EU-MX joint group provided a first version of the faults network thanks to the first performed field work.

The Acoculco area is intersected by NW-SE and NE-SW to ENE-WSW fault systems in mutual cross-cut relations, which suggests their contemporaneity. The faults belong to three different groups in terms of geometry and kinematics. The first group includes mainly NE-SW oriented normal faults. The second group comprises NW-SE faults with a typical strike- to oblique-slip movement. The last group concerns the caldera-rim faults, developed during caldera collapse (Calcagno et al. 2018).

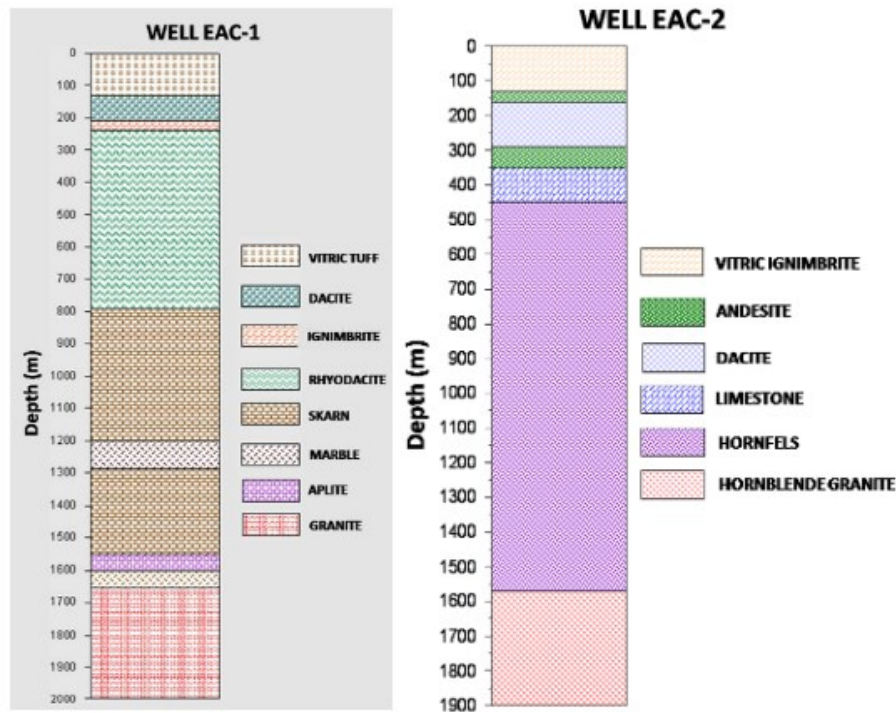


Figure 36: Lithologic column for well EAC-1 and EAC – 2 (Lorenzo-Pulido et al., 2010)

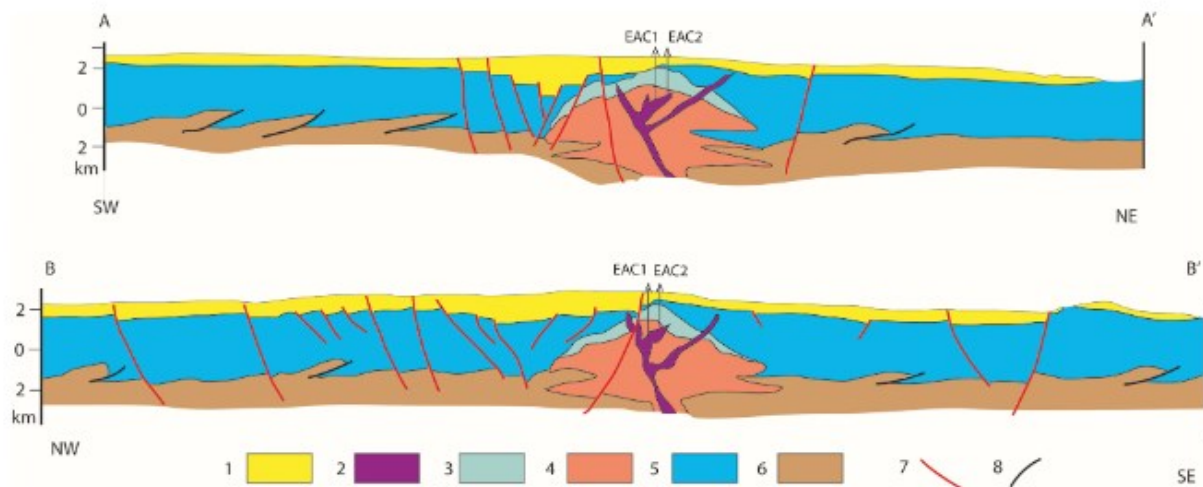


Figure 37: The two main cross-sections used for modelling the Acoculco area. Symbols: 1 – vulcanite (Pliocene-Holocene); 2– Quaternary dyke; 3 – skarn and marble; 4 – crust involved in thermal anomalies through time: magma chambers originating the different volcanic events are supposed to be developed within this volume; 5 – Jurassic-Cretaceous limestone; 6 – crystalline rocks, mainly phyllite (Paleozoic); 7 – Neogene-Quaternary normal to oblique slip faults; 8 – thrust faults related to the Laramide orogenesis (Oligocene) (Calcagno et al., 2018).

Five groups of rocks were modelled. The basement, which is the planned geothermal target at Acoculco, was split into four groups while all the overlying volcanic rocks were gathered in a single group. The basement includes, from bottom to top, phyllite and micaschist, and limestone and skarn, intruded by a granite (Calcagno et al., 2018).

### 4.3.2 First geomodel update

During the second year of the GEMex project an updated version of the regional scale Acoculco geomodel was carried out.

This version was presented at the second GEMex General Assembly held in Morelia, Mexico, in October 2018. The outline of this model update was described in the extended abstract submitted to the World Geothermal Congress 2020 related to an oral presentation, Figure 40.

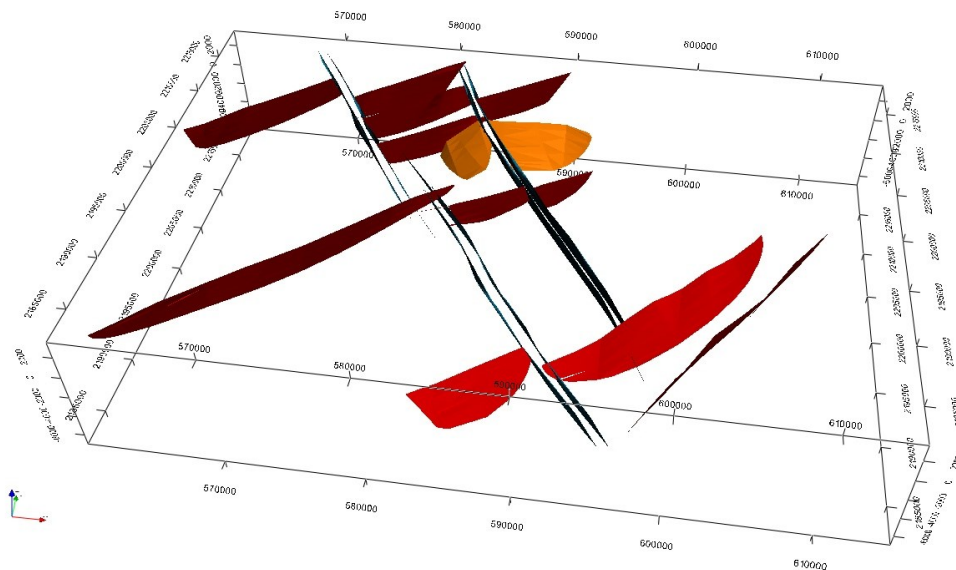


**Figure 39: The 3D visualisation of the updated faults system including the ‘Damage zones’, modelled as delimited by two sets of NNW-SSE striking parallel faults. Coordinate system is WGS84/UTM zone 14N (Calcagno et al., 2020).**

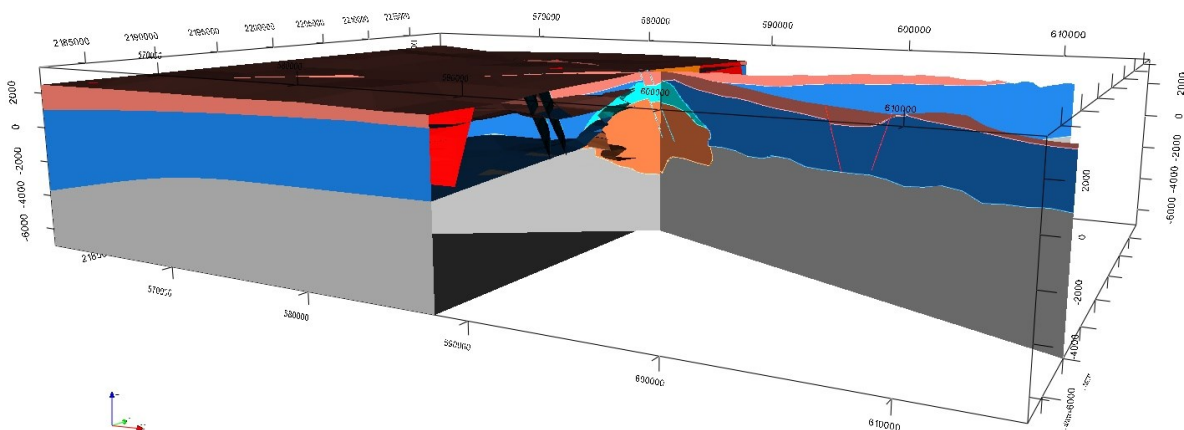


**Figure 40: The updated regional 3D geomodel of Acoculco with the new faults and the ‘Damage zones’. Coordinate system is WGS84/UTM zone 14N (Calcagno et al., 2020).**

### 4.3.3 Second geomodel update

The second model update at regional scale and the first and second releases of the local scale model are available in the VRE at the following link: <https://data.d4science.net/t5NF> together with the associated metadata sheets.

In January-February 2019 the EU-MX joint group carried out the last field work foreseen in GEMex project. The field work in Acoculco was focused mainly on the revision of the faults of the area that guaranteed a better comprehension of the structures of the regional area. Moreover, a detailed geological survey was accomplished in a smaller area in the surroundings of the EAC-1 and EAC-2 boreholes, so called local area.

The regional 3D geomodel of Acoculco was updated again thanks to the outcomes from the above mentioned field work (Figure 41). The principal difference with the previous version was related to the faults network. Field observations allowed to add some new NE-SW mainly normal faults and to depict with more accuracy the NW-SE faults. The latter were even better characterised from a kinematic point of view, in fact the resulting offset results from a first normal movement and a second oblique displacement.

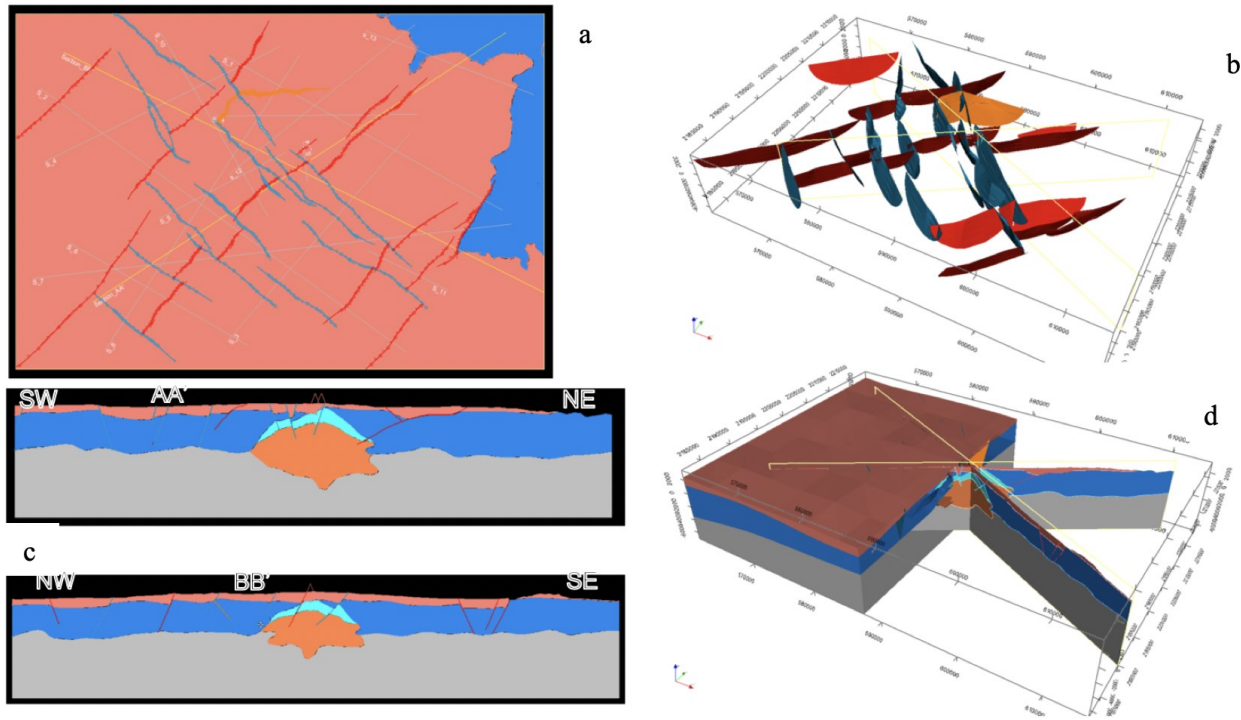


**Figure 41: The second updated regional 3D geomodel of Acoculco with the new faults. Coordinate system is WGS84/UTM zone 14N. a) The computed geological map, in orange, red and blue the updated faults network; b) the 3D view of the new faults network; c) the two computed cross-sections (AA' and BB'); d) the 3D view of the second updated Acoculco geomodel.**

As mentioned, the two deep boreholes EAC-1 and EAC-2 drilled by CFE resulted unproductive because they did not encounter any exploitable geothermal fluid. However, due to the high temperatures registered at both bottom holes, the Acoculco site was dedicated to the preparatory studies for an EGS development in the GEMex project. Thus, geophysical surveys (carried out in WP5) and stimulation modelling (performed in WP7) were focused nearby the two CFE boreholes.

The new and more detailed information of the area around the EAC-1 and EAC-2 wells gave the possibility to prepare a detailed local model aimed to better characterise this area and to provide detailed geometries for the stimulation models foreseen in the WP7 of GEMex project, which are necessary for the development of the area as an EGS.

The local model contains in its center the two boreholes and is 8.5 x 10.5 km horizontally spaced with a vertical dimension of 10.5 km in total. The model was built considering the results of the regional model, but it was refined with a more accurate and detailed faults network (Figure 42). Small faults that don't appear in the regional model for scale reasons are here included. In this local model the same five groups of geological units were used (i.e., from the top volcanites, limestones, skarns, granite). The two boreholes were included in the model again to constrain the model with direct data. This version of the local model was then the base for the following integrated model with the geophysical outcomes.

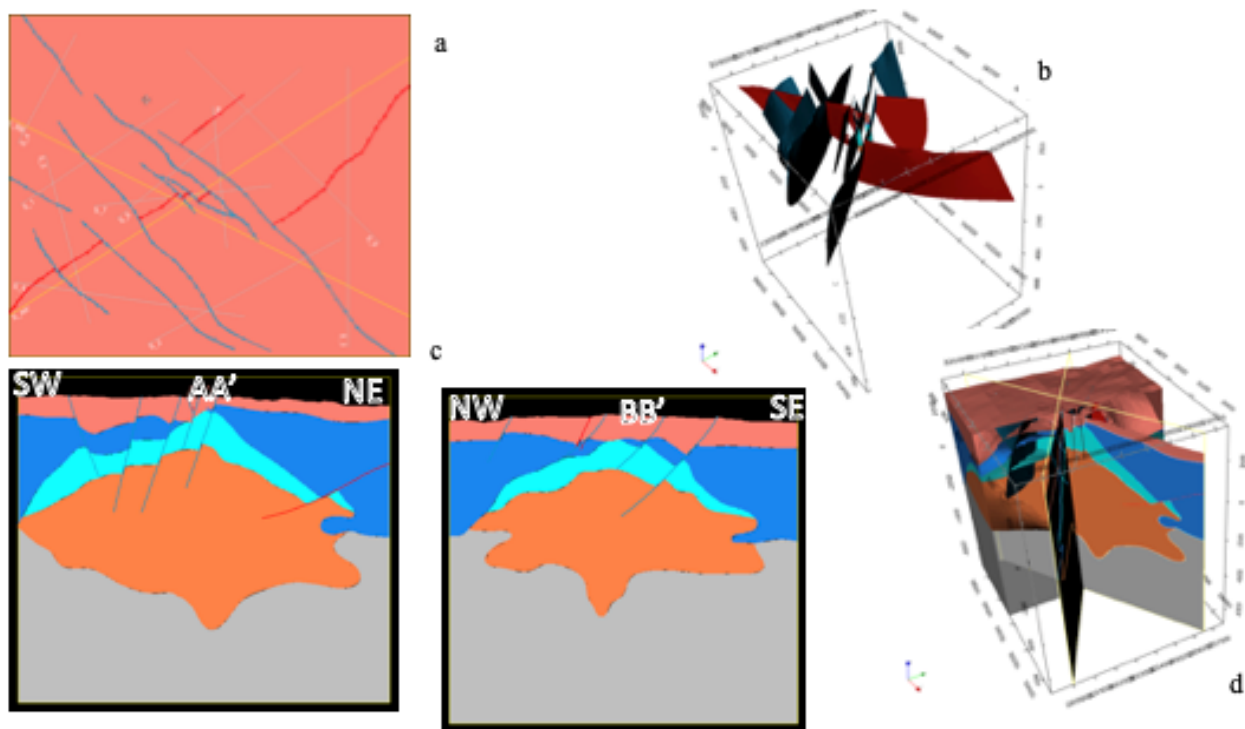


Figure 42: The second release of the local 3D geomodel of Acoculco with the detailed faults network. Coordinate system is WGS84/UTM zone 14N. a) The computed geological map, red and blue the detailed faults network; b) the 3D view of the new faults network; c) the two computed cross-sections (AA' and BB'); d) the 3D view of the local Acoculco geomodel.

#### 4.3.4 Integrated geomodel

The integrated geomodel at local scale is available in the VRE at the following link: <https://data.d4science.net/Ggw2> together with the associated metadata sheet.

To improve the accuracy of the Acoculco local geomodel, different kind of data were used. Most of them are the main outcomes of the geophysical surveys carried out in the local area during the GEMex project. In Table 4.1 the datasets considered for the integrated model are highlighted in the second part, however, not all the datasets were finally used to refine the Acoculco local model.

The team work at this point was crucial to decide which and how geophysical datasets had to be used directly in the improvement of the Acoculco local geomodel, and which were relevant for the definition of the geothermal conceptual model.

An important contribution was provided by the cross-plot and cluster analysis (see GEMex D5.12 for a full treatment of the topic) that allowed a quantitative integration of different geophysical datasets. Cross-plot are used to interpret geophysical datasets and can suggests various correlation between variables with a certain interval of confidence. The cluster analysis highlights set of data similar to each other and the data in different clusters are as different as possible. Among the different clustering approaches and outputs, we exploited the results coming from the supervised cluster analysis. In particular, we defined nine clusters, each of them characterized by a specific interval of resistivity and density (see GEMex D5.12 for details).

The process of data integration discussion was carried out by exploiting the capabilities of the tool “ParaView” (by Kitware), an open-source 3D data analysis and visualisation application that allowed to plot together different kind of datasets. The discussions results were used to upgrade the Acoculco local model within the

3D GeoModeller software package, by importing specific surfaces or body shapes. In particular the following checks and changes were performed:

1. The joint optimization of **VES** and **TEM**, the 2D **VES** resistivity profile and 3D **resistivity** model were used to provide insights for the verification of the depth of the volcanites bottom. The shape of the 60  $\Omega.m$  surface extracted from the 3D resistivity model was taken into account as possible limit between the more conductive volcanites and the underlying more resistive limestones. The same boundary value was even considered for the VES profiles. In the geomodel, a difference between the 60  $\Omega.m$  limit provided by the 2D vertical VES and the one by the 3D resistivity model has been widely observed (see Figure 43). The reason, briefly, is due to the different method sensibility. In fact the VES that provided the vertical profile are in general more sensible to the resistive rocks while MT measures that was used to prepare the 3D resistivity model are more sensible to the conductive rocks. For this reason, a clear constrain of the bottom of the volcanites was difficult to obtain. Moreover, the resistivity methods mainly highlight geophysical facies and not well defined lithological limits, thus the occurrence of volcanites more altered and consequently more affected by fluids circulation can be pointed out. However, the imported geophysical datasets showed a good correspondence in some spots with the lithological limit between the volcanites and the limestones (see Figure 43).

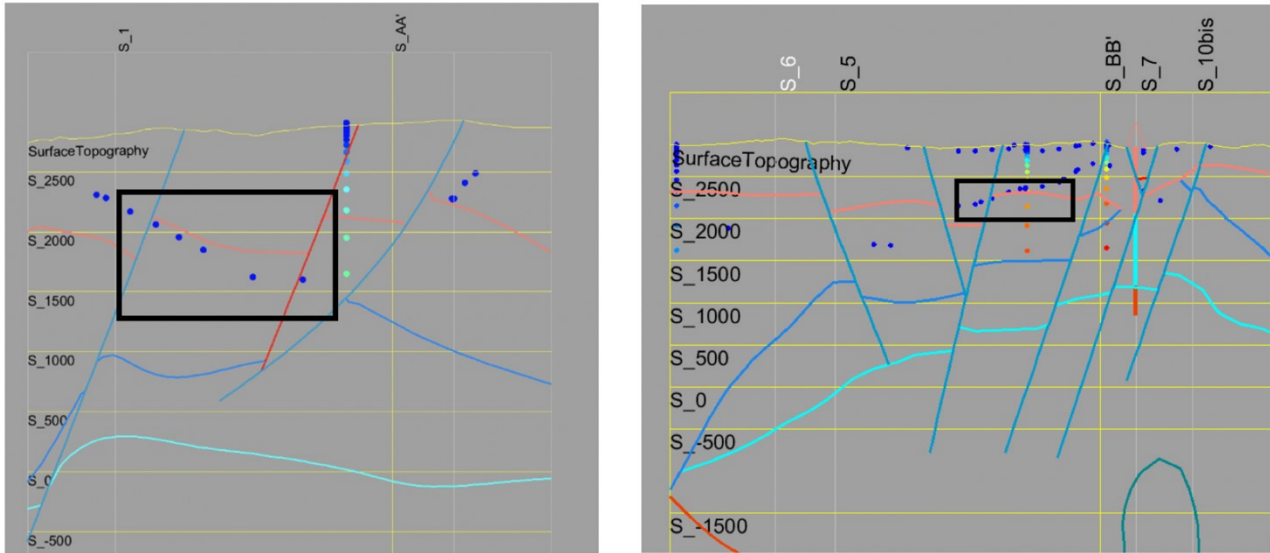


**Figure 43:** Part of the cross-section 10bis' on the left and part of the cross-section AA' on the right: VES is represented by the blue to light blue color ramp where colder colors stay for low resistive rocks while warmer color are referred to higher resistivity rocks. The blue dots (not in the vertical profile) are referred to the 60  $\Omega.m$  layer extracted from the 3D resistivity model. Inside the black box a good correspondence between the bottom of the volcanites and the 60  $\Omega.m$  layer.

In addition, the supervised cluster analysis recognized a low resistivity ( $R < 60 \Omega.m$ ) and low to high density ( $-0.05 \leq \delta D < +0.05 \text{ g/cm}^3$ ) volume of rocks possibly referable to the volcanites, as displayed in Figure 44.

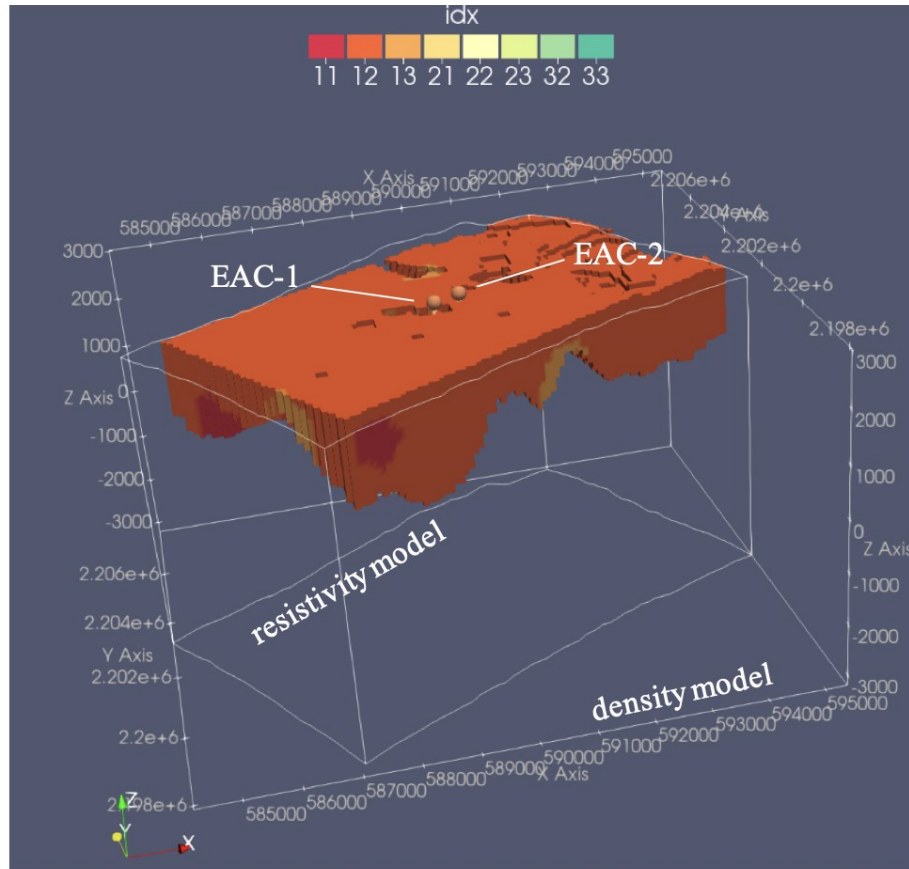
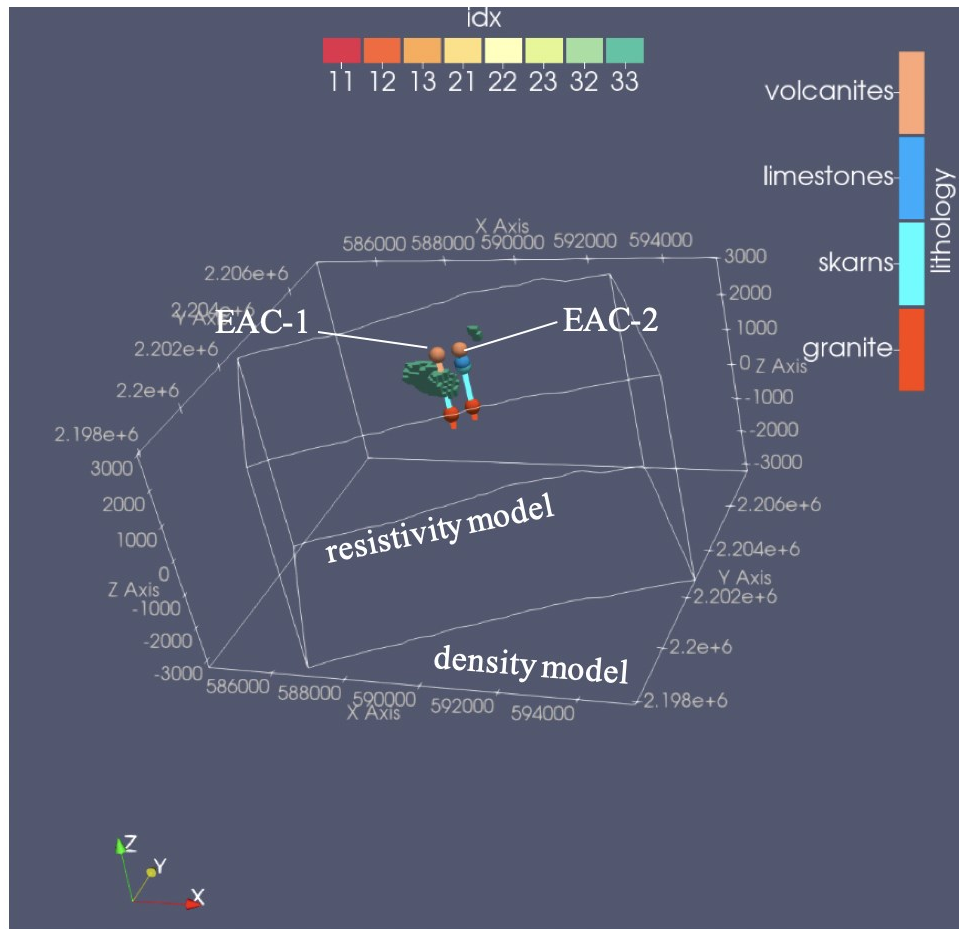
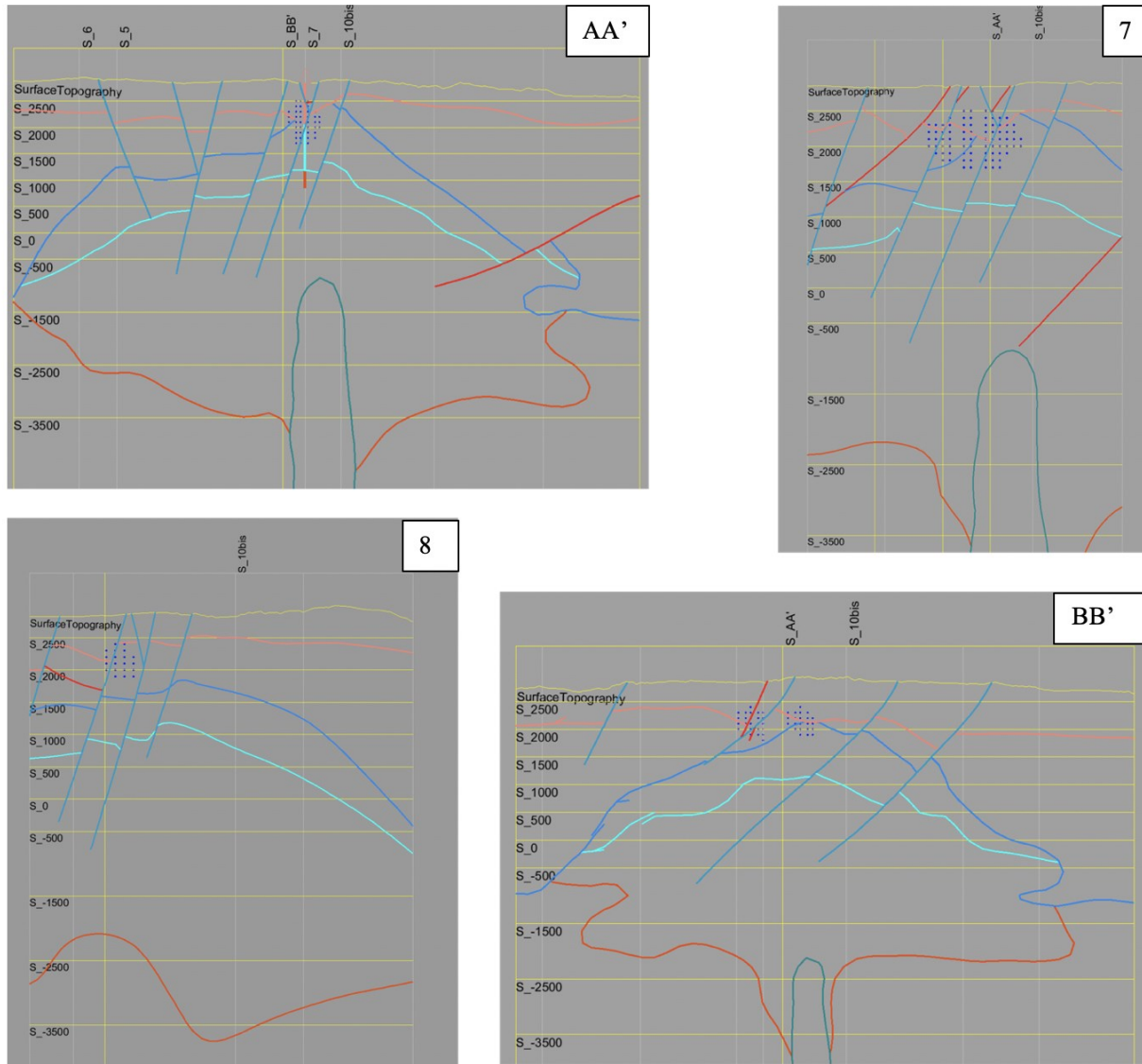


Figure 44: Low to high density and low resistivity ( $60 \Omega.m$ ) domains (clusters 11, 21, 31) coming from the supervised clustering that could partially represent the volcanites.

A **high-resistivity** and **high-density** body appearing northwest of the wells and partially overlapping EAC-1 could be interpreted as the **skarn** as well as a body with the same properties occur in the area of the *Alcaparrosa* manifestation. This is highlighted by the clusters analysis carried out by the above-mentioned supervised approach (see Figure 45). This distinctive cluster ( $R > 150 \Omega.m$  and  $\delta D > 0.05 \text{ g/cm}^3$ ) was imported in the geomodels and helped to adjust the boundaries of the skarns in different cross-sections (see Figure 46).



**Figure 45: High resistivity-high density domains from the supervised clustering model together with the simplified lithostratigraphic sequence of the two boreholes in the area of study. The borehole EAC-1 results partially inside a first volume of this kind of rocks, while a second volume occurs toward N from the EAC-2 borehole.**



**Figure 46: Blue dots represent the high resistivity-high density domain from the supervised clustering model imported in the AA', BB', 7 and 8 cross-sections. The occurrence of this cluster could suggest the presence of metamorphosed limestones in skarn facies and a former hydrothermal fluids circulation.**

2. A **new** young (6-5 ka if cooling – 50-80 ka if heating) magmatic **intrusive body** is inserted inside the existing granite. The thermal numerical simulation well fit the temperature data from the two borehole if the magmatic intrusion is supposed to be simplified in an ellipsoidal shape with an aspect ratio of 10 and a radius 500m (prolate ellipsoid) with a top depth at  $2300 \pm 400$  m. The new intrusion supposed geometry was also constrained by the 750° degree isotherm surface, which should highlight the part of volume of rocks partial melt. The 750° degree isotherm was then imported in the 3D geomodel to create the new geometry (see Figure 47). This young magmatic body (or the assemblage of more than one smaller magmatic intrusions), its depth, its shape and dimension are supposed to be the cause of the current thermal anomaly measured in the two boreholes.

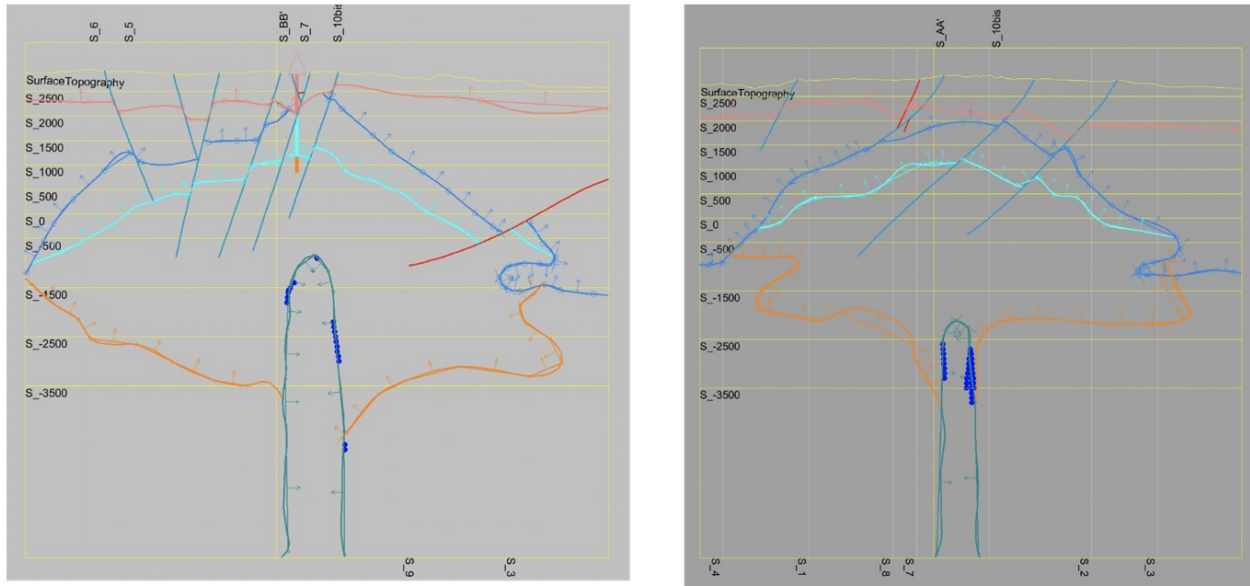


Figure 47: In both pictures are reported the blue dots that are related to the 750° degree isotherm from the regional thermal model and representing the shape of the supposed new younger intrusion. The blue dots position helped to infer the shape of the young intrusion within the previously (old) emplaced granite.

3. A normal **fault** NE-SW striking northward the boreholes and crossing *Alcaparrosa* manifestations area is included in the geomodel because of the existence of natural manifestation with a corresponding strike as well as the occurrence of one nearby seismic event registered in the seismic network set up in the period between 25<sup>th</sup> of April 2018 and the 16<sup>th</sup> of June 2019 by the GEMex project. Moreover, the presence of this fault can be even inferred by the high resistivity – high density cluster domain that occur in the underground of the *Alcaparrosa* area (see Figure 48). Thus, this faults can be related to the skarn facies possible generated by the hydrothermal circulation in this fault.

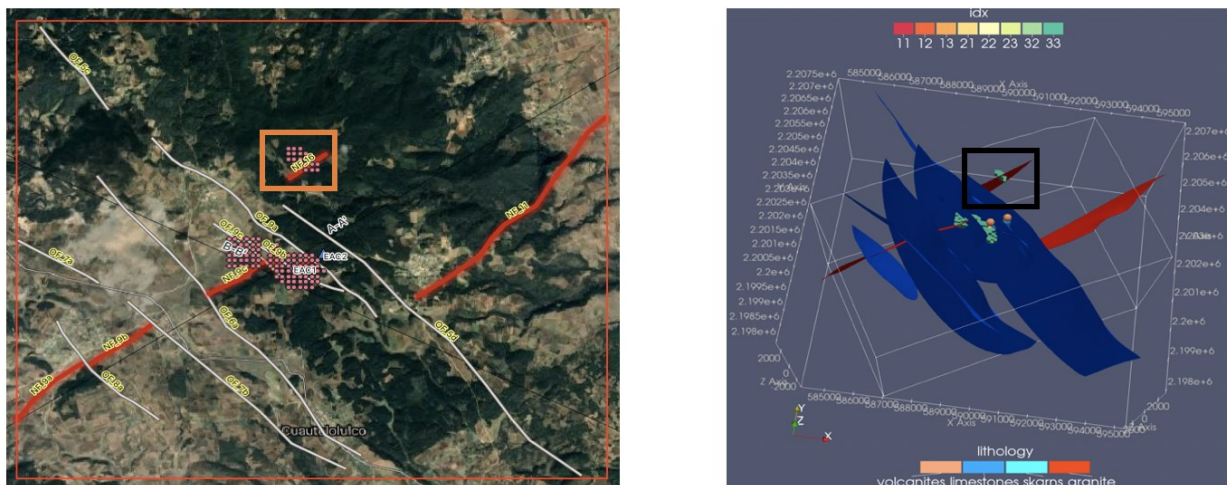
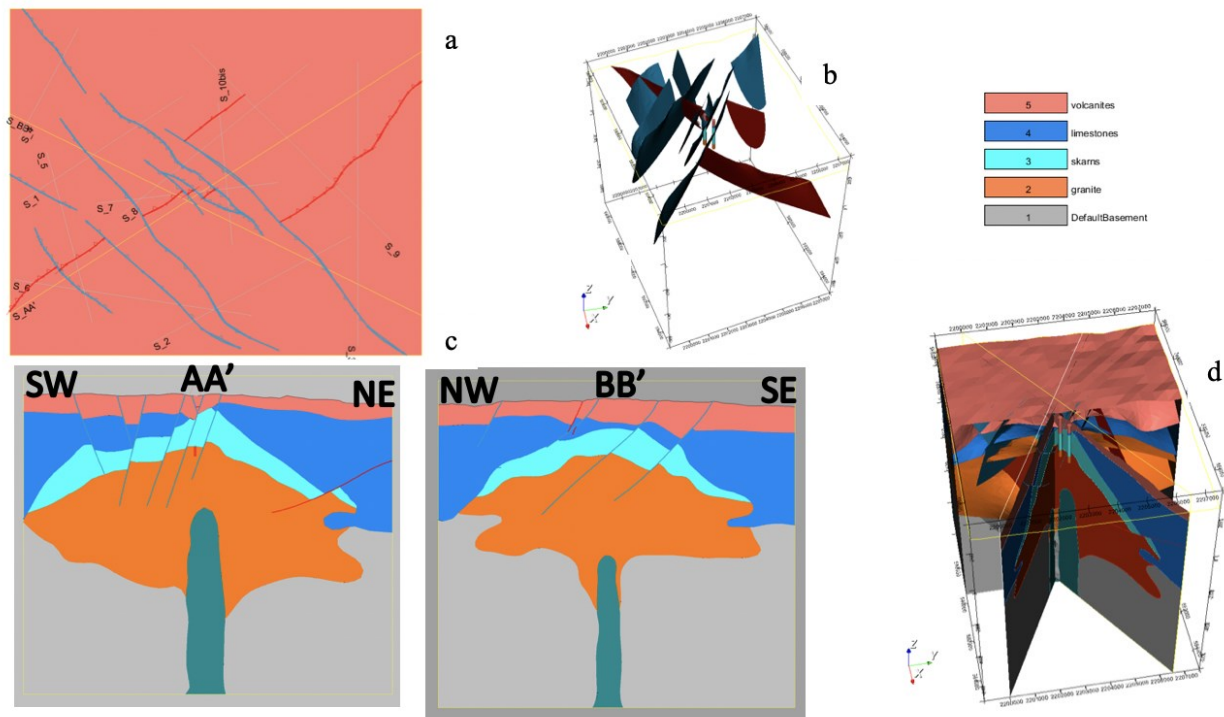


Figure 48: (Left) 2D map of the modelled faults at local scale (in light blue the NW-SE strike slip faults and in red the NE-SW normal faults). The pink dots represent the high resistivity – high density cluster domain projected in the surface. The fault in *Alcaparrosa* area is included in the indicated cluster (within the orange box). (Right) 3D representation of the faults and the high resistivity – high density cluster domain (in green). Within the black box the fault cutting the cluster.





**Figure 50:** The integrated local 3D geomodel of Acoculco. Coordinate system is WGS84/UTM zone 14N. a) The computed geological map, red and blue the detailed faults network; b) the 3D view of the new faults network; c) the two computed cross-sections (AA' and BB'); d) the 3D view of the local Acoculco geomodel. In this geomodel the bottom of the volcanites and part of the skarns are checked with geophysical data and cluster analysis, the young magmatic intrusion is added thanks to the Regional thermal model and the fault in the Alcaparrosa manifestation area is added.

#### 4.4 Interpretation – Conceptual model of the geothermal system

The conceptual model of Acoculco area is based on the integration among the results obtained: (i) during structural fieldwork, which produced the reconstruction of the regional stress field; and (ii) during geochemical and geophysical laboratory and fieldwork, carried out in the surroundings of the two existing boreholes, to be considered for EGS developments.

The structural fieldwork was mainly dedicated to collection of kinematic data on recent fault-slip surfaces (GEMex 4.1). The results are summarized as follows:

- Under the regional stress field, defined by a NNW-striking stretching direction, two main NNW- and NE-striking fault systems developed. These are accompanied by minor faults, with a slight different orientation, N- and E-striking respectively. The age of deformation is from Miocene to Present, as testified by the age of rocks, sediments and soil, involved in the faults activity.
- The NNW- and NE- striking faults are characterized by a dominant oblique right-lateral and normal movements, respectively. A second kinematic movement, with a dominant vertical displacement, is recognizable in the NNW-striking fault system. These features account for interpreting the NNW-striking faults as transfer faults, acting in the regional extensional regime which causes the NE-striking faults, too. Coeval processes of crustal uplift reactivated pre-existing structures with a dominant vertical movement.
- Although the regional stress is well defined, in terms of local stress, these results indicated a variability depending on kinematics.

- In the boreholes areas, the two previously mentioned fractures trends were also detected, in the frame of a general migration of deformation toward north-northwest. This latter process implies that the EGS chosen area, having sealed fractures, seems not be the most prone to be fractured in response to the stimulation test to be carried out by CFE in one of those wells.

Geochemical, geophysical, and thermal studies (GEMex 4.3, GEMex 5.3, and GEMex 3.4) carried out in the surroundings of the boreholes area indicate:

- CO<sub>2</sub> ground emission implies that most data are associated to soil respiration, reflecting low permeability conditions.
- T-strike alignments (from MT data) are in agreement with the trend of the regional structures.
- MT-maps and cross-sections show the strong influence of the hydrothermal alteration on the values of the resistivity data.
- Gravity data support discontinuities with the same trend of the regional structures.
- Seismicity is very scarce to absent.
- The high temperature anomaly ( $T > 320^{\circ}\text{C}$  at 1970 m b.g.l. in EAC-1 well) results from the presence of a recent magmatic input deeper than 3 km from the ground. The occurrence of distinct magmatic events during Pleistocene is responsible for the vigorous hydrothermal circulation, which sealed, almost locally, the fault-driven fluid path so that the actual temperature distribution is mainly controlled by conductive heat transfer processes.

Studies carried out on the EGS development feasibility indicate:

- Potential systems will rely on the fracture system and not on the low permeability of the rock matrix.
- Hydraulic stimulation treatments may improve the productivity of individual wells by improving the permeability of existing structures.
- Thermal and hydraulic stimulation of existing inflow zones is considered the most promising stimulation method for both high-temperature wells, especially in the deep granites (GEMex D7.2).

## 5 Conclusion

### 5.1 Way of working

The Los Humeros and Acoculco geomodels have been initiated since the very beginning of the project. Preliminary versions were constructed to give a coherent geological interpretation using the existing state of the art. They were updated using new data acquired in the field until the final integration. In the meantime, GEMex partners used the geomodels versions at different stages of their evolution to feed their own computations along the project (Table 5.1).

This advanced paradigm favoured a better collaboration of the various disciplines involved in the project. A common platform making possible cross-interpretation facilitated the interaction between EU and Mexican scientists. The overall interpretation was shared and agreed by the contributors as the common result of their cooperative work.

The construction of the geomodels of Los Humeros and Acoculco was conducted in a team work gathering European and Mexican colleagues. The geomodelling was processed in an interdisciplinary manner. The close connection between EU and MX was crucial in this process. The overall goal was to complete 3D geomodels representing a joint interpretation implemented interactively by geologists, geophysicists and geochemists rather than a conglomerate of distinct outcomes. The scientists compared, connected, discussed, and adapted their own interpretations in a common geometrical framework for a mutual result. This approach allows a better understanding of the geothermal systems by integrating complementary knowledge in an interactive process. It makes the interpretation co-constructed and then more robust and reliable.

<b>GEMex Work Package</b>	<b>Geomodel in use</b>	<b>Purpose</b>
Regional resource models WP3	Los Humeros regional	Hydrogeological simulation
	Los Humeros local	
	Acoculco regional	Thermal modelling
Tectonic control on fluid flow WP4	Los Humeros regional	Geological interpretation
	Los Humeros local	
	Acoculco regional	
Detection of deep structures WP5	Acoculco regional	Modelling inversion of geophysical EM data from CFE and literature
	Los Humeros regional	Seismic data analysis
	Los Humeros local	
	Los Humeros regional	Elastic modelling

	Los Humeros local	
Reservoir characterisation and conceptual models WP6	Los Humeros local	Understanding the relationship between the geological surfaces and the feed zones obtained from analysing the production data and heating up profiles of wells.
	Los Humeros regional Los Humeros local	Heat transport and fluid flow simulation
Concepts for the development and utilization of EGS at Acoculco WP7	Acoculco local Acoculco local integrated	Stimulation modelling
Concepts for the development of super-hot resources WP8	Los Humeros regional Los Humeros local Los Humeros integrated	Strategy for accessing super-hot resource

Table 5.1: The main uses of the geomodels within the GEMex consortium.

## 5.2 Achievements

The work performed for the geomodels of Los Humeros and Acoculco led to numerous achievements and communication. The main ones are presented respectively in Table 5.2 and Table 5.3.

Achievement	Description	Date	Link Folder (or file name) path
Integrated geomodel	Los Humeros integration scale	05/2020	<a href="https://data.d4science.net/mm5C">https://data.d4science.net/mm5C</a> VRE Folders > GEMex > WP3_Regional_Resource_Models > Task3.1_Integrated_regional_models > 20200507_LosHumerosIntegratedGeomodel
Integrated geomodel	Acoculco local scale	05/2020	<a href="https://data.d4science.net/Ggw2">https://data.d4science.net/Ggw2</a> VRE Folders > GEMex > WP3_Regional_Resource_Models > Task3.1_Integrated_regional_models > Acoculco_Integrated_Local_model
Los Humeros wells description	Fifty-seven wells provided by CFE described with sets of geological units and vertical or deviated geometry.	02/2020	<a href="https://data.d4science.net/nZcR">https://data.d4science.net/nZcR</a> Workspace > VRE Folders > CFE_DATA > 202002_LosHumeros_WellsDescription_2019update

Los Humeros updtated geomodel	Los Humeros local scale	10/2019	<a href="https://data.d4science.net/kvqX">https://data.d4science.net/kvqX</a> VRE Folders > GEMex > WP3_Regional_Resource_Models > Task3.1_Integrated_regional_models > 201910_LosHumerosUpdatedLocalModel
Acoculco updtated geomodels	Acoculco regional scale Acoculco local scale	05/2019	<a href="https://data.d4science.net/t5NF">https://data.d4science.net/t5NF</a> VRE Folders > GEMex > WP3_Regional_Resource_Models > Task3.1_Integrated_regional_models > 201905_GeologicalModels
Geomodels digest	Overview of the making of Los Humeros and Acoculco 3D geomodels	02/2019	<a href="https://data.d4science.net/Hp8S">https://data.d4science.net/Hp8S</a> VRE Folders > GEMex > WP3_Regional_Resource_Models > Task3.1_Integrated_regional_models > 20190221_GEMex_T3.1_3DGeomodels_Overview.docx
Acoculco updtated geomodel	Acoculco regional scale	11/2018	<a href="https://data.d4science.net/3R5b">https://data.d4science.net/3R5b</a> VRE Folders > GEMex > WP3_Regional_Resource_Models > Task3.1_Integrated_regional_models > 201811_AcoculcoRegionalModel
Los Humeros updtated geomodel	Los Humeros fault model local scale	11/2018	<a href="https://data.d4science.net/qotN">https://data.d4science.net/qotN</a> VRE Folders > GEMex > WP3_Regional_Resource_Models > Task3.1_Integrated_regional_models > 201811_LosHumerosLocalFaultModel
Acoculco preliminary geomodel	Acoculco regional scale	10/2017	<a href="https://data.d4science.net/h2rg">https://data.d4science.net/h2rg</a> VRE Folders > GEMex > WP3_Regional_Resource_Models > Task3.1_Integrated_regional_models > 201710_PreliminaryGeologicalModels > Acoculco
Los Humeros preliminary geomodels	Los Humeros regional scale Los Humeros local scale	10/2017	<a href="https://data.d4science.net/NA8B">https://data.d4science.net/NA8B</a> VRE Folders > GEMex > WP3_Regional_Resource_Models > Task3.1_Integrated_regional_models > 201710_PreliminaryGeologicalModels > LosHumeros
Information inventory	Identification and gathering of all known geological and geophysical information regarding the geothermal systems of Los Humeros and Acoculco	03/2017	<a href="https://data.d4science.net/PVXw">https://data.d4science.net/PVXw</a> VRE Folders >GEMex >Milestones > MS10_20170321_Final-Data_availability.xlsx

**Table 5.2: Main achievements of the geomodelling and integration process for Los Humeros and Acoculco.**

<b>Communications</b>	<b>Title</b>	<b>Date</b>	<b>Link</b> Folder (or file name) path
-----------------------	--------------	-------------	---

This report D3.1	Report on the geological integrated models of Los Humeros and Acoculco	05/2020	<a href="http://www.gemex-h2020.eu">http://www.gemex-h2020.eu</a>
Scientific paper and presentation (WGC2020)	Updating the 3D Geomodels of Los Humeros and Acoculco Geothermal Systems (Mexico) – H2020 GEMex Project	05/2020	N/A
Scientific paper (ADGEO)	Preliminary 3-D geological models of Los Humeros and Acoculco geothermal fields (Mexico) – H2020 GEMex Project	11/2018	<a href="https://doi.org/10.5194/adgeo-45-321-2018">https://doi.org/10.5194/adgeo-45-321-2018</a>
Scientific presentation (EGU2018)	3D preliminary geological models of Los Humeros and Acoculco (Mexico) H2020 GEMex project	04/2018	N/A
Analysis of CFE's geophysical model	Contents of the CFE-Leapfrog Geophysical model of the Los Humeros Caldera	2018	<a href="https://data.d4science.net/jfnb">https://data.d4science.net/jfnb</a> VRE Folders > CFE_DATA > Leapfrog Geophysical Model Los Humeros > GEMex_WP3_CFE-Leapfrog-Geophysical-Model_LH_20180206.pdf
Analysis of CFE's geological model	Contents of the CFE-Leapfrog Geological model of the Los Humeros Caldera	2017	<a href="https://data.d4science.net/JoCo">https://data.d4science.net/JoCo</a> VRE Folders > CFE_DATA > Leapfrog Geological Model Los Humeros > GEMex_WP3_CFE-LeapFrog-Model_20171024.pdf
Evanno's M.Sc. Thesis	3-D preliminary geological modelling of the Los Humeros geothermal area (Mexico)	2017	<a href="https://data.d4science.net/snwT">https://data.d4science.net/snwT</a> VRE Folders > GEMex > WP3_Regional_Resource_Models > Task3.1_Integrated_regional_models > 201710_PreliminaryGeologicalModels > LosHumeros > Gwladys_EVANNO_ENAG_2017.pdf

**Table 5.3: Main communications of the geomodelling and integration process for Los Humeros and Acoculco. Presentations done in GEMex meetings are not listed.**

### 5.3 Perspectives

Both for EGS and superhot fluid research, the work above described, beyond its own results, highlights the importance of the integration of data. Improvements to favour the merging of data is still necessary. In this view, studies on how homogenize the resolution of the different geophysical methods to depth is becoming crucial, considering the huge amount of data that can be produced. In particular, this is meaningful looking for superhot fluids, hosted in pockets, and for the location of the existing fracture systems in EGS perspectives.

Field and borehole data still represent the key-parameters for interpretation of geophysical data. In this view, the T-strike analyses from MT data resulted an efficient link between direct and indirect data, in order to give indications for the distribution and evaluation of tectonic structures. The integration between fractures reconstructed at surface and T-strike analysis might be considered as the first brick toward the total integration of the MT data, aimed to the reconstruction of the fractures network.

For Los Humeros, one relevant contribution of the integrated geomodel is the proposition of a relatively small area located south of Los Humeros village (Fig. 33), worth to be explored by CFE if the company decides a future searching for superhot geothermal resources.

For Acoculco, the integrated 3D geomodel and the resulting conceptual model can also be used by CFE as the base for further evaluation to assess the feasibility of the stimulation for an EGS development in this geothermal area.

The work performed to construct the various versions of the Los Humeros and Acoculco geomodels led to an interpretation of their respective geothermal system. In addition to the publications already issued by the team (Table 5.3), both geomodels and geothermal interpretations will be presented in forthcoming scientific papers.

## 6 Acknowledgement

The authors wish to thank the Comisión Federal de Electricidad (CFE, Mexico) for their assistance and support. This paper presents results of the GEMex Project, funded by the European Union's Horizon 2020 research and innovation programme under grant agreement No. 727550, and by the Mexican Energy Sustainability Fund CONACYT-SENER, Project 2015-04-268074. More information can be found on the GEMex Website: <http://www.gemex-h2020.eu>.

Thank you to all the GEMex partners who contributed in any way to the work presented in this report.

This report benefits of the estimable contribution of Victor Hugo Garduño who prematurely passed away during this EU-MX joint project.

## 7 References

- Avellán, D. R., Macías, J. L., Layer, P. W., Cisneros, G., Sánchez-Núñez, J. M., Gómez-Vasconcelos, Pola, A., Sosa- Ceballos, G., García-Tenorio, F., Reyes-Agustín, G., Osorio- Ocampo, S., García-Sánchez, L., Mendiola, F., Martí, J., López-Loera, H., and Benowitz, J.: Geology of the Late Pliocene – Pleistocene Acoculco caldera complex, eastern Trans-Mexican Volcanic Belt (México), J. Maps, in press, <https://doi.org/10.1080/17445647.2018.153107>, 2018.
- Bär, K., 2017.WP3: Contents of the CFE-Leapfrog Geological model of the Los Humeros Caldera, Mexico. GEMex internal report, 11 p.
- Bär, K., 2018.WP3: Contents of the CFE-Leapfrog Geophysical model of the Los Humeros Caldera, Mexico. GEMex internal report, 22 p.
- Calcagno, P., Trumpy, E., Gutiérrez-Negrín, L. C., Norini, G., Macías, J. L., Carrasco-Núñez, G., Liotta, D., Garduño-Monroy, V. H., Hersir, G. P., Vaessen, L., Evanno, G., and Arango Galván, C.: Updating the 3D Geomodels of Los Humeros and Acoculco Geothermal Systems (Mexico) – H2020 GEMex Project, In Proceedings of World Geothermal Congress 2020 (WGC2020), Reykjavik, Iceland, 27 April – 1 May 2020, 12 p.
- Calcagno, P., Evanno, G., Trumpy, E., Gutiérrez-Negrín, L. C., Macías, J. L., Carrasco-Núñez, G., and Liotta, D.: Preliminary 3-D geological models of Los Humeros and Acoculco geothermal fields (Mexico) – H2020 GEMex Project, Adv. Geosci., 45, 321-333, <https://doi.org/10.5194/adgeo-45-321-2018>, 2018.
- Calcagno, P.: 3-D GeoModelling for a Democratic Geothermal Interpretation, in: Proceedings of World Geothermal Congress 2015 (WGC2015), Melbourne, Australia, 7 pp., 2015.
- Calcagno, P., Baujard, C., Guillou-Frottier, L., Dagallier, A., and Genter, A.: Estimation of the deep geothermal potential within the Tertiary Limagne basin (French Massif Central): An integrated 3-D geological and thermal approach, *Geothermics*, 51, 496–508, 2014.
- Calcagno, P., Courrioux, G., Guillen, A., and Chilès, J. P.: Geological modelling from field data and geological knowledge, Part I – Modelling method coupling 3-D potential-field interpolation and geological rules, *Phys. Earth Planet. Int.*, 171, 147–157, 2008.
- Carrasco-Núñez, G., Bernal, J. P., Dávila, P., Jicha, B., Giordano, G., and Hernández, J.: Reappraisal of Los Humeros volcanic complex by new U/Th zircon and <sup>40</sup>Ar/<sup>39</sup>Ar dating: Implications for greater geothermal potential, *Geochem. Geophys. Geosy.*, 19, 132–149, <https://doi.org/10.1002/2017GC007044>, 2018.
- Carrasco-Núñez, G., López-Martínez, M., Hernández, J., and Vargas, V.: Subsurface stratigraphy and its correlation with the surficial geology at Los Humeros geothermal field, eastern Trans-Mexican Volcanic Belt, *Geothermics*, 67, 1–17, <https://doi.org/10.1016/j.geothermics.2017.01.001>, 2017a.
- Carrasco-Núñez, G., Hernández, J., De León, L., Dávila, P., Norini, G., Bernal, J. P., Jicha, B., Navarro, M., and López, P.: Geologic Map of Los Humeros volcanic complex and geothermal field, eastern Trans-Mexican Volcanic Belt, *Terra Digitalis*, 1, 1–11, <https://doi.org/10.22201/igg.terradigitalis.2017.2.24>, 2017b.
- Carrillo, J.; Pérez-Flores, M.; Gallardo, L.; Hernández-Márquez, O.; Schill, E.; Cornejo , N., 2020. 3D Joint Inversion of Gravity and Magnetic Data in Los Humeros and Acoculco Unconventional Geothermal Systems. Reykjavik, Iceland, April 26 – May 2, 2020, Proceedings World Geothermal Congress 2020.

Cloetingh, S., van Wees, J. D., Ziegler, P. A., Lenkey, L., Beekman, F., Tesauro, M., Förster, A., Norden, B., Kaban, M., Hardebol, N., Bonté, D., Genter, A., Guillou-Frottier, L., Ter Voorde, M., Sokoutis, D., Willingshofer, E., Cornu, T., and Worum, G.: Lithosphere tectonics and thermomechanical properties: An integrated modelling approach for Enhanced Geothermal Systems exploration in Europe, *Earth-Sci. Rev.*, 102, 159–206, 2010.

Evanno, G.: 3-D preliminary geological modelling of the Los Humeros geothermal area (Mexico), M.Sc. Thesis, ENAG/MFE- 088-GB-2017, 123 pp., 2017, available on VRE: <https://data.d4science.net/snwT>.

Ferrari, L., López-Martínez, M., Aguirre-Díaz, G., and Carrasco- Núñez, G.: Space-time patterns of Cenozoic arc volcanism in Central Mexico: from the Sierra Madre Occidental to the Mexican Volcanic Belt, *Geology*, 27, 303–306, 1999.

García-Palomo, A., Macías, J. L., Jiménez, A., Tolson, G., Mena, M., Sánchez-Núñez, J. M., Arce, J. L., Layer, P. W. Santoyo, M. A., and Lermo-Samaniego, J.: NW-SE Pliocene-Quaternary extension in the Apan-Acocolco region, eastern Trans-Mexican Volcanic Belt, *J. Volcanol. Geoth. Res.*, 349, 240–255, 2017.

GEMex D3.2 Report on the volcanological conceptual models of Los Humeros and Acocolco (UNIROMA3), available on the GEMex Website: <http://www.gemex-h2020.eu>.

GEMex D3.3 Report on the hydrogeological model of Los Humeros (BRGM), available on the GEMex Website: <http://www.gemex-h2020.eu>.

GEMex D3.4 Report on the regional resource assessment and geothermal models (UU), available on the GEMex Website: <http://www.gemex-h2020.eu>.

GEMex D3.5 Report on the analogue modelling of the interactions between regional tectonics and volcanoes (CNR), available on the GEMex Website: <http://www.gemex-h2020.eu>.

GEMex D3.6 Report on the analogue modelling of the collapse of caldera and volcanic edifices and the associated surface deformation (CNR), available on the GEMex Website: <http://www.gemex-h2020.eu>.

GEMex D4.1 Final report on active system (LH and AC) (UNIBA), available on the GEMex Website: <http://www.gemex-h2020.eu>.

GEMex D4.2 Final report on understanding from exhumed systems (UNIBA), available on the GEMex Website: <http://www.gemex-h2020.eu>.

GEMex D4.3 Final Report on geochemical characterization and origin of cold and thermal fluids (CNR), available on the GEMex Website: <http://www.gemex-h2020.eu>.

GEMex D5.2 Report on resistivity modelling and comparison with other SHGS (ISOR), available on the GEMex Website: <http://www.gemex-h2020.eu>.

GEMex D5.3 Report on the seismic structure of the Acocolco and Los Humeros fields (GFZ), available on the GEMex Website: <http://www.gemex-h2020.eu>.

GEMex D5.5 Report on seismic modelling (OGS), available on the GEMex Website: <http://www.gemex-h2020.eu>.

GEMex D5.6 Report on gravity modelling (KIT), available on the GEMex Website: <http://www.gemex-h2020.eu>.

GEMex D5.8 Report on 3D resistivity modelling with external constraint (ISOR), available on the GEMex Website: <http://www.gemex-h2020.eu>.

GEMex D5.10 Report on integrated geophysical model of Los Humeros and Acoculco (ISOR), available on the GEMex Website: <http://www.gemex-h2020.eu>.

GEMex D5.12 Report on implementation and validation protocol for EGS and SHGS (CNR), available on the GEMex Website: <http://www.gemex-h2020.eu>.

GEMex D6.3 Report on the numerical reservoir model used for the simulation of the Los Homeros reservoir (RWTH), available on the GEMex Website: <http://www.gemex-h2020.eu>.

GEMex D6.6. Report on the calibrated model for the super-hot reservoir at Los Humeros and its calibration against available field data (RWTH), available on the GEMex Website: <http://www.gemex-h2020.eu>.

GEMex D7.2. Report on optimised stimulation scenario for Acoculco (GFZ), available on the GEMex Website: <http://www.gemex-h2020.eu>.

Guillen, A., Calcagno, P., Courrioux, G., Joly, A., and Ledru, P.: Geological modelling from field data and geological knowledge, Part II, Modelling validation using gravity and magnetic data inversion, *Phys. Earth Planet. Int.*, 171, 158–169, 2008.

Gutiérrez-Negrín, L.C.A., Canchola-Félix, I., Romo-Jones, J.M. and Quijano-León., J.L., 2020. Geothermal Energy in Mexico: Update and Perspectives. *Proceedings World Geothermal Congress 2020*. In press.

Houlding, S. W.: 3-D Geoscience Modeling; Computer Techniques for Geological Characterization, Springer-Verlag, Berlin, Germany, 1994.

INEGI, 2016 – Continuo de Elevaciones Mexicano (CEM) - Digital Elevation Model (DEM). Last access 13/12/2016)

Jolie, E., Bruhn, D., López Hernández, A., Liotta, D., Garduño- Monroy, V. H., Lelli, M., Hersir, G. P., Arango-Galván, C., Bonté, D., Calcagno, P., Deb, P., Clauser, C., Peters, E., Hernández Ochoa, A. F., Huenges, E., González Acevedo, Z. I., Kielling, K., Trumpy, E., Vargas, J., Gutiérrez-Negrín, L. C., Aragón- Aguilar, A., Halldórsdóttir, S., González Partida, E., vanWees, J. D., Ramírez Montes, M. A., Díez León, H. D., and the GEMex team: GEMex – A Mexican-European Research Cooperation on Development of Superhot and Engineered Geothermal Systems. *Proceedings, 43<sup>rd</sup> Workshop on Geothermal Reservoir Engineering*, Stanford University, Stanford, CA, 2018.

Lajaunie, C., Courrioux, G., and Manuel, L.: Foliation fields and 3-D cartography in geology; principles of a method based on potential interpolation, *Mathemat. Geol.*, 29, 571–584, 1997.

Lesti, C., Giordano G., Salvini, F., Cas, R. (2008). Volcano tectonic setting of the intraplate, Pliocene-Holocene, Newer Volcanic Province (southeast Australia): Role of crustal fracture zones. *Journal of Geophysical Research*, 113, B07407, doi:10.1029/2007JB005110.

López-Hernández, A., García-Estrada, G., Aguirre-Díaz, G., González-Partida, E., Palma-Guzmán, H., and Quijano-León, J. L.: Hydrothermal activity in the Tulancingo–Acoculco Caldera Complex, central Mexico: Exploratory studies, *Geothermics*, 38, 279–293, 2009.

Lorenzo-Pulido, C., Armenta-Flores, M., and Ramírez-Silva, G. Characterization of the Acoculco Geothermal Zone as a HDR System, *GRC Transactions*, 34, 369–372, 2010.

Lucci, F., Carrasco-Núñez, G., Rossetti, F., Theye, T., White, J.C., Urbai, S., Azizi, H., Asahara, Y., Giordano, G., Anatomy of the magmatic plumbing system of Los Humeros Caldera (Mexico): implications for geothermal systems, *Solid Earth*, 11, 125–159, 2020.

Mallet, J. L.: *Geomodeling*, Oxford University Press, Oxford, New York, 2002.

Norini, G., Gropelli, G., Sulpizio, R., Carrasco-Núñez, G., Dávila-Harris, P., Pelliccioli, C., Zucca, F., and De Franco, R.: Structural analysis and thermal remote sensing of the Los Humeros Volcanic Complex: Implications for volcano structure and geothermal exploration, *J. Volcanol. Geoth. Res.*, 301, 221–237, <https://doi.org/10.1016/j.jvolgeores.2015.05.014>, 2015.

Olvera García E., Garduño-Monroy V.H., Liotta D., Brogi A., Bermejo-Santoyo G., Guevara-Alday J.A. (2019) - Neogene-Quaternary normal and transfer faults controlling deep-seated geothermal systems: The case of San Agustín del Maíz (central Trans-Mexican Volcanic Belt, México). *Geothermics* 86, <https://doi.org/10.1016/j.geothermics.2019.101791>

Paulsen, T. S., & Wilson, T. J. (2010). New criteria for systematic mapping and reliability assessment of monogenetic volcanic vent alignments and elongate volcanic vents for crustal stress analyses. *Tectonophysics*, 482(1-4), 16–28.

Sosa-Ceballos, G., Macías, J.L., Avellán, D.R., Salazar-Hermenegildo, N., Boijseauneau-López, M.E., and Pérez-Orozco, J.D.: The Acoculco Caldera Complex magmas: Genesis, evolution and relation with the Acoculco geothermal system. *Journal of Volcanology and Geothermal Research*, 358, pp. 288-306. Available at: <https://www.sciencedirect.com/science/article/abs/pii/S0377027318300131?via%3Dihub>, 2018.

Wu, Q., Xu, H., and Zou, X.: An effective method for 3-D geological modeling with multi-source data integration, *Comput. Geosci.*, 31, 35–43, 2005.



Coordination Office, GEMex project

Helmholtz-Zentrum Potsdam  
Deutsches GeoForschungsZentrum

Telegrafenberg, 14473 Potsdam

Germany